



**UNIVERSIDADE DE BRASÍLIA**  
**INSTITUTO DE GEOCIÊNCIAS**  
**PROGRAMA DE PÓS-GRADUAÇÃO EM GEOCIÊNCIAS APLICADAS**  
**E GEODINÂMICA**

**VITÓRIA RODRIGUES FERREIRA BARBOSA**

**ESTUDO DA DINÂMICA DO FÓSFORO NO TRIBUTÁRIO DO RIACHO  
FUNDO – LAGO PARANOÁ, DF**

**N° 185**

**BRASÍLIA, DF**  
**2021**



**UNIVERSIDADE DE BRASÍLIA**  
**INSTITUTO DE GEOCIÊNCIAS**  
**PROGRAMA DE PÓS-GRADUAÇÃO EM GEOCIÊNCIAS APLICADAS**  
**E GEODINÂMICA**

**ESTUDO DA DINÂMICA DO FÓSFORO NO TRIBUTÁRIO DO RIACHO  
FUNDO – LAGO PARANOÁ, DF**

**VITÓRIA RODRIGUES FERREIRA BARBOSA**

**DISSERTAÇÃO DE MESTRADO N° 185**  
**ÁREA DE CONCENTRAÇÃO: RECURSOS HÍDRICOS E MEIO**  
**AMBIENTE**  
**LINHA DE PESQUISA: GEOQUÍMICA AMBIENTAL**

**BRASÍLIA, DF**  
**2021**

**VITÓRIA RODRIGUES FERREIRA BARBOSA**

**ESTUDO DA DINÂMICA DO FÓSFORO NO TRIBUTÁRIO DO RIACHO  
FUNDO – LAGO PARANOÁ, DF**

Dissertação de Mestrado submetido ao Programa de Pós-Graduação em Geociências Aplicadas e Geodinâmica da Universidade de Brasília, como requisito parcial para obtenção do grau de Mestre em Geociências Aplicadas e Geodinâmica.

Área de concentração: Recursos hídricos e Meio Ambiente  
Linha de pesquisa: Geoquímica ambiental

Orientador: Geraldo Resende  
Boaventura

Coorientadora: Rejane Ennes Cicerelli

**BRASÍLIA, DF**

**2021**

Be

Barbosa, Vitória Rodrigues Ferreira  
ESTUDO DA DINÂMICA DO FÓSFORO NO TRIBUTÁRIO DO RIACHO  
FUNDO – LAGO PARANOÁ, DF / Vitória Rodrigues Ferreira  
Barbosa; orientador Geraldo Resende Boaventura; co  
orientador Rejane Ennes Cicerelli. -- Brasília, 2021.  
85 p.

Dissertação (Mestrado - Doutorado em Geociências  
Aplicadas) -- Universidade de Brasilia, 2021.

1. Fracionamento de fósforo. 2. Urbanização. 3.  
Sedimentos. 4. Material Particulado em Suspensão. 5.  
Contaminação. I. Boaventura, Geraldo Resende, orient. II.  
Cicerelli, Rejane Ennes, co-orient. III. Título.

**VITÓRIA RODRIGUES FERREIRA BARBOSA**

**ESTUDO DA DINÂMICA DO FÓSFORO NO TRIBUTÁRIO DO RIACHO  
FUNDO – LAGO PARANOÁ, DF**

Dissertação de Mestrado submetido ao Programa de Pós-Graduação em Geociências Aplicadas e Geodinâmica da Universidade de Brasília, como requisito parcial para obtenção do grau de Mestre em Geociências Aplicadas e Geodinâmica

Aprovado em 24 de setembro de 2021.

**BANCA EXAMINADORA**

---

PROF. GERALDO RESENDE BOAVENTURA  
UNIVERSIDADE DE BRASÍLIA  
ORIENTADOR

---

PROF. HENRIQUE LLACER ROIG  
EXAMINADOR INTERNO

---

PROF. ROZANE VALENTE MARINS  
EXAMINADORA EXTERNA

**BRASÍLIA, DF**  
**2021**

## **AGRADECIMENTOS**

Agradeço a todos que, de alguma forma, contribuíram para a realização dessa pesquisa.

Agradeço a minha família, meus pais, Silvia e Antonio Carlos e minha irmã Virginia, que sempre me apoiaram durante o mestrado e não mediram esforços para que eu pudesse alcançar meu objetivo. Agradeço a minha tia, Regina, por todo apoio, ajuda e os lanches.

Agradeço aos meus orientadores. Agradeço ao Prof. Geraldo Resende Boaventura pela oportunidade, suporte, ensinamentos, paciência e disponibilidade para a vida pessoal e profissional. Agradeço a Prof. Rejane Ennes Cicerelli pelos 5 anos de companheirismo, carinho, atenção, cuidado, paciência, broncas, conversas, discussões, por ser meu porto seguro quando pensava que tudo ia dar errado, por me incentivar, apoiar e sempre me ajudar a levantar. Agradeço ao Prof. Jeremie Garnier pelo apoio, confiança, por não desistir de mim, discussões, as inúmeras correções, paciência, sabedoria e os inúmeros desafios que você propôs. Durante esse período passei por um grande processo de autoconhecimento e crescimento pessoal e profissional que vocês me ajudaram a construir.

Agradeço aos meus amigos da pós-graduação Lyara, Hikari, Gabriella, Paula, Maria Elisa, André, Lucélia, Isa pelos momentos de felicidade e tristeza, pelas conversas e perceber que todo mundo está no mesmo barco. Agradeço ao Eltinho e ao Myller por toda a ajuda durante esse período, as explicações, conversas e os “açaís”. Agradeço aos meus amigos da graduação: Wedly e Ana pelas conversas, apoio, por me escutar e incentivar a continuar, e pelas saídas que ajudaram a esquecer um pouco os meus problemas e me deram força para continuar; Ao Edgar por toda a ajuda dele, principalmente nesta fase final do mestrado; a Carol pelas conversas reflexivas e os lanches; Christian que sempre me ajudou, apoiou e me deu suporte acadêmico durante esse período; Monique, Ianca, Babi, Matheus, Chris, Hugo e Caio pelos momentos de descontração. Agradeço aos meus amigos Lucas, Rayssa, Bruno, Carol, Maria Carolina pela amizade e carinho durante esse período.

Agradeço ao pessoal do LAGEQ, pelo aprendizado e apoio durante a execução deste trabalho.

Agradeço ao Mendes por todo suporte em campo, conversas, experiências essenciais para esse projeto

Agradeço ao Louis, Liszt, Catarina, Vivaldi, Felix, Leonoura e Yusuf por todo carinho e amor.

Agradeço a entidade Caboclo Boiadeiro Sete Cancelas por todos os conselhos, apoio, força e ajuda que me permitiram finalizar esse trabalho.

Agradeço a Companhia de Saneamento Ambiental do Distrito Federal (Caesb) e a ANA (Agência Nacional de Águas) pelos dados cedidos.

Agradeço ao Instituto de Geociências pela infraestrutura disponibilizada para execução dessa pesquisa.

Agradeço a Agência Reguladora de Águas (ADASA), Coordenação de Aperfeiçoamento de Pessoal de Nível Superior-Brasil (CAPES), Fundação de Apoio à Pesquisa do Distrito Federal (FAP-DF) e o Conselho Nacional de Desenvolvimento Científico e Tecnológico (CNPq) pelo apoio financeiro.

## **EPIGRAFE**

“The rain isn’t a big deal. Even if you’re the only one without an umbrella, it’s fine. Just get wet. Get wet and run.”

Myul Mang  
Doom at your service

Barbosa, VRF. Estudo da dinâmica do fósforo no tributário do Riacho Fundo – Lago Paranoá, DF (Dissertação – Mestrado). Brasília: Programa de Pós-Graduação em Geociências Aplicadas e Geodinâmica, Instituto de Geociências, Universidade de Brasília, 2021. 80 p.

## RESUMO

A eutrofização é um problema global que afeta diretamente a qualidade da água. O fósforo (P) de fontes pontuais e não pontuais leva ao seu enriquecimento nas águas superficiais e, portanto, auxilia no processo de eutrofização. O Lago Paranoá (LP), Distrito Federal (DF), Brasil, sofre com processos de eutrofização com recorrência, sendo os piores casos registrados na década de 70, 90 e em 2016, principalmente na região do Braço do Riacho Fundo (BRF) no qual está localizado uma Estação de Tratamento de Esgoto (ETE-Sul) e recebe águas da região mais urbanizada do DF. Considerando a situação acima é necessário obter informações sobre o processamento e transporte de P, as suas origens e destinos, as mudanças temporais e espaciais de P em amostras nos corpos hídricos do Lago Paranoá e do Córrego do Riacho Fundo (RFS), tributário do BRF. Foram investigadas amostras de água superficial e material particulado em suspensão (SPM) coletados de 2015 a 2020 no LP e RFS; perfil de sedimento de 600 cm; e amostras de sedimento de fundo (0 -15 cm) no LP em 2016. As amostras são parte do banco de dados do Laboratório de Geoquímica da Universidade de Brasília (UnB). O fósforo total (TP), metais e nutrientes foram determinados para as amostras. As determinações para as amostras de água foram realizadas pelo ICP-MS. Para as demais amostras foram realizadas digestões ácidas para determinação de metais, nutrientes e perda ao fogo; e para as amostras de sedimento foram analisadas as quatro frações de P: fracamente ligado a P (Lo-P), P ligado a Alumínio (Al-P), Ferro (Fe-P) e Cálcio (Ca-P). A determinação de metais, P e suas frações foram realizadas pelo ICP-OES. O fósforo dissolvido (DP) apresentou baixa concentração e variação. O TP no SPM mostrou concentrações entre 900 e 100000 mg kg<sup>-1</sup>, assim como os sedimentos com concentração de P variaram de 400 a 7000 mg kg<sup>-1</sup>, concentrações máximas próximas à ETE-Sul. No perfil sedimentar, o TP variou aproximadamente de 120 mg kg<sup>-1</sup> a 1500 mg kg<sup>-1</sup> com

os maiores percentuais das frações de fósforo ligado a ferro e a alumino, 61% e 27% respectivamente. Os maiores teores de P são acompanhados por altas concentrações de P, LOI, C, Ca e Mn nos intervalos de 200 a 250 cm e 300 a 450 cm, refletindo mudanças no ambiente, como períodos anterior e posterior a instalação das ETE e o início da urbanização. Com relação às frações de P, a sequência de abundância geral nos sedimentos foi IP >> OP e Al-P> Fe-P> Ca-P> Lo-P, foi verificada diferenças marcantes de concentração de acordo a localização espacial. A distribuição de Al-P e Ca-P apontou para um aumento da contribuição antropogênica, sendo suas maiores concentrações próximo as ETE-Sul ou de fontes antrópicas. A determinação de P no SPM e dos sedimentos mostrou ser um indicativo essencial da qualidade ambiental do LP.

**Palavras-Chaves:** Fracionamento de fósforo; urbanização; sedimentos; material particulado em suspensão; contaminação.

Barbosa, VRF. Study of phosphorus dynamics in the tidal stream of Riacho Fundo – Lago Paranoá, DF (Dissertation – Master). Applied Geosciences and Geodynamics Postgraduate Program, Brasília: Institute of Geosciences, University of Brasília, 2021. 80 p.

## ABSTRACT

Eutrophication is a global problem that directly affects water quality. Phosphorus (P) from point and non-point sources leads to its enrichment in surface waters and, therefore, helps in the eutrophication process. Lake Paranoá (LP), Federal District (DF), Brazil, suffers from recurrent eutrophication processes, with the worst cases recorded in the 70s, 90s and 2016, mainly in the Riacho Fundo Branch (BRF) region in which is located a wastewater treatment plant (WWTP-South) and receives water from the most urbanized region of the DF. Considering the situation above it is necessary to obtain information about the processing and transport of P, such as its origins and destinations, such as temporal changes and spaces of P in our water bodies of LP and Riacho Fundo Stream (RFS), tributary of the BRF. Collected surface water and suspended particulate matter (SPM) collected from 2015 to 2020 in the LP and RFS were investigated; 600 cm sediment profile; and as a bottom sediment (0 -15 cm) in the LP in 2016. As part of the database of the Geochemistry Laboratory of the University of Brasília (UnB). Total phosphorus (TP), metals and nutrients were determined for as accused. Determinations for water standards were carried out by ICP-MS. For as others corrected, acid digestions for determination of metals, nutrients and loss to ignition were eliminated; and for the sediments, the four fractions of P were analyzed: weakly bound to P (Lo-P), P bound to Aluminum (Al-P), Iron (Fe-P) and Calcium (Ca-P). The determination of metals, P and their fractions were performed by ICP-OES. Dissolved phosphorus (DP) showed low concentration and variation. The TP in the SPM configured between 900 and 100000 mg kg<sup>-1</sup>, as well as the sediments with P concentration ranged from 400 to 7000 mg kg<sup>-1</sup>, maximum percentages close to the WWTP-South. In the sedimentary profile, the TP ranged approximately from 120 mg kg<sup>-1</sup> to 1500 mg kg<sup>-1</sup> with the highest percentages of phosphorus bound to iron and aluminum, 61% and 27% respectively. The highest P contents are accompanied by

high priority P, LOI, C, Ca and Mn in the ranges of from 200 to 250 cm and from 300 to 450 cm, reflecting changes in the environment, such as periods before and after installation of ETEs and the beginning of urbanization. Regarding the P fractions, the sequence of general abundance in the sediments was IP >> OP and Al-P> Fe-P> Ca-P> Lo-P, marked differences in concentration according to spatial location were verified. The distribution of Al-P and Ca-P pointed to an increase in the anthropogenic contribution, with their greatest practices being close to ETE-Sul or from anthropogenic sources. The determination of P in the SPM and of the sediments revealed to be an essential indicator of the environmental quality of the LP.

**Key-Words:** Phosphorus Fractionation; Urbanization; Sediments; Suspended Particulate Matter; Contamination

## **LISTA DE FIGURAS**

Figura 1 - Exemplos de fontes de P difuso entrando em sistemas aquáticos (sumidouros) são ilustrados (adaptado de Macintosh et al., 2018). ....	13
Figura 2 - Fluxograma metodológico da dissertação (Autor, 2021). ....	20
Figure 3 - Map of Paranoá Lake, including the design sampling. ....	27
Figure 4 - Principal Component Analysis (PCA) of dissolved (4A and 4B), ....	33
Figure 5 - Principal Component Analysis (PCA) of SPM(5A and 5B). ....	34
Figure 6 - Vertical distribution of phosphorus and other elements in sediment cores from BRF. ....	35
Figure 7 - Vertical profiles of phosphorus and others elements from the mouth of the RFS (4LB). ....	35
Figure 8 - Principal Component Analysis (PCA) of Sediments (8A and 8B). ..	36
Figure 9 - The concentration of P in shallow waters (Figure 4 - A); SPM (Figure 4 - B); and sediment (Figure 4 – C). ....	38
Figure 10 - P speciation relation with species (Lo-P; Al-P; Fe-P, and Ca-P) in the sediment until 15 cm of depth; and B - P speciation in sediment profile for 4LB point. ....	42
Figure 11 - Graphics Biplot of sediments of AlxP; FexP; CaxP; ZnxP; TixP; and MnxP. ....	45
Figure 12 - PCA for the species of P and metals. ....	48
Figura 13 – Esquema do método para determinação de formas de fósforo inorgânico em sedimentos superficiais.....	84

## **LISTA DE TABELAS**

Table 1 - Identification, type, number and collected date of samples. ....	26
Tabela 2 - Coordenadas dos pontos de amostragem.....	72
Tabela 3 - Composição amostras dissolvidas.....	74
Tabela 4 – Composição do SPM .....	78
Tabela 5 - Concentração química dos sedimentos.....	80
Tabela 6 - Concentração química de P e suas frações nos sedimentos .....	82

## **LISTA DE SIGLAS**

1L: Bananal Region – Região do Bananal

2L: Gama Region – Região do Gama

3L: Center of LP Region- Região do Centro do Lago

4L: Riacho Fundo Region- Região do Riacho Fundo

5L: Torto Region- Região do Torto

Al-P: Alluminium bound to Phosphorus – Alumínio ligado ao Fósforo

BCR: European Community Bureau of Reference

BRF: Riacho Fundo Branch – Braço do Riacho Fundo

Caesb: Companhia de Saneamento Ambiental do Distrito Federal.

Ca-P: Calcium bound to Phosphorus – Cálcio ligado ao Fósforo

CMS: Concentration of Suspending Material – Concentração do Material em Suspensão

DF: District Federal – Distrito Federal

DP: Dissolved Phosphorus – Fósforo Dissolvido

EPA or USEPA: Environmental Protection Agency - USA

EUA: Estados Unidos da América

Fe-P: Iron bound to Phosphorus – Ferro ligado ao Fósforo

ICP – OES: Inductively coupled plasma optical emission spectrometry – espectrometria de emissão óptica com plasma indutivamente acoplado

ICP - MS: Inductively Coupled Plasma - Mass Spectrometry - espectrometria de massa com plasma indutivamente acoplado

LDPE: low-density polyethylene - Polietileno de baixa densidade

LMB: lanthanum-modified bentonite ,

Lo-P: Loosely bound to Phosphorus – Fracamente ligado ao Fósforo

LP: Paranoá Lake – Lago Paranoá

MAP: mean annual precipitation – média anual de precipitação

MCE: mixed cellulose ester -

OECD: Organization for Economic Co-Operation and Development

P: Phosphorus - Fósforo

PCA: Principal component analysis – Análise de principal componente

PI: Phosphorus inorganic form – Fósforo Inorgânico

PIA: P inactivation agents

P-Org: organic phosphorus - Fósforo Orgânico

POT: organic species of P – Total de Fósforo Orgânico

PT: Portuguese - Português.

RFS: Riacho Fundo Stream – Córrego do Riacho Fundo

RSD: relative standard deviations – Desvio Padrão Relativo

SCE: sequential chemical extractions – Extração química sequencial

SMP: Suspend Particulate Matter – Material particulado em suspensão

TCAP: thermally-treated calcium-rich attapulgite

Log Kd: Distribution Coefficient – Coeficiente de Distribuição

TIP: total inorganic phosphorus – Fósforo Inorgânico Total

TP: Total Phosphorus – Fósforo Total

WHO: World Health Organization (WHO)

WTR: water treatment residuals – Tratamento de águas residuais

WWTP: Waste Water Treatment Plant – Estação de Tratamento de Esgoto

## SUMÁRIO

<b>1. INTRODUÇÃO .....</b>	<b>12</b>
1.1. INTRODUÇÃO .....	12
1.2. OBJETIVOS .....	16
1.2.1. Objetivos Gerais .....	16
1.2.2. Objetivos Específicos .....	16
1.3. MATERIAIS .....	16
1.3.1 – Área de Estudo .....	16
1.3.2 – Amostragem.....	18
1.4. ESTRUTURA DA DISSERTAÇÃO.....	19
<b>2. ANÁLISE DOS RESULTADOS        THE BEHAVIOR OF PHOSPHORUS IN URBAN RESERVOIRS – SPECIES, FRACTIONS, AND CHARACTERIZATION OF PHOSPHORUS .....</b>	<b>21</b>
2.1. ABSTRACT .....	21
2.2. INTRODUCTION.....	22
2.3. METHODS .....	24
2.3.1. Study area .....	24
2.3.2. Design Sampling and sample preparation .....	26
2.3.3. Analytical methods.....	28
2.3.4. Quality and Control .....	30
2.3.5. Statistical analysis .....	31
2.4. RESULTS AND DISCUSSIONS .....	32
2.4.1. Main properties.....	32
2.4.2. Distribution of Total Phosphorus (TP) in the Paranoá Lake .....	37
2.4.4. Speciation of P and metals and the implications for LP .....	44
2.4.5. Comparison around the world .....	49
2.5. CONCLUSIONS .....	51
2.6. ACKNOWLEDGMENTS .....	52
<b>3. CONSIDERAÇÕES FINAIS .....</b>	<b>53</b>
<b>4. REFERÊNCIAS BIBLIOGRÁFICAS.....</b>	<b>55</b>
<b>ANEXOS .....</b>	<b>72</b>



## 1. INTRODUÇÃO

### 1.1. INTRODUÇÃO

Atualmente, o Distrito Federal (DF) é a terceira área mais urbanizada do país (IBGE, 2016). Geralmente em regiões metropolitanas tem elevada quantidade de águas residuais de origem difusa e pontual despejadas em reservatórios ou rios próximos (Liu et al., 2015; Savage et al., 2010). Um dos principais problemas dessa situação é a eutrofização dos recursos hídricos, que é um fenômeno pelo qual um ecossistema é enriquecido por nutrientes, principalmente fósforo (P) e nitrogênio (N) (Karim Morsy et al., 2017)

O processo de eutrofização é um importante problema que atinge córregos e corpos de água doce relacionado a ação antrópica, causando prejuízos sociais, ecológicos e econômicos aos sistemas associados (Bitschofsky and Nausch, 2019). São estimados nos Estados Unidos da América (EUA), na Inglaterra e no País de Gales um investimento aproximado de \$100 milhões de dólares por ano no tratamento deste problema ou na mitigação dos efeitos deste processo na qualidade dos ecossistemas aquáticos (Macintosh et al., 2018).

O fósforo é considerado a maior ameaça para o ecossistema de lagos no mundo, pois é o nutriente limitante que controla o estado trófico de corpos d'água (Tu et al., 2019; Worsfold et al., 2016). Foi verificado que após a redução significativa da entrada de P em corpos hídricos a melhoria da qualidade dos corpos hídricos de água doce que sofrem com a eutrofização. Assim, tornou-se cada vez mais óbvio que o entendimento do comportamento do P é essencial para avaliação ecológica (Meinikmann et al., 2015). As relações entre os *inputs* de P, a concentração ambiente de P na coluna d'água e a resposta ecológica são complexas (Withers and Jarvie, 2008). Dependendo das condições do local (ou seja, inclinação, capacidade de retenção de sedimentos etc.), o transporte difuso de P ocorre como partículas ou P dissolvido em fluxo superficial, escoamento superficial canalizado, drenagem ou águas subterrâneas.

Comparativamente, em sistemas naturais os sistemas hídricos possuem baixa concentração de P, relacionado a baixa solubilidade e volatilidade dos compostos de P (Persson and Jansson, 1988). Os principais fluxos de P observados são entre a biota marinha e o oceano/água, entre a biota do solo e o solo, do solo para a superfície

do oceano e erosão/intemperismo das rochas. Porém com as ações antrópicas passaram a representar um aumento significante de P em ambientes aquáticos, relacionados a poluição urbana e a agricultura (Figura 1).

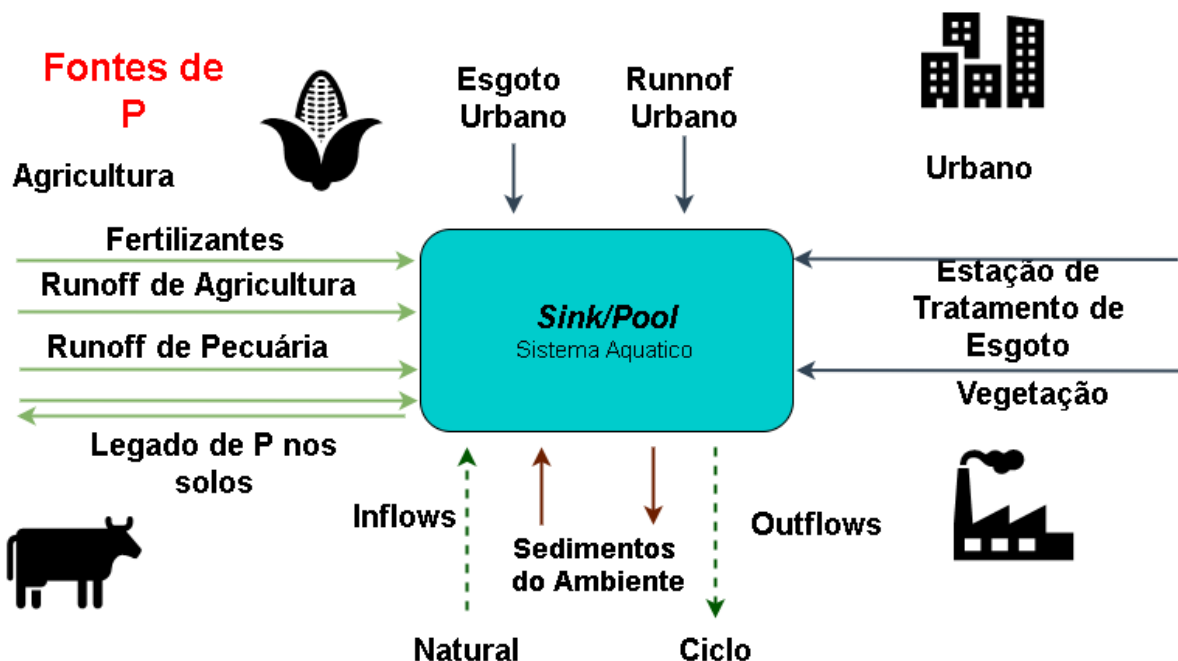


Figura 1 - Exemplos de fontes de P difuso entrando em sistemas aquáticos (sumidouros) são ilustrados (adaptado de Macintosh et al., 2018).

A fim de inibir o desenvolvimento do processo de eutrofização, muitos estudos são feitos para compreender o comportamento dos nutrientes, especialmente o P, e desacelera o problema ao redor do mundo (Dugopolski et al., 2008; Frumin and Gildeeva, 2014; Lürling and van Oosterhout, 2013; Meinikmann et al., 2015). Este é um problema global, no qual a maior parte de lagos eutrofizados se localizam na África, seguidos pela Oceania, América do Sul, América do Norte, Europa e Ásia. Por exemplo, Victoria Lake na África e Erie Lake na América do Norte (Li et al., 2021). Cada corpo hídrico possui variáveis que interferem no processo de eutrofização que precisam ser estudadas com cuidado, considerando localização, clima, solos, geologia, concentração naturais de P no ambiente, e demais parâmetros de qualidade de água.

Assim como no resto do mundo, o DF sofreu com este problema no Lago Paranoá (LP), que se iniciou a partir de 1959. Nesta época o reservatório começou a receber os esgotos domésticos da cidade, além de outras entradas difusas de fósforo e de despejos de matadouros clandestinos. Como consequências no final da década

de 70 aconteceu, o que é considerado o maior desastre ecológico do LP até hoje, um *bloom* da cianobactéria. A *Microcystis aerugionsa* encontrada principalmente no braço do Riacho Fundo (BRF), causou a primeira grande mortandade de peixes (Angelini et al., 2008; Fonseca, 2001; Starling et al., 2002). Após este incidente, medidas mitigadoras foram adotadas, como a aplicação de algicida, adição de sulfato de alumínio e a retiradas das macrofilas do LP (Fonseca, 2001) para diminuir a biomassa vegetal e implantação de tratamento de efluentes domésticos nas Estações de Tratamento de Esgoto (ETEs - WWTP) para o controle da entrada de nutrientes.

Apesar do monitoramento das águas com análises físico-químicas e microbiológicas e gestão dos efluentes realizados pela Companhia de Saneamento Ambiental do Distrito Federal (Caesb), o problema retornou com uma intensidade preocupante nos anos de 1982, 1997 e em 2012 (Dias, 2011). Pinho e Santos (2016) verificaram valores de P acima de 100mg/m<sup>3</sup>, níveis acima dos aceitáveis e possivelmente associados ao *bloom* de algas que ocorreu em 2016. Diversos trabalhos como Amorim et al., (2019), Barbosa et al., (2019); Dias., (2017); Franz et al., (2014), Philomeno (2007) e Pinho e Santos (2016) apontam que as áreas mais atingidas e possíveis reincidências por esse problema são os braços do Riacho Fundo e Bananal.

Em um contexto em que os corpos hídricos de água doce estão em foco e a busca de tratamento de contaminantes nesses sistemas, o gerenciamento de poluentes que impossibilitam o uso da água, como P, é um assunto atual (Withers, 2019; Withers and Jarvie, 2008). Em circunstâncias locais em como a da crise hídrica em 2016 - 2017, atual seca de Brasília e utilização abusiva dos mananciais de água do DF, o LP passou a ser utilizado para o abastecimento público. Desse modo, se tornou essencial melhorar, controlar e manter a qualidade de suas águas. Para fins de gestão de qualidade da água, é essencial determinar cargas e fluxos de frações de P em corpos de água, para investigar processos de ciclagem local, na restauração de ecossistemas eutróficos e gerenciar os impactos socioeconômicos no corpo d'água(Cordell et al., 2009; Withers and Jarvie, 2008; Worsfold et al., 2016).

A ETE-Sul atua com sistema de lodos ativados a nível terciário, por meio de Sistema Phoredox, que inclui a remoção biológica de nutrientes e o polimento final por meio de processo físico-químico. A remoção do fósforo ocorre por intermédio de

microrganismos que realizam a desfosfatação. Por fim, o polimento final consiste na retenção de sólidos e fósforo residuais através da floculação química (Caesb, 2019; Pinho and Santos, 2016). Os relatórios Caesb apontam valores flutuantes de P total dissolvido na saída da ETE Sul (Caesb, 2019). Porém atualmente sabe-se que a gestão do P dissolvido sem considerar aporte pelo material particulado e pelo sedimento de fundo associado as reações na coluna d'água é insuficiente. O P transportado na forma sólida (adsorvido ou na estrutura dos minerais do sedimento) pode ser liberado por mudanças nos parâmetros da água, se tornando disponível para bactérias e algas que auxiliam no processo de eutrofização (Frankowski and BolaŁek, 1999; Hosomi et al., 1982; Yu et al., 2017).

Assim, se faz necessário melhorar o conhecimento sobre a fracionamento sólida ou partição do P nos materiais transportados até o lago. Assim como, quantificar as suas frações que participam de sua dinâmica, neste ambiente, entre o compartimento sólido-líquido. Existem poucos estudos em regiões tropicais que focam nos componentes particulados do P, sua dinâmica líquido-sólido e a sua relação com períodos chuvosos e secos. É necessário compreender os processos físicos, químicos e biológicos que ocorrem durante o transporte do P em corpos hídricos, na coluna de água e na interface água-sedimento entre elas mudanças de fases de particulado ou dissolvido e orgânico ou inorgânico (Avilés et al., 2006; Bitschofsky and Nausch, 2019; Ni et al., 2015; Persson and Jansson, 1988). Cada espécie de P possui características de retenção e comportamento diferentes, portanto, apresentam contribuições distintas para o processo de eutrofização (Bao et al., 2018).

A presente pesquisa se propõe estudar o fluxo de P ao longo do braço do Riacho Fundo para aperfeiçoar a gestão deste elemento no corpo hídrico. O entendimento das origens, destino, tipos e formas do P presentes na área de estudo em escala temporal e espacial auxiliará no desenvolvimento de indicadores para melhorar gestão ambiental do LP.

## 1.2. OBJETIVOS

### 1.2.1. Objetivos Gerais

O principal objetivo desta pesquisa é compreender os fluxos ou ciclo de P no LP, principalmente na região BRF.

### 1.2.2. Objetivos Específicos

- Implementar no laboratório e aplicar metodologias para determinar o P total e diferentes frações de P em água doce, solo e sedimento;
- Determinar as principais fontes, fracionamento e destinos pontuais e não pontuais de P ao longo da BRF;
- Quantificar P em sedimentos e associar com processos de sedimentação ao do histórico do LP;
- Avaliar os impactos do P na qualidade da água da BRF;

## 1.3. MATERIAIS

### 1.3.1 – Área de Estudo

A área de estudo é o tributário do Riacho Fundo, localizada na porção sudoeste da bacia hidrográfica do Lago Paranoá, na região centro-oeste do DF. Esta região engloba a Unidade Hidrográfica do Riacho Fundo (UHRF) e o Lago Paranoá. O local de estudo é localizado no bioma Cerrado no centro do Brasil, com altitudes que variam de 1000 m a 1250 m de altura. O clima é caracterizado por duas estações bem definidas, a seca de maio a setembro e a chuvosa de outubro a abril, com a precipitação anual entre 1500 e 1750 mm e temperatura média anual de 20-21°C (WHO, 2017). A região está incluída no Planalto Central, que é caracterizado por planaltos extensos e paisagem ondulante. A geologia é marcada pela presença de crostas lateríticas e saprolitos de rochas metassedimentares, quartzitos e rochas metamórficas do grupo Paranoá-Canastra (Campos and Freitas-Silva, 1998). Os

principais solos encontrados na região são latossolo vermelho escuro, latossolo vermelho-amarelo e cambissolos (Reatto, 2004; Reatto-Braga and Correia, 2000).

O Lago Paranoá (LP) é um reservatório artificial urbano localizado na cidade de Brasília – DF, construído em 1959. É considerado um lago artificial profundo, com profundidade média de 14 m (máx. 38 m, próximo da barragem) e uma área de 37,5 km<sup>2</sup>. O reservatório tem uma capacidade máxima de armazenamento de 498 x 106 m<sup>3</sup>. Ele está inserido na Bacia do Lago Paranoá, que é constituída por cinco sub-bacias: Torto, Bananal, Riacho Fundo, Gama e Lago Paranoá. As sub-bacias localizadas ao norte são as mais preservadas devido à influência do Parque Nacional de Brasília, áreas menos densamente povoada e com vegetação preservada. As sub-bacias ao sul, no entanto, são mais urbanizadas e densamente povoadas, portanto, mais impactadas, principalmente devido às práticas de desmatamento, exploração de cascalheiras, movimentação de solo, dentre outras (ADASA, 2017).

O tempo de detenção hidráulica costumava ser aproximadamente 0,82 anos (Ferrante et al. 2001), mas devido à redução da vazão através da barragem aumentou para mais de 2 anos durante o período de estudo. Essa redução de vazão foi necessária para permitir a captação da água do lago para abastecer a população durante a grave crise hídrica registrada no período de 2016 a 2017. Além disso, o Lago Paranoá recebe efluentes de duas estações de tratamento de esgoto (ETE Norte e ETE Sul). Segundo Mar da Costa et al. (2016), as estações de tratamento operam utilizando processos semelhantes, Lodos Ativados com remoção biológica de nutrientes (N e P), seguido de tratamento adicional de flotação para melhorar a remoção de P.

A UHRF abrange as 7 regiões administrativas (RA) com população total de aproximadamente de 393,708 habitantes, representando um aumento de 27% de 2004 (CODEPLAN, 2017; IBGE, 2016) e com área de aproximadamente 200 km<sup>2</sup>. Esta região é a mais populosa do DF com uso e ocupação do solo é variado (CODEPLAN, 2017). A região apresenta colônias agrícolas, setores industriais, ocupação urbanas planejadas como o Guará, ocupação urbanas não planejadas e desordenadas como Vicente Pires e um lixão. O Ribeirão Riacho Fundo deságua diretamente no Lago Paranoá com vazão média anual de 4,04m<sup>3</sup>/s, possui uma área de drenagem de 225,48km<sup>2</sup>, sendo seu curso principal de 13km. Seus principais

afluentes são os córregos Vicente Pires, Guará e Ipê. Essa sub-bacia apresenta a maior densidade e diversidade de ocupação, compreendendo as Regiões Administrativas do Riacho Fundo, Núcleo Bandeirante, Guará, Candangolândia além de outras áreas residenciais como as Mansões Park Way e Águas Claras, o Setor de Indústria e Abastecimento e áreas de atividade agrícola (Ferrante et al., 2001; CODEPLAN, 1994).

O Braço do Riacho Fundo (BRF) é a região do LP que recebe as águas do RFS. Essa região possui histórico de eutrofização e alterações ambientais (Barbosa et al., 2019; Cunha, 2015; Dias, 2017; Mar da Costa et al., 2016b). Estudos anteriores mostram que a região possui as maiores concentrações de nutrientes e condições mais propícias para a eutrofização (Barbosa et al., 2019). Pesquisas anteriores demonstraram perda extrema de solo e altas taxas de assoreamento em BRF (2,5 cm/ano de 2007 a 2009 com maior deposição de material granulométrico na fração areia (de Aquino et al., 2018; Franz et al., 2014).

### **1.3.2 – Amostragem**

Para a realização desta pesquisa foi utilizado dados de diversos compartimentos, localizações e períodos. Desse modo parte dos dados utilizados são oriundos de outras atividades de pesquisa, trabalhos de mestrado e doutorado, pesquisas realizadas pela Universidade de Brasília (UnB), como de Dias (2017) – dados obtidos durante os anos de 2015 a 2016 - e Oliveira (2021) – dados obtidos de 2016 a 2018 - levantamento de campo dos entes envolvidos, como o Caesb, e dados primários levantados na presente pesquisa. Dados coletados de 2019 a 2021 foram realizados pelo autor.

A escolha dos pontos de amostragem considerou o uso e cobertura do solo, a fim de encontrar possíveis fontes contaminantes. Assim temos pontos próximos a área de nascentes ou com vegetação local preservada, próximo a regiões altamente urbanizadas, próximas a ETE ou possíveis contribuição para lançamentos de resíduos e efluentes, montante e jusantes de corpos hídricos. Para o estudo serão trabalhadas amostras de solos, sedimentos, perfil sedimentar, material particulado em suspensão (MPS) e água superficial, onde serão realizadas extrações totais e parciais para determinação de P total, frações de fósforo orgânico e inorgânico.

Para a coleta do perfil sedimentar foi utilizado o perfilador do tipo Core Sampler da empresa Eijkelkamp com tubo de acrílico de 2 a 5m de comprimento, os quais foram vedados, após a perfuração, para evitar o escape do material pela base durante a remoção deste do leito do lago. Ainda com o tubo no local amostrado, mediu-se a espessura da lâmina d'água para posterior cálculo da espessura da coluna de sedimentos (Oliveira, 2021). Os sedimentos de fundo foram coletados por meio do Piston-Corer da Uwitec Sampling Equipment. As amostras utilizadas foram coletadas nos anos de 2016 e 2018, nos quatro braços e no centro do LP por Dias (2017) e Oliveira (2021).

Para a coleta de água superficial foram utilizados frascos de polietileno, com capacidade de 2 litros, previamente lavados com solução ácida (HCL 10%). E após a coleta, em laboratório as amostras foram filtradas em membranas de 0,22µm de porosidade e armazenadas em tubos estéreis. A partir dos filtros é obtido o MPS, no qual foi realizado procedimentos para análise geoquímica.

#### 1.4. ESTRUTURA DA DISSERTAÇÃO

Esta dissertação está dividida em três capítulos teóricos. A organização deste trabalho de pesquisa, com a descrição do conteúdo de cada capítulo, é brevemente descrita a seguir:

Capítulo 1: Descreve uma introdução à dissertação, com breve apresentação do assunto. Esta parte enfatiza a descrição dos objetivos e a motivação encontrada para a escolha de um tema de trabalho. E também possui parte que introduz a área de estudo e os materiais utilizados nesta pesquisa. E, por fim, como está constituída a dissertação, que corresponde a esta seção.

Capítulo 2: Mostra os resultados e discussões que estão presentes na forma de artigo.

Capítulo 3: Consiste nas considerações finais e recomendações, traz os apontamentos finais dessa dissertação com indicativos de trabalhos a serem realizados futuramente.

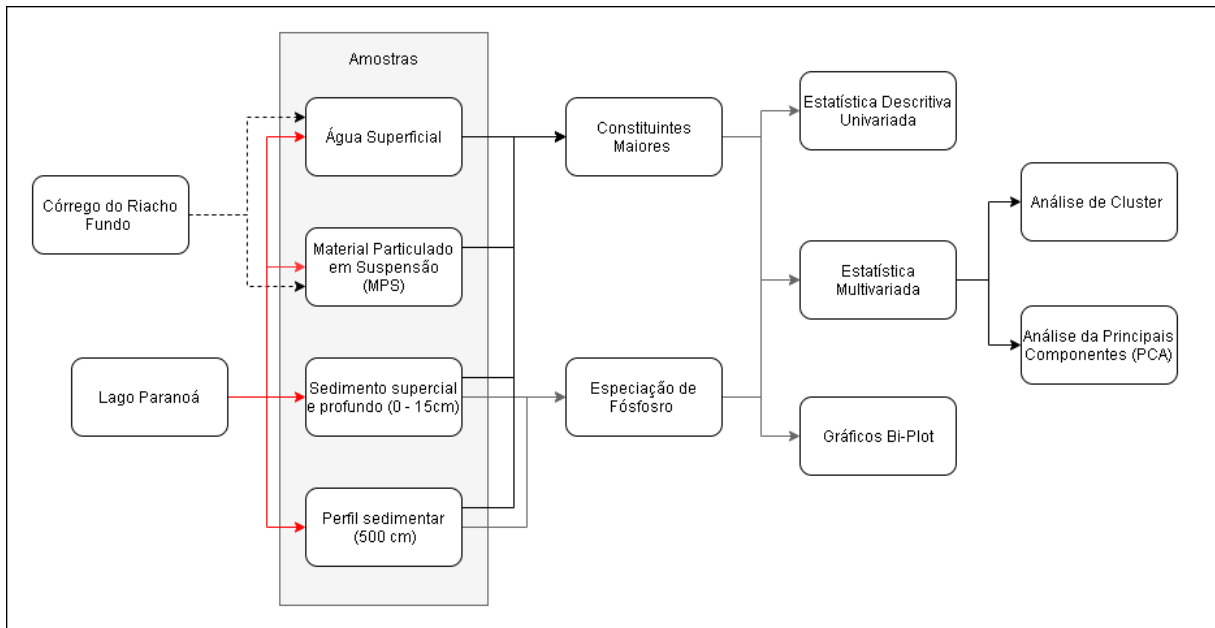


Figura 2 - Fluxograma metodológico da dissertação (Autor, 2021).

## 2. ANÁLISE DOS RESULTADOS

### THE BEHAVIOR OF PHOSPHORUS IN URBAN RESERVOIRS – SPECIES, FRACTIONS, AND CHARACTERIZATION OF PHOSPHORUS

Vitória Rodrigues Ferreira Barbosa<sup>1,2</sup>; Jeremie Garnie<sup>1,2</sup>; Rejane Ennes Cicerelli<sup>1,2</sup>; Geraldo Resende Boaventura<sup>1,2</sup>; Myller Tonha<sup>1,2</sup>; Derlayne Dias Roque<sup>1,2</sup>; Elton Oliviera<sup>1,2</sup>; Marie-Paule Bonnet<sup>2,3</sup>; Patrick Seyler<sup>2,4</sup>; Marco Ianniruberto<sup>1,2</sup>; Sergio Koide<sup>1</sup>

<sup>1</sup> Post-Graduation in Applied Geosciences and Geodynamics, Geoscience Institute, University of Brasilia. Asa Norte, 70910-900 Brasilia - DF, Brazil. +55 (61) 3107698

<sup>2</sup> Joint International Laboratory LMI OCE “Observatory of Environmental Change’, UnB/IRD, Brasilia, DF, Brazil

<sup>3</sup> French National Research Institute for Sustainable Development (IRD) – UMR Espace-DEV, University of Montpellier, France

<sup>4</sup> French National Research Institute for Sustainable Development (IRD) – UMR HSM, University of Montpellier, France

#### 2.1. ABSTRACT

Phosphorus (P) from point and non-points sources lead to P enrichment in surface waters and thus to eutrophication. To gain deeper insights into P processing and transport, the temporal and spatial changes of P along urban bodies waters samples from the Paranoá Lake (LP), and the Riacho Fundo Stream (RFS) were investigated. Surface water and Suspend Particulate Matter (SPM) samples were taken from 2015 to 2020 in LP and RFS, sediment profile, surface, and deep sediment samples in LP in 2016. Concentrations of metals, nutrients, and Total Phosphorus (TP) was analyzed for all samples, and the sediment samples were also analyzed for four P fractions: loosely bond to P, P bound to Al, Fe, and Ca. The dissolved phosphorus (DP) did not show significantly varied. The TP in SPM showed concentration varied (from 900 to 100000 mg kg<sup>-1</sup>), as well the sediments with P concentration ranged from 400 to 7000 mg kg<sup>-1</sup>. The minimum concentrations were detected at sites close to RFS

or in Torto Branch, and maximum concentrations near to WWTP-South. In sedimentary profile, TP has high concentrations in the intervals from 200 to 250 cm and from 300 to 450 cm, reflecting changes in environment. Concerning P forms, the overall abundance sequence in grab sediments was IP >> OP and Al-P > Fe-P > Ca-P > Lo-P, whereas in core sediments it showed marked differences spatial location. The relative abundance of the inorganic species (Fe-P) was controlled by the mineralogy of the sediments. While the Al-P and Ca-P distribution pointed to an increased anthropogenic input, the relative abundance of P fractions provided information on the P origin, incorporation processes, and evolution over time. This information permitted to identify the main P sources, the WWTP-South, and destination of P, the sediments.

## 2.2. INTRODUCTION

Currently, the eutrophication process is the main problem faced by most surface water bodies (Zhao et al., 2020) and has been a global environmental concern for decades (Ashley et al., 2011; Bennett et al., 2001; Karim Morsy et al., 2017). The occurrence of this phenomenon is related to excessive nutrients, such as nitrogen (N) and phosphorus (P) in water bodies, causing the growth of algae and plant life (Karim Morsy et al., 2017). According to the Organization for Economic Co-Operation and Development (OECD, 1982), the P, known to control primary productivity, is responsible for 80% of these processes.

The phosphorus input can be from punctual and non-punctual sources. Usually, inputs to the lakes come from industrial discharges, sewage, runoff from agriculture, construction sites and urban areas (Jarvie et al., 2015, 2002; Macintosh et al., 2018; Némery and Garnier, 2007; Sarvajayakesavalu et al., 2018). Phosphorus usually occurs in surface waters in particulate form (Broberg and Persson, 1988; Cooper et al., 2015; Persson and Jansson, 1988; Sandström et al., 2020). The dissolved state of phosphorus may become associated with particles as they settle out of the water column and sink to the bottom (Hupfer et al., 1995; Moura et al., 2020; Shilla et al., 2009). The relationships between P supply, P concentration in the region, the water column, the suspended particulate material (SPM), and the sediment and ecological response are complex. The P cycle includes several biotic and abiotic transformation processes, such as dynamic biotic, uptake/release, adsorption/desorption, precipitation/dissolution, and advection/diffusion in the water column and solid

particulate. These processes vary according to bio-physical-chemical conditions, like pH, redox condition, sedimentation rate, sediment grain size, chemical composition, availability of metal-oxyhydroxides phases, biodiversity, and quantity (Frankowski et al., 2002; Frankowski and BolaŁek, 1999; Pardo et al., 1999; Reitzel et al., 2013; Wan et al., 2011).

Numerous previous studies show that most P embeds themselves into different sedimentary pools. Thus, sediments play a key role that can act as a source or a sink of P. To better understand the role of P, several sequential chemical extractions (SCE) were developed to assess P solid partition in a sample, separating P pools based on the extractants and the order of their use (Macintosh et al., 2018; Persson and Jansson, 1988; Thin et al., 2020). Currently, solid partition approach considers organic and inorganic species of P. The species of inorganic P can be found in forms of loosely bound P (Lo-P), P bound to Al (Al-P), P bound to Fe (Fe-P), and P bound to Ca (Ca-P). This solid partition approach is based on the diversity of phosphorus bioavailability and release potential in different lake environments (Jiang et al., 2011). Information on the various chemical species of P in the lake is useful for understanding: if the sediments act as sink or pool of P, proper methods to reduce internal loading of P, quantify the risk of P release from deposits, and figure out rehabilitation strategies for eutrophicated water bodies.

Lakes close to urban conglomerates are normally degraded by anthropic activities (Bao et al., 2018; Bhateria and Jain, 2016; Grochowska et al., 2019). The Paranoá Lake (LP), Brasília, DF, Brazil is an urban lake with multiple uses, from humidity control to public water supply (Liporoni, 2012) and presents a historic of eutrophic processes, particularly expressive in the Riacho Fundo Branch (BRF - 4L), located in the lake's southwest area (Barbosa, 2019; Fonseca, 2001). Diverse studies are conducted in the LP, especially regarding water quality. Mar da Costa et al., (2016) verified the occurrence of organic micropollutants in Paranoá Lake waters and Wastewater Treatment Plant (WWTPs) effluents. Cunha, (2015), Mar da Costa et al., (2016); Pinho and Santos (2016) show that BRF has the worst Water Quality Index (IQC) with the variables Total phosphorus (TP), Nitrogen Series, Total solids, metals, and coliforms with major influence. Echeverria (2007) presents that anthropic impact is associated with an urbanization increase. Barbosa et al., (2019) the most recent study, analyzed the balance of nutrients P and N in the LP. The results show external

inputs of N and P to the LP, emphasizing the southern region tributaries, more specifically Riacho Fundo and the wastewater treatment plants.

Eutrophication has a recurrent history in LP, with significant occurrences in the 70s, 1982, 1997, 2012, and 2016 (Angelini et al., 2008; Laporoni, 2012; Pinho and Santos, 2016). Barbosa (2019) shows that BRF is the most affected by high concentrations of P and N; thus, the P cycle in this region should be explored. The history of eutrophication in the LP along with previous studies highlight the importance of spatially and temporally understanding the states, the different compartments, the sources, behavior, fate, and transport of the P concentration in the LP, specifically in the BRF. The present study aims to (1) determine the flux of P in LP, specifically in the BRF, (2) characterize anthropogenic sources of P and their transport along with the LP; (3) investigate P solid partition and potential bioavailability of P in sediment and consequent environmental risk; and (4) explore how the P-fraction in sediments have spatially and temporally varied in LP and in its different levels over the recent past decades.

## 2.3. METHODS

### 2.3.1. Study area

The Paranoá basin, has a total area of approximately 1034 km<sup>2</sup>, accounting for 18% of the territory of the Federal District (DF). This region is part of the Planalto Central, characterized by extensive plateaus and a rolling landscape. The geology is characterized by sedimentary deposits. The lithology composed by metasedimentary rocks of Meso- and Neoproterozoic rocks (schists, quartzites, and metamorphic silt), comprising pelitic, psammitic, and carbonate metasediments from Paranoá-Canastra-Araxá Group (Campos and Freitas-Silva, 1998). These geological units are covered by Red oxisol, (acidic, rich in iron, and alumini), which covers approximately 85% of the catchment area (Freitas et al., 1998). The Oxisols are very leached, deep, well-drained soils, without major impediments to agricultural mechanization, dystrophic, alic, with low available water retention capacity. The Cambisols, second main type of soil occurring in the watershed, are strongly drained, shallow to deep soils, brown or brownish-yellow in color, with high to low base saturation and chemical activity of the

colloidal fraction (EMBRAPA, 1978; Embrapa Solos, 2018; Sobral et al., 2015). The regional climate is characterized by two well-defined seasons: a dry season (May–September) and a rainy season (October–April), with mean annual precipitation (MAP) of 1,600–1,700 mm and mean annual temperature of 21.9°C(WMO, 2010).

Paranoá Lake (LP) is an urban reservoir located in the city of Brasília (capital of Brazil). The lake has a surface area of 38 km<sup>2</sup>, a volume of 498\*10<sup>6</sup> m<sup>3</sup>, a water residence time of 0.82 years, a medium-depth of 14 m, and a maximum depth of 40m. It is located in the urban perimeter of Brasília. There are four branches formed of different main tributaries: the creak Bananal (1L) and Torto (5L) entering from the north, and the creak Riacho Fundo (4L) and Gama (2L) entering from the south (Fonseca, 2001). It is used for power generation, recreational purposes, and provides humidity to the city during the dry months. Since the water crisis in 2017, it has been used as a source of drinking water (Barbosa et al., 2019). Due to its ecological, economic, and social importance, some works on water quality (Amorim et al., 2019; Merschel et al., 2015) fauna and flora diversity (Petrere et al., 2006; Starling et al., 2002) and geochemistry have been carried out in the lake (Barbosa, 2019; Dias, 2017, 2013; Franz et al., 2014). The Riacho Fundo Stream, with a length of approximately 13 km and a discharge of 4.5 m<sup>3</sup>/s (Adasa, 2011), is the main tributary of the Riacho Fundo Branch (BRF). It drains an area covered by various land use and cover types, including a landfill, sewage treatment plant, agriculture, preserved natural areas, and a high urban density that varied from 3.66 to 88.64 (hab.\*ha) in 2015 (CODEPLAN, 2017). The high urbanization increases the stormwater runoff rates with high suspended solids loads (Aquino, 2017; Dias, 2017, 2013). Furthermore, this region is known for suffering silting and eutrophication processes (Aquino, 2017).

LP is an artificial freshwater reservoir, which was built in 1959. In the first decades after the city foundation, untreated or poorly treated sewage was released into the lake, leading to increased nutrient concentration and eutrophication (Fonseca, 2001). In 1993, two WWTPs, Brasilia Norte (Brasilia North – WWTP North) and Brasilia Sul (Brasilia South – WWTP South), were built. Both WWTPs run similar processes encompassing activated sludge, nitrification and denitrification mechanisms, biological phosphorous removal, followed by an additional flotation treatment to upgrade phosphorous removal (ADASA, 2017; Liporoni, 2012). Since their installation and

commissioning, it is estimated that nutrient release into the Lake has decreased by 70% (Starling et al., 2002).

### 2.3.2. Design Sampling and sample preparation

The sampling design aims to assess various P compartments and characterize spatial and temporal P sources and distribution. A total of 181 samples were collected in the years 2015 and 2020 during both rainy and dry seasons. The samples include shallow waters (N= 103), suspended particle material (SPM) (N= 34), and lake surface sediments (N= 11), lake bottom sediments (N= 16), a 6.60-meter sedimentary profile (N= 12 samples) and topsoil (N= 5) (Figure 3 and Table 1). The concentration of metals measured in the topsoil was considered as naturally occurring components, once they were collected in areas without anthropic influence (Oliveira, 2021).

Table 1 - Identification, type, number and collected date of samples.

ID	Sufarce Water	SPM	Lake Sediment	Sedimentary Profile	Soils	Date
1LA	3	1	1			2018 <sup>1"</sup> ; 2016 <sup>1"</sup>
1L*	3					2018 <sup>1"</sup> ; 2016 <sup>1"</sup>
2L	2	1	1			2018 <sup>1"</sup> ; 2016 <sup>1"</sup>
3L	3	1	4			2018 <sup>1"</sup> ; 2016 <sup>1"</sup>
4LB	3	1	4	12		2018 <sup>1"</sup> ; 2016 <sup>1"</sup>
4LC	6		4			2018 <sup>1"</sup> ; 2016 <sup>1"</sup>
4LD	4		4			2018 <sup>1"</sup> ; 2016 <sup>1"</sup>
4LE	1	1	3			2018 <sup>1"</sup> ; 2016 <sup>1"</sup>
4LF	1		4			2018 <sup>1"</sup> ; 2016 <sup>1"</sup>
4S*	42	7				2020 <sup>1""</sup> ; 2019 <sup>3""</sup> ; 2017 <sup>3""</sup> ; 2016 <sup>2"</sup>
4S*	31					2020 <sup>1""</sup> ; 2019 <sup>3""</sup> ; 2017 <sup>3""</sup> ; 2016 <sup>2"</sup>
5L	3	1	1			2018 <sup>1"</sup> ; 2016 <sup>1"</sup>
CX1				2		2017 <sup>2"</sup>
OX1				2		2017 <sup>2"</sup>
OX2				1		2017 <sup>2"</sup>

Annotation: In the ID of points the first character: - Number means the region; 1: Bananal Branch; 2 Gama Branch; 3 Lake Center; 4 Riacho Fundo Branch; 5 Torto Branch. Second character: - Letter means location: L: Lake; S: Stream. Third character: - Letter means different location. \* Different coordinates of points collected. In Date the superscript numbers: <sup>1</sup> Dry Season; <sup>2</sup> Rainy Season; <sup>3</sup>Dry and Rainy Season. The ' represente the autor of colect: ' Dias, 2017; " Oliveira, 2021; " Autor, 2021.

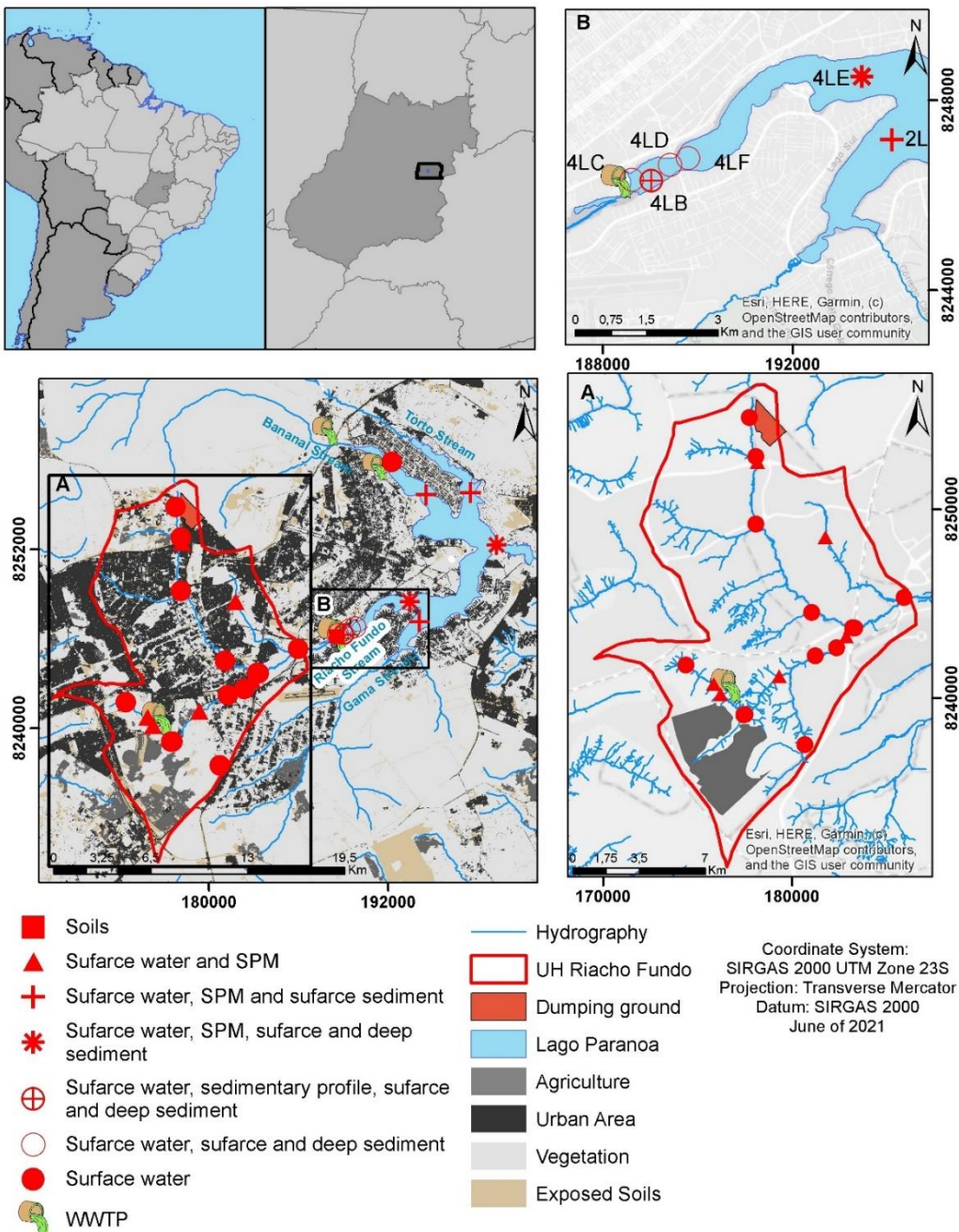


Figure 3 - Map of Paranoá Lake, including the design sampling.

Figure 3 and Table 1 show the sampling points in LP (12 points) and Riacho Fundo Stream (20 points). The sampling points at the Bananal Branch (1L) and the Torto Branch (5L) are considered the most preserved regions of LP, both in its northern part. The first point of sampling is located after the WWTP-North and receives material from urban areas (as the central part of Brasília) and natural regions (as the area of the National Park of Brasília). The second one passes through an area with agricultural activities and some urban agglomerations. In the south, Riacho Fundo Branch (BRF)

(4L) is considered the most polluted region (Salles and Bredeweg, 2009) and receives mostly urban material, while Gama Branch (2L) passes through a mix of preserved, agricultural, and residential areas (Moura, 2008; Moura et al., 2010).

Five sampling points were located in the Riacho Fundo Branch: one of them close, downstream, to the discharge of effluents from WWTP South (4LC) and the second one close to the Riacho Fundo Stream (4LB). The other points, 4LD and 4LF and 4LE, were sampled to understand the dynamics and mobility of the element, after two expected P inputs (Riacho Fundo Creek and WWTP-South). Soils were collected in an area without anthropic influence (the cerrado field) (Ox1 (x: -15.684°; y: -47.855°); Ox2 (x:-15.603°; y: -47.641°); and Cx (x:-15.547°; y: -47.834).

The surface sediments were collected using a Piston-Corer by Uwitec Sampling Equipment, with polyethylene tubes (50 cm long by 9 cm in diameter). The surface sediments, with depths varying from 0 to 30 cm, were sliced. The topsoil (0-20 cm depth) was collected using a plastic shovel. All samples were preserved in ice-packed boxes and taken to preparation in the laboratory. The sediments and soils were air-dried, homogenized, and crushed in agate hand grail and pistil.

Surface water was collected and stored in 1 L precleaned low-density polyethylene (LDPE) bottles and preserved in ice-packed boxes for further filtration in the laboratory. In the laboratory, the water samples were filtered using mixed cellulose ester (MCE) membrane filters (Millipore), previously acid-cleaned HNO<sub>3</sub> 5% V/V, dried at 60°C and weighted 0.2 µm (Baird et al., 2017). After filtration until filter saturation, the membrane was collected, dried to 60 °C and weighed in the laboratory to calculate the SPM mass.

### **2.3.3. Analytical methods**

#### *2.3.3.1. Water analytical methods*

The water physicochemical parameters, as temperature, pH, and electric conductivity, were measured with portable multiparameter equipment by the WTW brand and multi-model 350I, in the field.

Four aliquots of the filtered water were separated. The two first ones were not acidified and were separated for alkalinity analysis by the automatic titration method

with H<sub>2</sub>SO<sub>4</sub>, 0.02M in the Scott Tritoline Easy equipment in the laboratory and for dissolved anions analysis - (F<sup>-</sup>, Cl<sup>-</sup>, PO<sub>4</sub><sup>3-</sup>, SO<sub>4</sub><sup>2-</sup>, NO<sub>3</sub><sup>-</sup>) by ion chromatography with conductivity suppressed in the Dionex equipment, model ICS90, from the Geochemistry Laboratory of UnB. The two others were acidified by distilled HNO<sub>3</sub> and used for the determination of major elements by inductively coupled plasma optical emission spectrometry (ICP-OES - Agilent equipment, from the Geochemistry Laboratory of UnB) and trace elements by ICP-MS (Inductively Coupled Plasma - Mass Spectrometry - Thermo Scientific®, iCAP Q, USA, at Hydro Sciences Montpellier Laboratory, France). The Detection Limited (LD) was calculated based on the signal-to-noise approach of at least five blank determinations, resulting in LD for 0.015 µg L<sup>-1</sup> for the ICP-MS in analyses of water samples and 0.07 µg g<sup>-1</sup> for the analyses of solid samples.

#### *2.3.3.2. Sediments analytical methods*

The solid samples (sediments, soil, and SPM) were weighed in Savillex® PFA vials and digested in two independent replicates on a hot plate using a multiple-step double-distilled acid. The procedure with HF, HNO<sub>3</sub>, H<sub>2</sub>O<sub>2</sub>, and HCl (Merck) determines major, minor, trace, and rare elements. The final solid was redissolved with 10 mL of HCl 2 mol/L and centrifuged for further analysis. The partition of metals associated with acid soluble (F1), reducible (F2), oxidizable (F3), and residual (F4) solid phases was also analyzed according to the extraction protocol of the European Community Bureau of Reference (BCR) (Rauret et al., 1999). The concentrations of elements were determined by ICP- OES and ICP-MS using the same procedure used for filtered water samples. Total carbon and nitrogen of sediments and soil were analyzed by using a TOC-LCPN analyzer (Shimadzu Corp., SSM-5000, Japan).

#### *2.3.3.3. Sequential P extraction and total P*

Total phosphorus (TP) in the sediment was analyzed using two types of procedure: (1) determination by igniting the sediment at 550 ± 10°C in a muffle furnace followed by shaking the sample with 1N H<sub>2</sub>SO<sub>4</sub> for 16hr according to Wildung and

Schmidt (1973) and (2) total digestion of the sediment with a double-step distilled acid procedure with HF, HNO<sub>3</sub>, H<sub>2</sub>O<sub>2</sub> and HCl.

Organic P was determined by a procedure starting with an extraction using 1 mol/L HCl to remove inorganic phosphorus. Then, the residue was placed in a porcelain crucible and calcinated in a furnace for 1 h at 450 °C. After that, the residue was extracted again with 1 mol/L HCl to remove the phosphorus associated with the organic matter of the sediment (Pardo et al., 1999; Williams et al., 1976). Only some samples were chosen for this analysis, considering the content of P, location, and depth. The chosen samples were soils, superficial, and bottom sediment from 4LC, 3L, 4LB, and 4LE.

The P extractions in sediments and soils were performed in two independent replicates using suitable chemical reagents purchased from Sigma Aldrich (Canada). The four different phases of P in sediment were on 1.0 g dry weight and 50 mL extractants at room temperature using an orbital shaker. The sequential P extraction method used in the present study determines P distribution in loosely bound (Lo-P), aluminum bound (Al-P), iron-bound (Fe-P), and calcium bound (Ca-P) phosphorus (Aydin et al., 2010, 2009a, 2009b; Frankowski et al., 2002; Frankowski and BolaŁek, 1999). The extractant solutions were all prepared using high-purity water (> 18.2 mΩ, Milli-Q System®), with respectively 1.0M ammonium chloride (NH<sub>4</sub>Cl), 1.0M ammonium fluoride (NH<sub>4</sub>F), 0.1M sodium hydroxide (NaOH) and 1.0M H<sub>2</sub>SO<sub>4</sub>. The extraction time depended on the extractants (varying from 1 to 18 hrs), and all rinse steps were held in 15 min. After each extraction and rinsing step, the supernatant was separated by centrifugation at 4000 rpm for 15 min at room temperature. The phosphorus concentrations were determined by ICP-OES (5100, Agilent, USA). The total inorganic phosphorus (TIP) was reported as the sum of different inorganic phosphorus fractions, Lo-P, Al-P, Fe-P, and Ca-P.

### 2.3.4. Quality and Control

For analytical quality assurance of TP determined in sediments, certified reference materials were used: NIST (San Joaquin Soil SRM 2709a and Estuarine sediment 1646a), and for water, the analysis used NRC (SLRS-5) and Mississippi-03 (CRM Environment Canada). The difference between the analytical result found in the

present study and the reference material was less than 5 %, thus the result was assumed consistent. The sum of each phosphorus species was compared with the TP in the sediment sample to verify the accuracy due to the lack of suitable standard reference material. The results of the sum ranged from 93.6 to 99.6%. The relative standard deviations (RSD) of the replicates in elements and SEP analysis was around  $\pm 10\%$ . For each set of analyses, blanks were also used for background correction. Re-analysis of 15% of the samples to control the analytical quality resulted in relative standard deviations of less than 5%.

For the determination of TP, different methodologies were used. The test was performed with reference material, the certificate reference international material NIST (Estuarine sediment 1646a). The detection limit for phosphorus was above 0.150 mg/L, and 0.0010 mg/L for the ICP-OES and ICP-MS analyzes. The accuracy of the standard samples for (1) and (2) methods was on average  $\pm 5\%$  of the certified values, and the standard deviations of the triplicates ranged from 95% to 110%.

### 2.3.5. Statistical analysis

The data of P speciation, the other elements and physicochemical parameters were assessed by the Kolmogorov–Smirnov test. Student's t-test for variables with normal distribution and the Mann–Whitney test for variables with non-normal distribution were used for mean comparisons between the field and literature results. Pearson correlation analysis was employed with a two-tailed test of significance to study the relationship between the measured parameters.

The principal component analysis (PCA) is a multivariable analytical tool that allows data reduction, assisting in the characterization of a system using the means for a small number of new variables (Loska and Wiechula, 2003). The analysis of the varimax rotation of standardized component loadings was conducted to investigate the main factors controlling the P species, determine the similarities and differences in the chemical composition of the samples, as well as define their environments, and identify possible different sources of P (Bernardi et al., 2012; Jiang et al., 2011; Lyra et al., 2010; Thin et al., 2020). In this study was made total of 5 PCA. The dissolved elements PCA involved 18 water parameters and 30 points from Paranoá Lake and 73 points from Riacho Fundo Stream, the SPM PCA used 5 points from LP and 27 points from

RFS, the third PCA combined the anterior analysis. The sediment PCA used data from LP (26 points), Soils (5 points) and the sedimentary profile (12 points). Statistical analysis was carried out in the Statistica software version 10.0.

## 2.4. RESULTS AND DISCUSSIONS

### 2.4.1. Main properties

The dissolved substances were mainly composed of  $\text{SO}_4$ , Ca, Na, Cl,  $\text{NO}_3$ , K, Si, and Mg. All the concentrations were below the dissolved concentrations recommended by World Health Organization (WHO) (WHO, 2017), Environmental Protection Agency - USA (EPA or USEPA)(USEPA, 2000), and established by Brazilian Governance guidelines by the resolution nº 357/05, (CONAMA, 2005), aimed at water quality.

The Figure 4-A and 4-B represents the PCA of the dissolved. The total percentages of variance were 46%. The PCA variables (Figure 4-A) Na, K, Gd,  $\text{SO}_4$ , Cl, and Si were strongly negatively correlated with PC1 (31.25%) and PC2 (14.67%). These elements are characteristic of domestic sewage, especially the Gd, Cl, and  $\text{SO}_4$ , that act as tracers for this type of origin (Atinkpahoun et al., 2018; Louis et al., 2020). In this same quadrant, the Mn, P, and  $\text{NO}_3$  are weakly related to this group, which means that these elements have not significantly participated in the dissolved phase (Berbel et al., 2015; Mar da Costa et al., 2016b; Yu et al., 2021) It is important to observe in Figure 4-B, the PCA with the distribution of samples with the same configuration, which are from the points that correspond to sewage influence.

Figure 4-A also presents the second group of elements, composed mainly of Sr, Ca, Cu, and Mg predominantly. This assemblage is related to urban regions, especially with urban construction material. Figure 4-B shows that points with a similar configuration – strongly correlated with PC2 and negatively with PC1 – are from intensely urbanized areas. The opposite is the characterization is the water springs. In this case, an increase in urbanization from below-right to above-left is observed (da Silva et al., 2013).

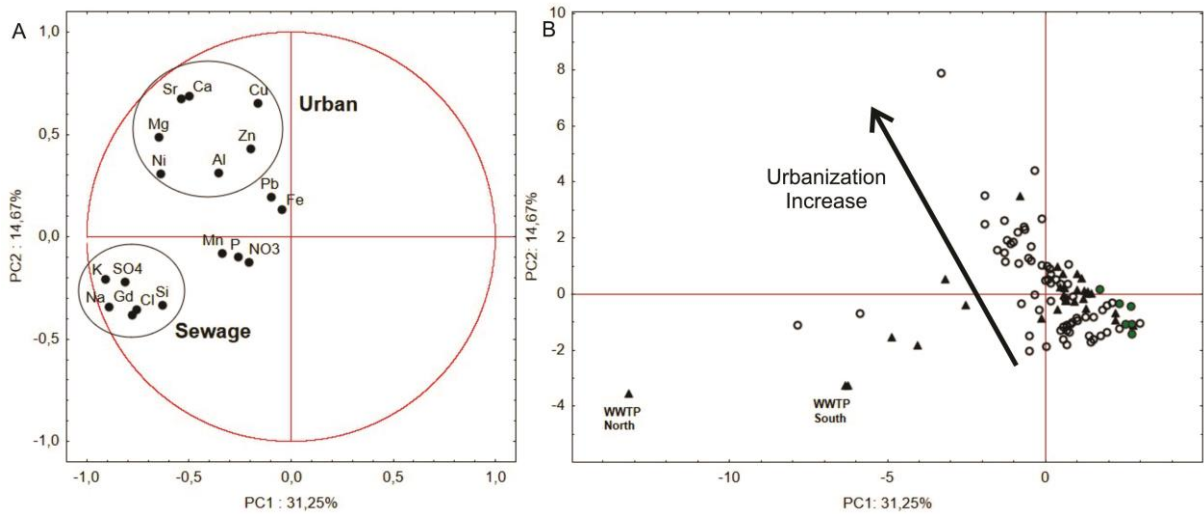


Figure 4 - Principal Component Analysis (PCA) of dissolved (4A and 4B),

In this way, the water quality in the stream can be separated into two groups, one close to the headwater and the other close to urban areas. The concentrations of Na, P, K, Ca, Ni, Gd, Cl, and SO<sub>4</sub> were higher in points near WWPT and in urban regions than in preserved areas like water springs in the RF In the LP, higher concentrations were observed close to WWTP, mainly related to the elements Al, Zn, and Gd. According to Berbel (2008), Bhateria and Jain (2016) and Pedreira et al., (2018) these elements in high concentration is used to trace sewage.

In relation to SPM, the higher value average of concentrations of elements follows the order Al >>> Fe >>> Ca >>> P >> Na > Mg > K. Spatially, the variation of elements did not follow a unique pattern. However, temporally, it was observed a tendency related to seasons, as Aquino (2017) and Franz et al., (2014) observed. In the point 4LC, a high concentration of P, Cu, Zn, and Gd was observed, which can be related to anthropic activities, as Maia (2003) already identified.

The PCA exploratory approach for the SPM is the Figure 5-A and 5-B. The SPM variables correlate with first factor (PC1) representing 49.12% of the total variance, and the second factor (PC2) accounts for 22.2% of the total variance. The grouping of elements (5-A) can be related to different sources. The assemblage of Pb, Al, Gd, Th, K, and  $\Sigma$ REE (Sum of Rare Earth Elements) indicates natural origin (with negative PC1 and positive PC2). The negative PC1 and PC2 can be related to anthropic sources, differentiated from sewage, with the set of Cu, Zn, and Fe, and some urban factors, with the set of P, Mg, Sr, Na, and Ca, mainly associated with carbonates. The Figure 5-B shows the PCA of cases, and it is possible to distinguish the WWTP from others

points. In relation to the other points, as shown in Figure 5-B, it is not possible to define with clarity the different sources or land use and cover, once those similar points have different configurations.

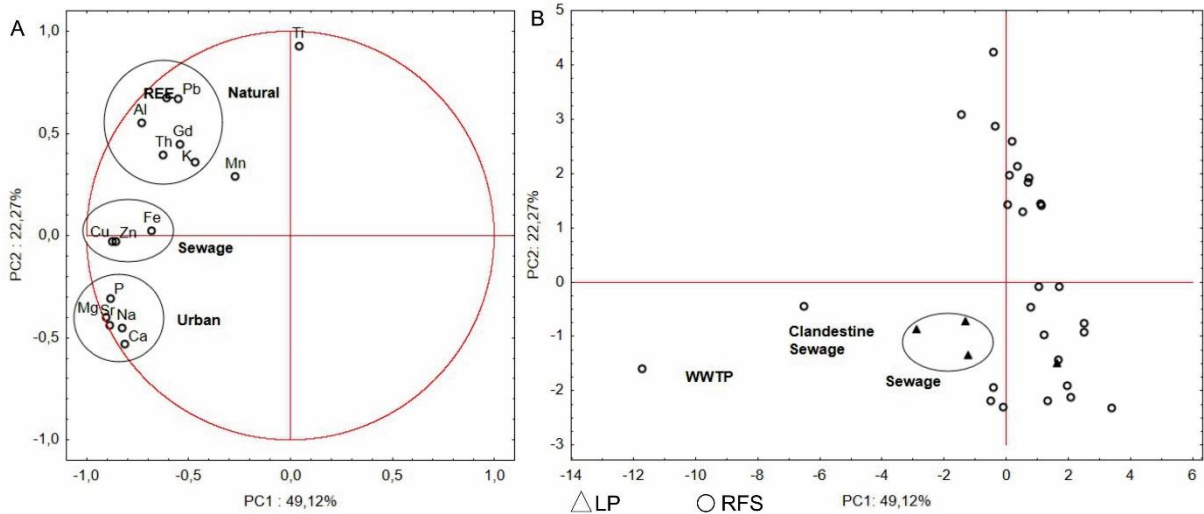


Figure 5 - Principal Component Analysis (PCA) of SPM(5A and 5B).

Figure 6 represents the concentration of main elements (Al, Fe, Mn, Ca, Mg, Zn, and P) for points from BRF, lake center point (3L) of sediments, and soil samples to compare chemical composition in natural and anthropized areas. The average concentrations of the elements in the sediments and soil followed this order: Al >> Fe >> K >> Ti >> Ca >> S >> Mg >> P >> Na. In all samples, Al and Fe concentrations were homogeneous. Their origin is related to laterites and Fe-Al rich soil (Red oxisol). Since the local geology and pedology are abundant in Al and Fe, the high concentration of these elements is normal (Echeverria, 2007; Maia, 2003; Moura et al., 2010).

The biggest difference observed was in 4LC, comparing the lake points and soils, mainly for Ca, Mg, Zn, and P (red points). Also, a trend of concentration increase of Mg and Mn was observed towards the center of the LP, as it, is indicated by the arrows in Figure 6. This can be an indication of decrease of anthropic influence.

Figure 7 presents the concentrations of SiO<sub>2</sub>, Th, Al, Fe, Mn, Ca, Mg, Zn P, LOI (Loss On Ignition), C, and N in sediment profile (from the exit point of the BRF – Point 4LB). Figure 7 compares the concentrations of these substances in sediment collected at different intervals and shows temporal changes. Above 450 cm, low concentrations of P, Zn and Mn may be related to the unaltered environment. Above, diverse variations were observed from 300 to 450 cm, mainly from Ca, Mg, P, LOI, C, and N. The interval

from 200 to 250 cm contains significant variations for Al, Mn, and P. These two intervals might represent drastic changes in the deposition environment, and may be related to the start of urbanization, eutrophication events, start of WWTP and efficiency of P removal treatment.

Figures 6 and 7 show the elements concentrations in the soil samples (Ox1; Ox2; and Cx). As expected, the Cambisols was rich in Fe, Mn, Ca, Zn and Mg and the Oxisols was richer in Al and Th.

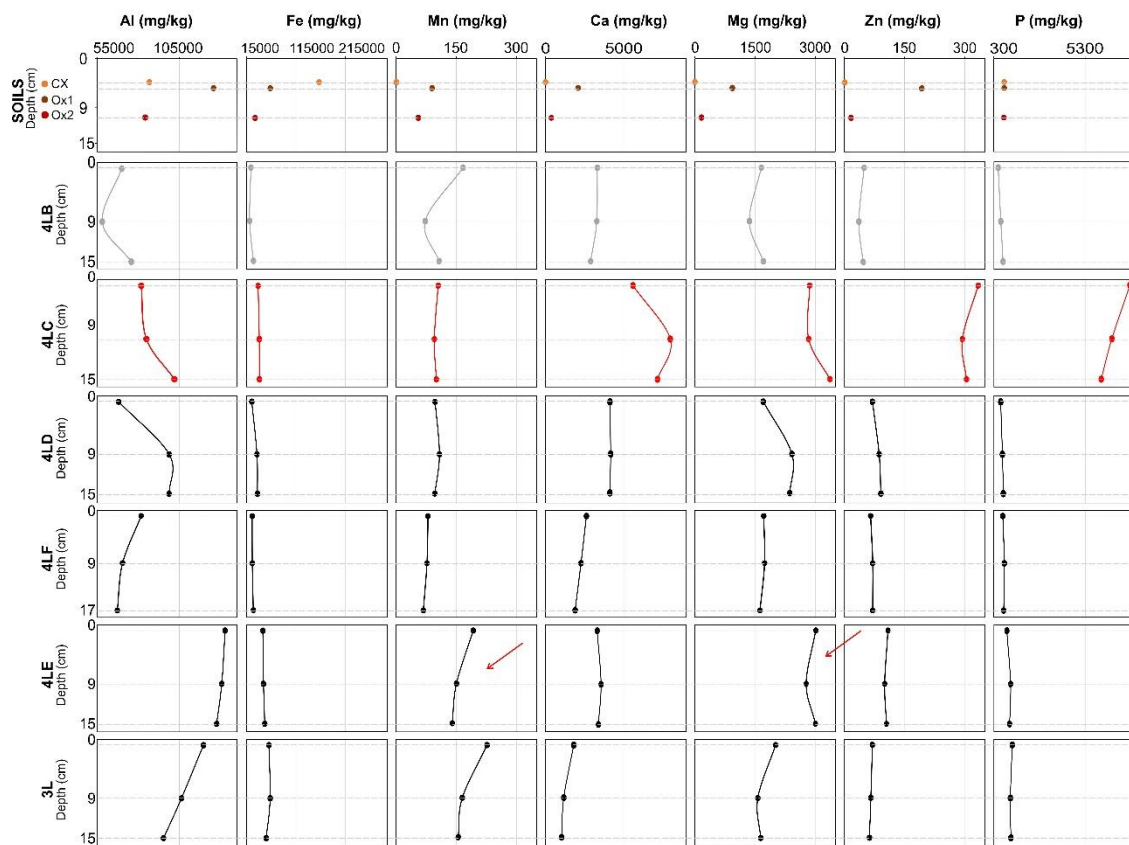


Figure 6 - Vertical distribution of phosphorus and other elements in sediment cores from BRF.

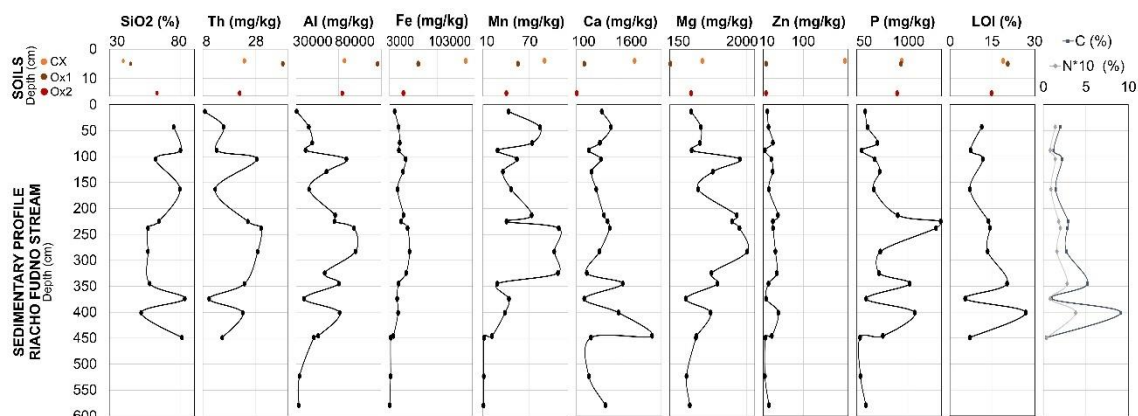


Figure 7 - Vertical profiles of phosphorus and others elements from the mouth of the RFS (4LB).

The TP in soils varied from 790 to 910 mg kg<sup>-1</sup>, that is in agreement with the local geology. According to Pavinato et al., (2020) in this region, the concentration of native P is from approximately < 200 mg kg<sup>-1</sup> to 800 mg kg<sup>-1</sup>. Cerrado soils are naturally low in phosphorus and have a low cation exchange capacity, very low available P contents and high capacity of P adsorption.

In Figure 8, the PCA for all soils and sediments was performed (lake sediments (0-15 cm), profile sediment and soils) to evaluate the TP and metals aiming to understand the relations. The sediments PCA accounted for 76.4% of the total variance for two principal axes. The PC1 axis accounted for 47.91% and PC2 axis accounted for 28.53%. The group A is characterized by presence of Mn, Al, Ti, Fe, Mn and V, with strongly negative PC1 and positive PC2. The anthropic group is characterized for strongly negative PC2. The presence of P, Zn, Ca and Mg is associated with strongly negative PC1. In Figure 8-B, the WWTP (in red) and BRF points (black points) were separated from others points. This can be related to larger concentration of P in these points than other points. The behavior of other elements is similar in this region, as Zn. For this peculiarity, the BRF must be considered separately.

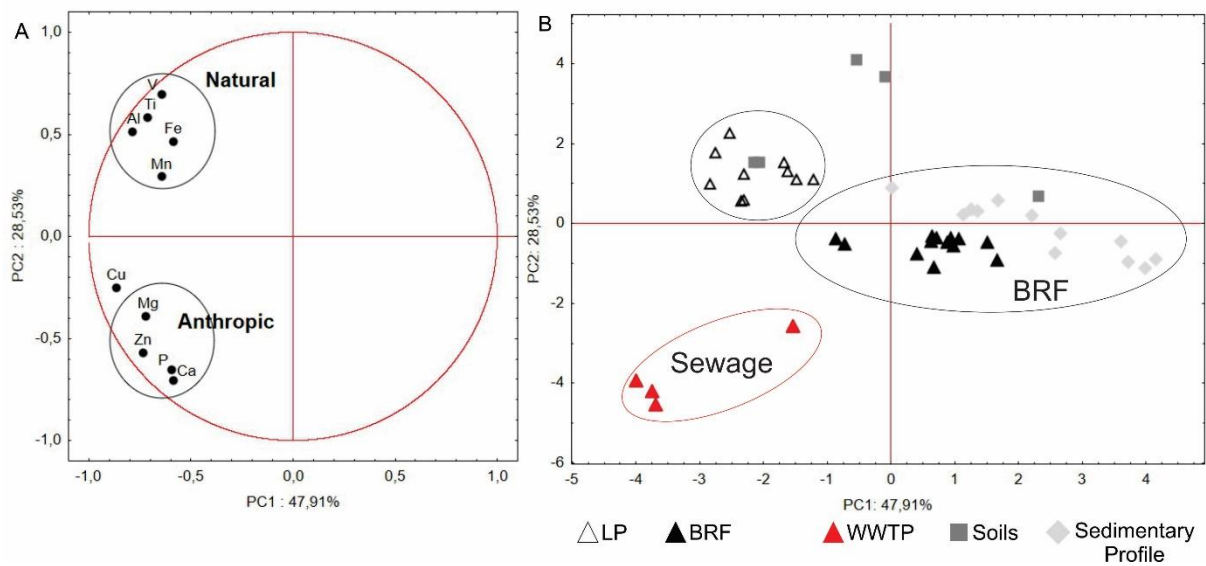


Figure 8 - Principal Component Analysis (PCA) of Sediments (8A and 8B).

In Figures 4-B, 5-B and 8-B, the points from WWTP are in the same quadrant; however, it is possible to see a distance between them WWTP South and WWTP North. The WWTP-North is more distant from other points and the WWTP-South is closer to the BRF points, showing the possible relation between them. The LP has two

WWTPs, the south and the north, with similar treatment of biological nutrient removal and final refinement. However, the differences are observed in the projected flow, efluent current flow, and service area (Caesb, 2019). The WWTP-South was built to support 1,500 L/s flows and operates with 1,319 L/s for the 17,330 ha of area. However, the WWTP-North can support 920 L/s flows and acts with 450 L/s, attending 9,139 ha of area. The difference between the WWTP projection and demand is visible, considering that the south region is the most urbanized. The dissolved P concentration of these points is around  $20 \text{ mg L}^{-1}$  and does not show significant difference. However, in the SPM and sediment, the region of WWTP-South had at least 4 times more P in these compartments than WWTP-North.

#### **2.4.2. Distribution of Total Phosphorus (TP) in the Paranoá Lake**

Figure 9 shows the medium distribution of P in surface waters (Figure 9-A); SPM (Figure 9-B); and sediment (Figure 9-C).

The concentration of P in surface water (Figure 9-A) showed the range of below detection limit (LD) -  $20 \mu\text{g L}^{-1}$ , with the maximum value in 4LC (single red point in Figure 9-A), although the other points did not exceed  $10 \mu\text{g L}^{-1}$ . The dissolved phosphorus (DP) in surface waters can be found in different forms, such as inorganic orthophosphates, condensed or polyphosphates, organic phosphates (Worsfold et al., 2016). The inorganic phosphorus or orthophosphates ( $\text{PO}_4^{3-}$ ;  $\text{HPO}_4^{2-}$ ;  $\text{H}_2\text{PO}_4^-$ ; and  $\text{H}_3\text{PO}_4$ ) are the main directly available form of P (bioavailable) for planktonic algae and bacteria. The species of phosphates can change according to pH (Boström et al., 1988; Nunes, 2010; Worsfold et al., 2016). In the LP, the range of pH was from 6.68 to 7.5, and consequently P under predominant forms  $\text{H}_2\text{PO}_4$  and  $\text{HPO}_4^2$  (Barbosa, 2019). However, the main form of orthophosphate in natural waters is  $\text{PO}_4^{3-}$  (Spivakov et al., 1999). In previous studies as Barbosa (2019), higher concentrations of orthophosphate ( $\text{PO}_4^{3-}$ ) were observed during the rainy season in the points 1L (North), 2L tributary (South), and close to the dam. However, during the dry season, the highest concentrations were relative to the WWTP.

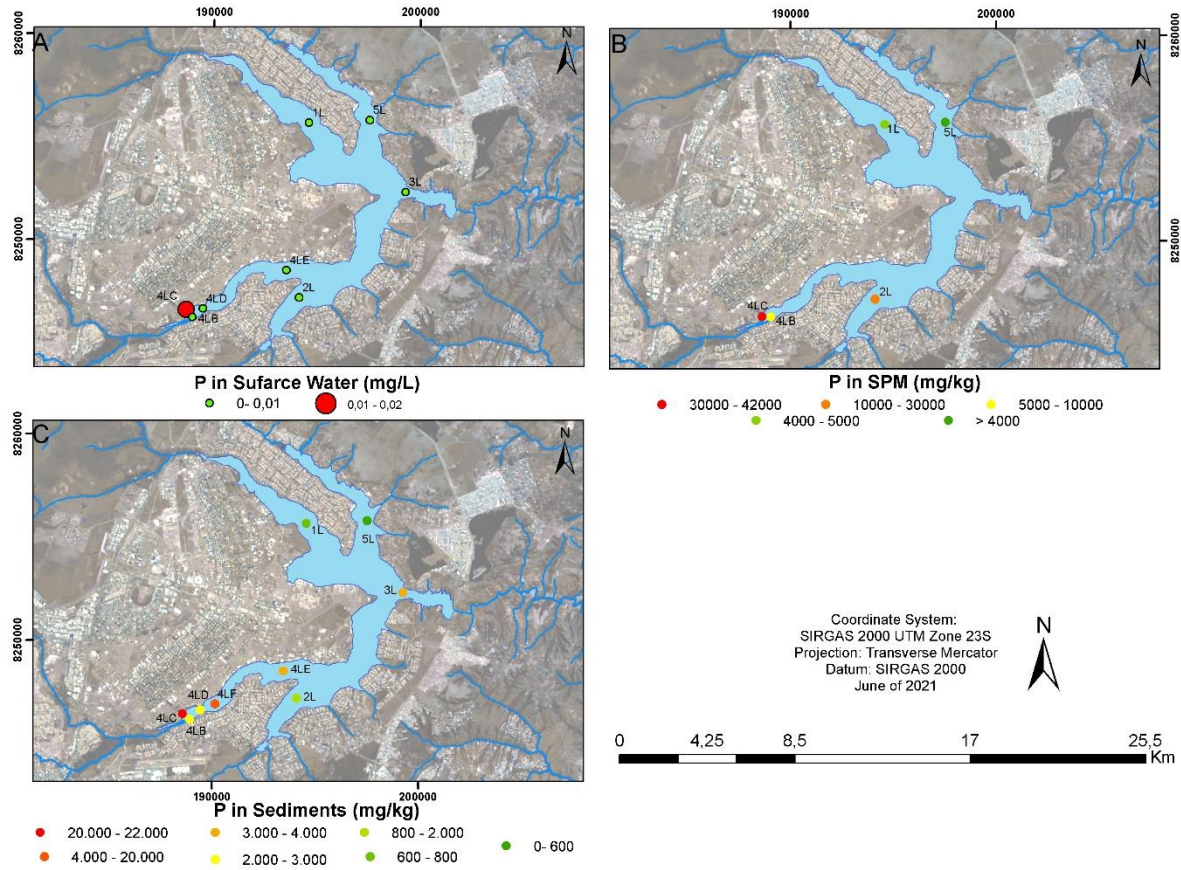


Figure 9 - The concentration of P in shallow waters (Figure 9 - A); SPM (Figure 9 - B); and sediment (Figure 9 – C).

Analysis of dissolved phosphorus data ( $\text{PO}_4^{3-}$  and POT) carried out by the Company of Sanitation of the Federal District (Caesb) in the LP detected the organic species of P (POT) in water with higher concentrations than inorganic P (Barbosa, 2019; Barbosa et al., 2019; Caesb, 2019). In other words, the main component in dissolved phosphorus is organic, which originates from excretion, decomposition, death, or autolysis of biomolecules (Macintosh et al., 2018).

This study showed higher concentrations of TP in point 4LC, followed by the points 1LC and 1LB (located near to the WWTP) with a range from 23 to 8  $\mu\text{g L}^{-1}$ . The other points (3L, 5L, and 2L) showed lower concentrations, ranging from 7 to 8  $\mu\text{g L}^{-1}$ . In the affluent from Riacho Fundo Branch, RFS, the variation was from 4 to 200  $\text{mg L}^{-1}$ . Low concentration of P was observed in the water in the RFS and in the LP, despite the presence of punctual sources anthropic of P, which did not present significant contribution significantly contribute to the aquatic ecosystem.

The concentration of P in SPM (Figure 9-B) varied between 900 and 100,000 mg kg<sup>-1</sup>. The largest concentration in LP was observed in 4LC, above 40,000 mg kg<sup>-1</sup>, followed by 2L and 4LB. The lowest concentration was found in the north region of LP (above 3,000 mg kg<sup>-1</sup> and 9,000 mg kg<sup>-1</sup> in the points 5L and 1L, respectively). In the Riacho Fundo Stream, the concentration ranged from 900 to 100,000 mg kg<sup>-1</sup>. In the SPM, the particulate P can be composed of many minerals from erosion, amorphous precipitates and sorbed reaction products (Holtan et al., 1988).

Phosphorus-containing particles can be originated by (1) Biologically produced cells of plants, bacteria, and animals; (2) Weathering products; and (3) Direct precipitation of inorganic phosphorus or sorption to others. According to the concentrations of P found in soils and in the SPM the hypothesis (2) is not applicable. Unfortunately, in order to determine the origin of options 1 or 3, it is necessary to apply different techniques that were not used in this work. Worldwide, the proportion of organic and inorganic particulate phosphorus varies. For example, in Green Bay (USA), Chao, and Tai Lake (China), the organic portion is predominant. However, in river waters, the inorganic part is dominant (Feng et al., 2020; Yang et al., 2021).

The P has the tendency to be retained by sediments, through a series of physical, chemical, and biological processes that allow the temporary or permanent phosphorus storage in the solid phase (Holtan et al., 1988). The log Kd (Distribution Coefficient) reflects the relative affinity of solid phase and water phase for P. The log Kd ranged from 4.50 to 7.52, without high variation. It was observed that the higher the log Kd value, the better the solid phase's ability to adsorb and retain P. The points from the BRF showed that the concentration of suspending material (CSM) was three times bigger than other points, which indicates that this region suffers from silting process (Dias, 2013).

Figure 9 – C shows the concentration of P in sediments from 1 to 15 cm of depth in the Paranoá Lake. The P in lake sediment ranged from above 400 -7,000 mg kg<sup>-1</sup>. The highest concentration was found in 4LC (4,000 to 7,000 mg kg<sup>-1</sup>), where they were four times superior to most of the others points. An exception to this point, the high concentration was in point 3L with 1,300 mg kg<sup>-1</sup>. The lowest concentration was found in 4LB and 5L, with a concentration of P above 400 mg kg<sup>-1</sup> and above 500 mg kg<sup>-1</sup>,

respectively. Barbosa (2019) observed TP ranges from 40 to 556 mg kg<sup>-1</sup>, with an average of 220 mg kg<sup>-1</sup>, in sediments in LP.

The surface sediments of the BRF and the LP had the highest concentration of P. The differential of these portions of sediment interacts directly with the water column. Thus, the P is mobile and easily released to the overlying water column (Mao et al., 2021; Tang et al., 2010).

In China, the USA, and Canada, the concentration of P in the order above 500 mg kg<sup>-1</sup> in the sediments represents an increased P release risk, according to the environmental dredging common standard (Barik et al., 2019; Xiang and Zhou, 2011). In Brazil, the concentration is 2000 mg kg<sup>-1</sup> according the CONAMA n° 454. The CETESB (Companhia Ambiental do Estado de São Paulo – São Paulo Environmental Company) developed the Sediment Quality Criterion, where evaluate P concentration and considering the concentration of P between 750 to 1,500 mg/kg, as it can be considered regular, and they are having an impact on the water body. And concentration above 1,500 mg/kg, considered to have a high impact and are classified like poor. According to the concentrations observed in the superficial sediment of the LP, most points in the LP present risk, except for the 4LB point in the rainy season. However, it is necessary to evaluate these reference values once the tropical climate influences the conditions for the liberation of P to water.

The region of BRF has some different factors from the LP. In this case, each point must be analyzed with attention. The point 4LB receives the material of an urban river with a flow rate of 5 L/s. The water body runs through an urban perimeter with a sanitary system of sewerage and a minor WWTP (that does not have procedures for P treatment). Still, there is release of clandestine sludge, considerable urban runoff, and does not cross agricultural areas. Nevertheless, the sediments of this region show major participation in sand granulometry. They are rich in SiO<sub>2</sub>, Al<sub>2</sub>O<sub>3</sub>, and Fe<sub>2</sub>O<sub>3</sub>, with a good correlation with Ca<sup>2+</sup>, Mg<sup>2+</sup>, Sr<sup>2+</sup>, and Ba<sup>2+</sup> (Dias, 2017). This demonstrated association with carbonates with anthropic origin (construction civil). From data analysis, it was evident that from all the tributaries of LP, the Riacho Fundo Stream has the lowest contribution of P to the LP. The concentration of P can be originated from some dissolved material that transforms to solid or material related to construction, once that showed a strong correlation ( $r > 0.75$ ) with Ca, Mn, and Sr.

The 4LC is the point downstream near to WWTP-South. This region is the biggest contributor in terms of nutrients and organic matter for LP. These sediments are silt/clay in granulometry with high P, Ca, Cu, Zn, and Mg concentrations. These assemblies are strongly associated with sewage (Atinkpahoun et al., 2018; Berbel et al., 2015). The liquid effluent released by WWTP, with the flow rate of 1,125 L/s, is within limits established by federal law. However, the particulate content is not defined by the legislation. Comparing the high concentration of some elements with anthropic characteristics in the SPM and previous studies (Bitschofsky and Nausch, 2019; Rönspieß et al., 2020), it can be concluded that WWTP can contribute with these elements under the particulate form. This input in particulate form of P has been related to a lack of control.

The 4LD had a concentration of P ranging from 500 - 800 mg kg<sup>-1</sup>. This point is the "region of the mix," where Riacho Fundo Stream's water and the WWTP are mixed. For this reason, the concentration is slightly inferior to the subsequent points.

This study verified that the South region of the LP, especially the BRF region, is the main receiver and accumulator of P, as proven by Barbosa (2019). Thus, the WWTP-South is the main source of P, and the Riacho Fundo Stream is the second major source. The main form of the P is in sediment in particular form (SPM) as a major pollutant. The dissolved P has not significantly participated in the system, once P is strongly sorbed on particulate matter and bacteria probably consumes rapidly the release. The origin and end of P are in the sediment form, possibly transported in the particulate form associated with some oxides and led bed in proximity.

The analysis of P in LP suggests that the P is mainly originate from an alocitone source and from the BRF watershed. In water analysis, SPM, sediment, and bibliographic reference (Broberg and Persson, 1988; Cooper et al., 2015; Yin et al., 2017), it was observed that most of the phosphorus that enters aquatic systems is in particulate form, which eventually reaches the Lake (Fox et al., 2016; Jiang et al., 2011; Owens and Walling, 2002). The water flow in this region is mild; thus, it facilitates the dispersion of P and sustainable long-term storage of phosphorus in sediments. As a result, it is visible that the WWTP-South had some influence in the Lake, and this is near its perimeter.

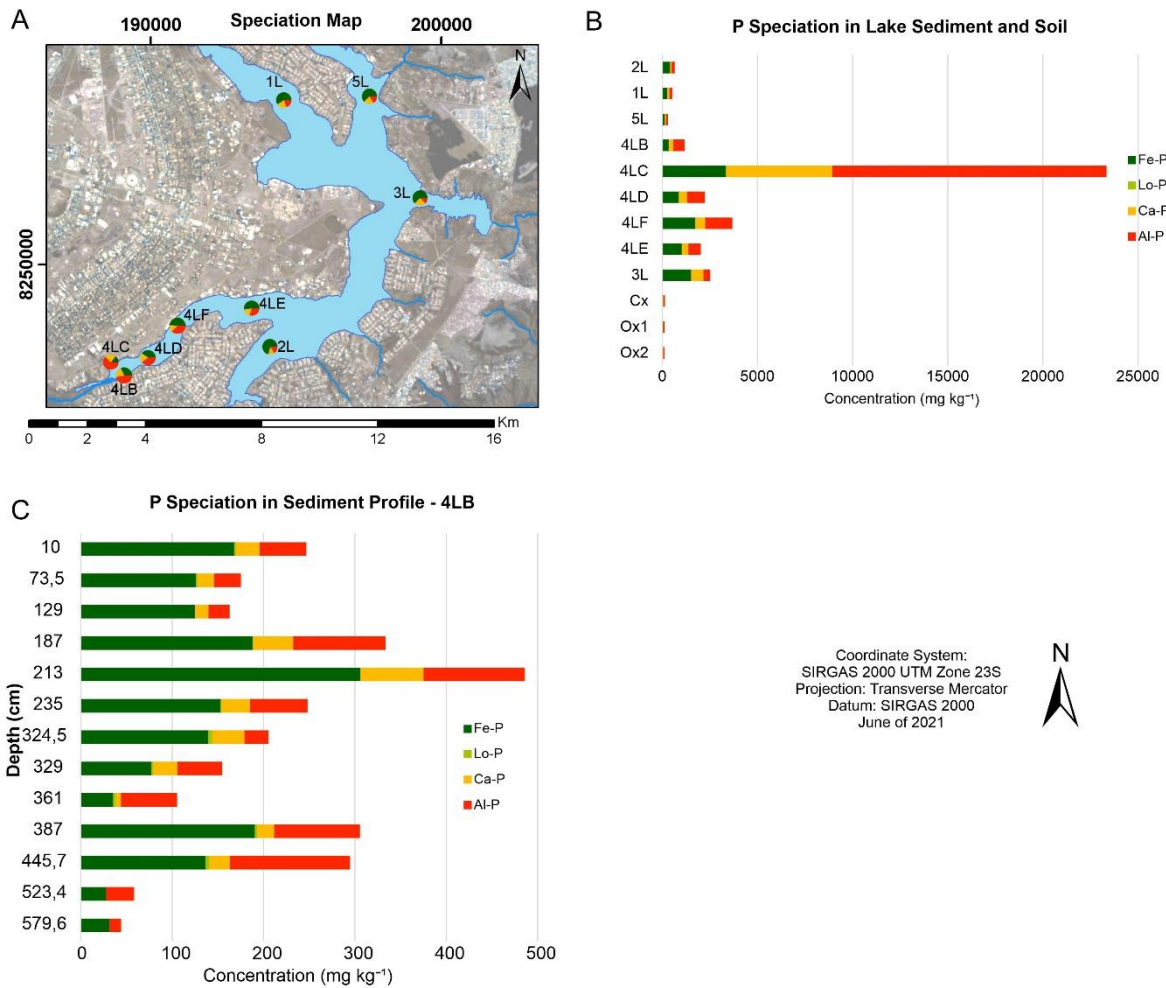


Figure 10 - P speciation relation with species (Lo-P; Al-P; Fe-P, and Ca-P) in the sediment until 15 cm of depth; and B - P speciation in sediment profile for 4LB point.

Figure 10-A showed the P fractionation relation with species (Lo-P; Al-P; Fe-P, and Ca-P) in the sediment until 15 cm of depth. The different fractions of P are distinguished by spatial and concentration distribution, in which the relative abundances of phosphorus forms follow the order: Al-P (52 %) > Fe-P (27 %) > Ca-P (21 %) > Lo-P (0.30 %). The minor concentration was in the north region (Torto Branch), where dominant presence of Fe-P species was observed. The Fe-P showed to be a natural or non-anthropic species, once it was predominant in the most preserved points. In the south area, the BRF region, the Al-P species were more predominant. It was verified the occurrence of substitution of the Al-P for Fe-P as it moved away from WWTP.

Lo-P ranged from LD to 27.38 mg kg<sup>-1</sup>, with an average of 4.35 mg kg<sup>-1</sup> and represented < 0.30% of total of P. The maximum of Lo-P was found in 4LC, the average concentration in this point was 12.40 mg kg<sup>-1</sup>, which represents a much higher value

compared to the other points, which may be attributed to the proximity to the main source. This species did not show significant results compared with other species.

Lo-P (loosely adsorbed P) concentration is also named water-soluble, labile, exchangeable + carbonate - associated, and hydrolyzed P. The Lo-P species is considered the most important parameter for assessing P bioavailability in the sediment (Bramha et al., 2014; Persson and Jansson, 1988). It is available in the form of orthophosphate ( $\text{PO}_4^{3-}$ ), and it can directly get incorporated into algae and ultimately robustly promote eutrophication (Bigaj et al., 2013; Fonseca, 2001; Yang et al., 2016).

The absolute concentrations of Al-P, Fe-P, and Ca-P species in the sediments varied from 40 – 5,000; from 60 -1,000; and 55 – 3,000  $\text{mg kg}^{-1}$  with an average of 765, 409, and 314  $\text{mg kg}^{-1}$ , respectively. The concentration of all three fractions of P was observed to be high in the southern portion of LP. Point 4LC had a higher concentration of Ca-P, Fe-P, and Al-P with concentrations of above 1,400, 3,300, and 5,500  $\text{mg kg}^{-1}$ . This species has a high positive correlation ( $r>0.75$ ) with Ca, Zn, Mg, Pb, Na, and between each other.

As observed above, the sedimentary P was mainly present in the inorganic form (PI), ranging from above 250 to 10,000  $\text{mg kg}^{-1}$ . In the LP, the minimum concentration was found in the 4LB, of 250  $\text{mg kg}^{-1}$ . The organic phosphorus (P-Org) analysis was made for some samples selected in function of the concentration of P and location. The concentrations of organic P were low comparing to inorganic P, ranging from above 85 to 100  $\text{mg kg}^{-1}$ . Barbosa (2019) found a range from 10.1 to 82  $\text{mg kg}^{-1}$  corroborating with the results found in this research. In BRF, the corresponding value found by Barbosa (2019) was approximately 50  $\text{mg kg}^{-1}$ . Again, the maximum concentration was found in 4LC, near to the WWTP.

The results found are consistent with previously published studies and other references, which suggested that the concentration of P-Org in sediments is lower than PI (Aydin et al., 2010, 2009a, 2009b; Gunduz et al., 2011). Normally, P-Org is an immobilized portion in the sediment (Søndergaard et al., 1996), and it is difficult to become bioavailable from microbial remineralization. In Profile sediment (4LB) (Figure 10-B) total P concentrations of all P fractions (Lo-P, Al-P, Fe-P and Ca-P), and PT concentrations of each fraction in sediment profiles (0 – 600 cm) are shown in Figure 10. TP concentration in sediments ranged from 120 to approximately 6000  $\text{mg kg}^{-1}$ . Sedimentary P was mainly present in the inorganic form, with total PI concentrations ranging from above 40 to 485  $\text{mg kg}^{-1}$ (Figure 10). In 2 samples of sedimentary profile

(P1 and P5), P-Org was determined, with values of 70 and 170 mg kg<sup>-1</sup>. The species Fe-P and Al-P represent most of the P in the samples as PI (average 60% and 25%, respectively). The minimum values (below 100 mg kg<sup>-1</sup>) of PI were found in the deep portions of the sedimentary profile, above 450 cm. The maximum concentrations of TP were found in depth 235 to 241 cm in the sedimentary profile. The rank order of P fractions in the whole sediment profile was Fe-P (28 – above of 300 mg·kg<sup>-1</sup>), Al-P (11 – 130 mg·kg<sup>-1</sup>), Ca-P (0 – 485 mg·kg<sup>-1</sup>) and the Lo-P (0 – 4.3 mg·kg<sup>-1</sup>).

In the sedimentary profile low concentrations of P and its species was observed in deeper portion. The exceptions were the intervals from 235 to 241 cm, 329 to 361 cm, and 387 from 415 cm, with average concentration of P above 1,100 mg kg<sup>-1</sup> (Figure 10). These intervals were also richer in Carbon (C), Ca, and organic matter (corresponding to LOI) Al-P, Fe-P and Ca-P. The first interval (235 to 361 cm) presented darker color and has a coarse granulometry. The second interval was characterized by a dark color and fine granulometry and presented a high content of LOI. The last portion corresponded to dark gray and fine sediment and was above unaltered material from LP. The second and third intervals compatible can be with the first release of non-treated sewage in the LP. In other words, in this period the WWTP did not exist in the LP. Between these two intervals, an abrupt decrease of P concentration is found, can be related to mitigating actions. In this interval, the increase of Al-P was observed, and it was the only point where Al-P was superior to Fe-P in the sedimentary profile. The first interval can be related to the granulometry and a big urban expansion.

#### **2.4.4. Speciation of P and metals and the implications for LP**

The relation between P and other elements is likely to form mineral phases with or act as a binding surface with the elements. The mineralogy of the study area is composed in the total fraction by quartz and kaolinite, followed by gibbsite and illite. In the clay fraction, the predominant mineral is kaolinite, followed by gibbsite and illite; and quartz which is considered as minor and trace. As trace constituents in both fractions, goethite, hematite, rutile and anatase were found (Dias, 2017; Moreira and Boaventura, 2003). The clay minerals (gibbsite, hematite, goethite) or precipitated with Ca, Fe or Al may offer sites to P and this is rapidly immobilized by sorption, and convert into strongly sorbed moderately and non-labile stable P forms, depending on the

intrinsic mineralogy (Huser, 2012; Paulo S. Pavinato et al., 2020). A series of bi-plot (Figure 11) was made to understand the relation between the elements, P, and its species.

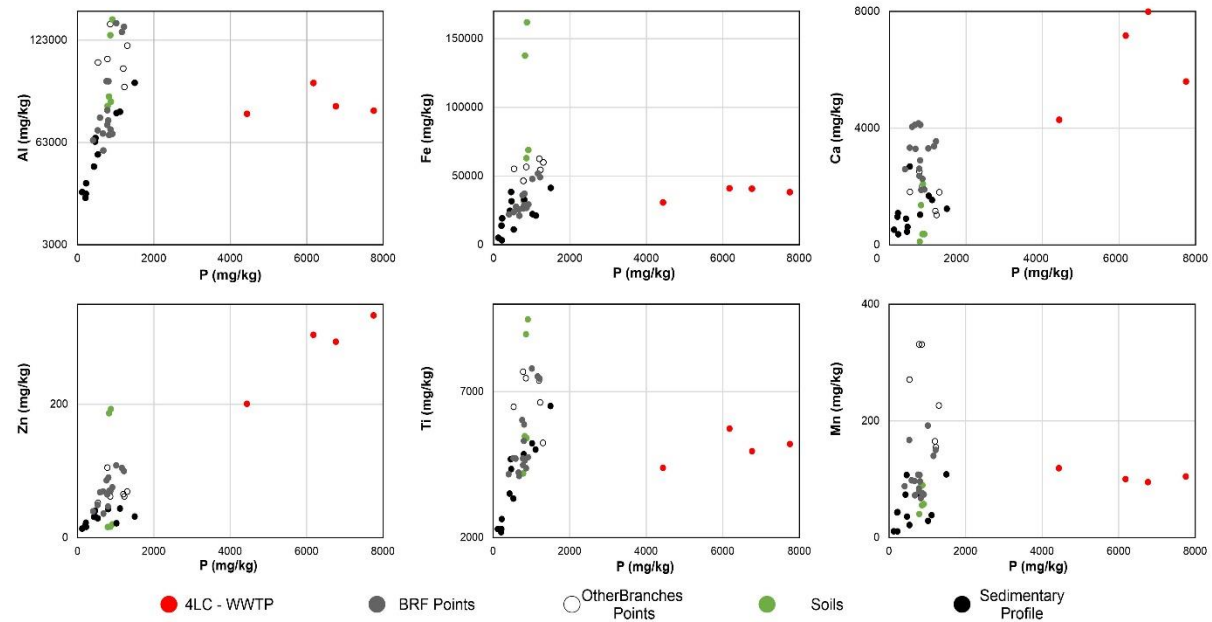


Figure 11 - Graphics Biplot of sediments of AlxP; FexP; CaxP; ZnxP; TixP; and MnxC.

The relation of Al and P was analyzed in the graphs PxAl (Figure 11). It was easily separated into three groups. The first one (red), with high values, relates to 4LC, the point surrounding the WWTP. The second group (gray) is related to points of BRF with intermediary concentration. The last group is composed by samples from sedimentary profile, where has the some altered samples (0-5 cm samples of sediment) and un-altered samples (above 400 cm samples).

In the graphics, the increase of Al, P, and Al-P was verified. It is possible to conclude the presence of anthropic inputs of P and Al, mainly in 4LC, where both elements are high. In this particular point, it was observed the growth of both elements. The surprising fact was an increase of P and Al-P in the order of 1,000 times, while the growth of Al was 100 times. This suggests that a significant part of Al-P is originated from WWTP sources and comes in the Al-P particulate forms. In other words, the process of binding of Al and P did not take place in the water column. The major concentrate of this fraction in superficial sediment corroborates with this hypothesis.

In consideration to bibliographic information, the high Al and P near WWTP must be related with the most successful and used method to suppress internal P-loading. This technique is applied in WWTP-South and uses aluminum sulfate (Alum), which has an high affinity for phosphorus. Between pH 5 and 8.5, the dissolved Al undergoes hydrolysis to form solid amorphous  $\text{Al(OH)}_3$  (a white floc) and  $\text{H}^+$ , leading to a subsequent decline in pH (Boisvert et al., 1997; Dugopolski et al., 2008). This floc grabs phosphorus and other particles as it settles to the bottom of the Lake (Lin et al., 2017; Reitzel et al., 2013). Once deposited on the surface sediment, the freshly formed Al floc is highly susceptible to resuspension events that may lead to redistribution of the Al floc in weeks or months after Al application (Rott et al., 2017). There are cases with relatively large areas in which resuspension of sediment-rich in Al-P occurs (Berbel et al., 2015; Kleeberg and Grüneberg, 2005; Tiecher et al., 2017).

In 2016 occurred a eutrophication process in BRF. The high intensity of this event in BRF can be related to a higher concentration of P in the sediment in this region, to a possible resuspension or bioavailability of P, or maybe to P release from Al-P. From 2016 to 2017, Brasilia faced a hydric crisis caused by the reduced volume of rain 2016. The climate factors that affected the water residence time modified other water characteristics as pH, redox conditions, and water levels. Also, the affluent current flow, the quantity of sewage, and concentration in this period can be affected by climate factors.

In other points, the Al-P, although in low concentrations, but still representative, can be related to P sorption. The inorganic solids, such as ferric oxyhydroxides, aluminum oxyhydroxides, calcium compounds (as calcite and aragonite), and clay minerals (as illite, montmorillonite, and kaolinite), have a high affinity for phosphate (Gatiboni et al., 2021; Persson and Jansson, 1988; Reitzel et al., 2013). Thus, these compounds can serve as adsorption sites in sediments. This feature can explain the high concentration of Fe-P in LP, that in some points corresponds to more than 50% of the total of P. The higher Fe-P and Al-P concentrations resulted from the high active Fe/Al oxides content in the sediment. Most of these materials originated from the erosion of rich in Fe/Al oxides soil. The graphic FexP corroborates to this, once Fe increase did not show association with the P (Figure 11).

The vertical profiles of lake sediments showed a TP decreased with the depth, except for the points 4LD and 3L. This can be an association between phosphorus and the redox cycle of aluminum and iron. The Al /Fe-oxides provide sorption sites for P, so the sedimentation continues. The dissimilatory Fe reduction occurs in the reduced depth zone of sediments, leading to the release of phosphate to pore waters. In this way, the Fe(II), and P are dissolved and can then migrate upward into the oxidized zone of the sediment column, where the reoxidation of iron leads to the renewed scavenging of phosphate by the freshly precipitated Al/Fe-oxides (Huser, 2012; Persson and Jansson, 1988).

The Ca-P determined by this method consists of apatite bound with P and P bound to carbonates (Frankowski et al., 2002; Persson and Jansson, 1988). The species represent the third most abundant in the P species in LP, but its distribution is different. In Graph CaxP, it was observed that some samples – lake sediment – have an increase of Ca and P. This behavior was mainly observed in the point 4LC, and similar to the AlxP Graph. However, Soils and profile sediment samples showed growth of Ca, as well as the rise of Ca-P in lake sediment, particularly in 4LC (red points), with a strong influence of P.

Most points showed low contribution of Ca-P in the TP, except for 4LC and 3L (Figure 11). These samples presented different behavior with other species, once Ca-P had an important role. In 4LC, the Ca-P is the second most abundant species. Possibly, the Ca comes from the anthropical source, once the geology does not provide calcium-carbonate. The use of NaOH (caustic soda) or Ca(OH)<sub>2</sub> (lime milk) to treat the pH is known (Rott et al., 2017). In waters with high pH values, ores susceptible to the precipitation of products such as Ca(OH)<sub>2</sub> and CaCO<sub>3</sub> occur, which can serve as adsorbents for phosphonates (Tang et al., 2019; Yin et al., 2013). In this case, the effect of pH causes CaCO<sub>3</sub> precipitation, and P may be co-precipitated or adsorbed to the precipitate (Persson and Jansson, 1988; Wang et al., 2013). This form is non-bioavailable and difficult to release P to water because it is relatively stable, which can be attributed to the permanent burial of P in sediments (Hanrahan et al., 2005). However, under weakly acidic conditions, it can be partly released (Hanrahan et al., 2005; Rott et al., 2017). The Mg, Ca, and P have a high correlation ( $r>0.80$ ). All these elements showed an anomaly in the 4LC region. The Mg is related to MgCO<sub>3</sub>, a substance used in the treatment of sewage, assisting in the pH control.

Graph ZnxP showed a behavior similar to graphs AlxP and CaxP. In Figure 11, the alteration of Zn in the profile was accompanied by P and Ca. The Zn in the LP system is anthropic (Dias, 2013; Maia, 2003). The high concentrations of Zn were related to a high concentration of P found in the WWTP. The soils and the sedimentary profile did not indicate a significant increase.

The Ti was a geogenic element, without anthropic sources, as observed through PCA. The Graph TixP behavior was similar to FexP, with a high P content in WWTP and no changes in concentrations of Ti. In the soils and sediments with less influence of anthropic activities, the increase of Ti was observed.

In Figure 12 has two PCAs, Figure 12-A and 12-B is the PCA for the species of P and metals. As observed, the principal components could explain 73% of the total variance. For the analysis of PCA was observed the strong correlation between P, Al-P, and Fe-P ( $p>0.9$ ). The Ca-P shows moderate correlation ( $0.7 < p < 0.9$ ). The differential is the Lo-P, which has a strong correlation with PC1 and moderate positive with PC2.

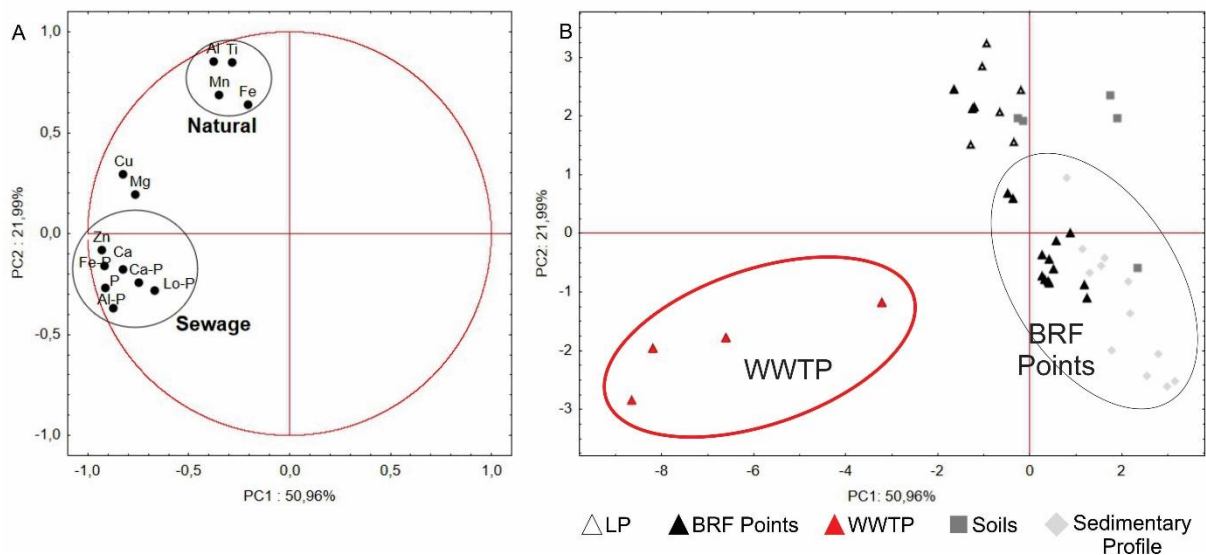


Figure 12 - PCA for the species of P and metals.

In Figure 12-A, it is possible to separate two groups of elements assembling. The first group, with Al, Ti, Mn, and Fe, can characterize a terrigenous origin. The second group is composed of all species of P, with Zn, and Ca, highlighting out an anthropic source. Unfortunately, it is not possible to distinguish from punctual and non-punctual sources. In this case, PC2 is the decisive factor, with a positive or negative association for source determination. Figure 12-B shows that the WWTP points are

isolated, again related to the high concentration of P and its species. The points from BRF region are too separated from others points to the LP.

#### **2.4.5. Comparison around the world**

The TP in sediment from Lake Paranoá (except for 4LC) ranged from above 100 – 1,400 mg kg<sup>-1</sup>, and in 4LC, in front of WWTP-South, it ranged from above 4,000 to 7,000 mg kg<sup>-1</sup>. Barbosa (2019) observed TP ranges from 74 to 556 mg kg<sup>-1</sup>, with an average of 220 mg kg<sup>-1</sup>, in sediments in LP. In the Cruzeta and Gargalheiras Reservoirs (Northeast of Brazil), the TP varied from 487 to 1,081 mg kg<sup>-1</sup> and from 711 to 982 mg kg<sup>-1</sup>, respectively. These Brazilian reservoirs are in the semiarid region, where factors as precipitation, temperature and erosion have a strong influence (Cavalcante et al., 2018). Lake Honggen (China) has a TP range from 850 to 2,133 mg kg<sup>-1</sup> in sediments, considering an urban lake with multiple-use and eutrophication historical, similarly to LP (Jiang et al., 2011; Zhu et al., 2013). In Lake Chilika, a protected area from India with eutrophication cases, TP was measured from a minimum of 244 mg kg<sup>-1</sup> and a maximum of 2150 mg kg<sup>-1</sup>, both in the post-monsoon season (Barik et al., 2016).

These phosphorus concentrations in sediments show that the intervals of values found in LP were not out of range compared with other lakes from different systems. Considering the P concentration of 600 mg kg<sup>-1</sup>, that presents minimum ecological risk (Zhang et al., 2016), only 32% of 43 samples are below this value in this study. The input of P in the LP, except for the BRF, can be from different industries, urban activities (e.g., use of detergents), agriculture, recreation, stormwater runoff, and atmospheric deposits (Jiang et al., 2011; Macintosh et al., 2018; Worsfold et al., 2016).

Lo-P showed a positive correlation with other species of P, P, Mg, Zn, Ca, and Pb. The contribution of Lo-P was similar to other lakes in the world. Lake Chilika (India), Lake Mazalah (Egypt), Lake Myall (Australia), Lake Hongfeng (China), and Lake Lugano (Swiss and Italy) have the lowest (less than 1%) Lo-P concentrations (Abdel-Satar & Goher, 2009; Barik et al., 2016; Jiang et al., 2011; Shilla et al., 2009; Tu et al., 2019). Using superficial sediment samples of rainy and dry seasons of 4LC and 4LB, it was observed that the variation of Lo-P was not significant.

In other regions, it is verified that the geological background and use and occupation of soil strongly influence the concentration of species. For example, Lake Erie (USA) and Lake Hongfeng (China), where the Ca-P is the most abundant species, was related to detrital sediments or terrigenous sources (Jiang et al., 2011; Williams et al., 1976). In the Gargalheiras and Cruzeta Reservoirs, the P form was present mainly as P-BD (Redox-sensitive (Fe, Mn bound) P), which was related to internal P source in water bodies (Cavalcante et al., 2018). This behavior is also observed in Lake Myall (Australia) (Shilla et al., 2009). In Lake Manzalah (Egypt), the Al-P is dominant, representing 48;39% of TP in the Lake and is related to different pollution sources, as sewage inputs (Abdel-Satar and Goher, 2009).

Considering the historical eutrophication, the monitoring and gestion of dissolved P in the watershed and data from WWTP South, we suggest that the P release from the sediment certainly contributes substantially to this problem, once particulate P concentration is high and can be released associated to pH and conductivity changes and also early diagenesis process occurring in the sediment. Therefore, factors like the sedimentary rate, residential water, pH, sedimentation and oxygenation of water column are essential for developing algae bloom. To avoid this process, an effective treatment to control of particulate P input, P's release and mitigate the nuisances caused by eutrophication. As far as we could verify, our study indicates that the studied region can benefit from in-lake geoengineering techniques that immobilize the potential releasable P pool in water and sediment (Lürling and van Oosterhout, 2013).

Many techniques can be employed in water bodies to reduce eutrophication. The first auxiliary action is to work with the direct input of nutrients. In this case, it would improve the WWTP system, especially in the treatment for the particulate that is launch in the effluent. The second possible source of P is the sedimentary pool. Even if the outside input were treated, the intern load could cause problems. Several techniques can be used to control legacy P stored in sediments, as sediment dredging and in situ sediment inactivation by application of products.

## 2.5. CONCLUSIONS

The present study presents a coupled analysis of P to investigate the variation of this element in urban lakes to evaluate possible environmental impacts. The results showed an appropriate and necessary tool for understanding the cycle of P in the LP. This strategy showed that the analysis restricts to water, generally made by primary sanitation institutions, is limited for environmental issues of the Paranoá lake. The implementation of this methodology for water resources management strengthens the understanding of the eutrophication process and efficiently supports decision-making.

The presented results indicate that although the water did not have harmful phosphorus concentrations to the ecosystem, it had other sources. It is necessary to take some measures to reduce the P concentrations, especially the Al-P and Fe-P, in sediment. The main region is BRF, mainly the point 4LC – near WWTP South – to mitigate possible environmental risks in LP.

The main form of P input was sediment, in particulate, which was verified in this study. The concentration of dissolved P did not present significant participation in the study, and it was weakly associated with sewage, within limits established by the legislation. However, the SPM and sediments show high concentration values of P in the BRF region, which can be related to anthropic sources, mainly to untreated sewage and also the effluent of WWTP.

The South WWTP P contribution seems to be local, restrict to the BRF branch. The other possible P source in the BRF was associated with Riacho Fundo Stream (4LB), with clandestine untreated sewage and construction material associated with urban areas. The other watershed of the LP do not show high and alarming concentrations of particulate P.

Most of the sediments from points in LP show the ecological risk for the Lake. In natural soils, the P speciation was dominated for Fe-P and Ca-P. In the sediments of BRF, the P speciation was different, dominated by Al-P. This region has the most available species of P in the sediment, and the surface sediments tend to retain P due to the formation of iron oxy-hydroxides, mainly Al-P oxides, during the flocculation processes that occur in WWTP. According to several variables as the early diagenesis and pH and redox changes, and also water level, flow velocity or residence time, the P can be bioavailable to the environment. In this way, part of the eutrophication

process, as observed in 2016 in BRF branch, can be related to P release from sediment.

## 2.6. ACKNOWLEDGMENTS

This study was financed in part by the Coordenação de Aperfeiçoamento de Pessoal de Nível Superior - Brasil (CAPES), Agência Reguladora de Águas (ADASA), Conselho Nacional de Desenvolvimento Científico e Tecnológico (CNPq), and Fundação de Apoio à Pesquisa do Distrito Federal (FAP-DF). God bless us. The authors acknowledge the students and researchers who participated in field investigations. The authors acknowledge the staff from the Geosciences Institute of UnB, and Hydrosciences Montpellier.

### 3. CONSIDERAÇÕES FINAIS

Nesta pesquisa a dinâmica do P no Braço do Riacho Fundo do Lago Paranoá – DF foi estudada a partir de uma abordagem integrada de ferramentas geoquímicas com extrações químicas (simples e sequenciais) e fracionamento em diferentes compartimentos. Foi verificado as concentrações de P total e suas frações em água, sedimento e em solos. Desse modo, foi possível compreender melhor o comportamento geoquímico do P, e seus possíveis efeitos no ambiente.

Na água foi verificado que o P total dissolvido apresentou concentrações baixas, e as maiores concentrações foram encontradas próximas as ETEs. Ainda assim, os valores não se mostram significativos e não afetam as características da água do reservatório. No P dissolvido foi observado que a porção orgânica é superior a inorgânica. A Caesb e alguns estudos como este, Barbosa (2019) e Pinho & Santos (2016) focam somente na porção dissolvida, e ainda não investigam a parte orgânica do P. Considerando que a maior concentração de P é orgânico no dissolvido e observando a correlação do P com outras componentes orgânicos, este deve ser considerado para a realização de um estudo específico.

No sedimento foi verificado maiores concentrações de P, principalmente no particulado, com ênfase nos pontos de BRF. Este foi considerado a principal forma de entrada do P no LP e a compartimento particulado sua principal forma de transporte, sendo a ETE-Sul, a principal fonte é alóctone. Portanto, algumas medidas específicas para controlar o aporte de P devem ser destinadas à essas fontes. Desse modo, este estudo identificou que os sedimentos são os principais compartimentos de armazenamento de P, ou seja, grande parte deste nutriente é retida na coluna sedimentar.

O fracionamento de fósforo nos sedimentos identificou uma grande quantidade de Al-P na região de BRF e de Fe-P no LP. Ambas as formas são disponíveis, o que pode representar um risco à eutrofização. As frações Al-P e Ca-P se apresentam com características e como *inputs* antrópicos. Estas frações estão associadas a forma de tratamento de água e esgoto adotadas pela ETE-Sul e tem suas influências limitadas a região do BRF.

Neste estudo não foi possível avaliar as condições físico-químicas envolvidas na possível mobilização do fósforo para a coluna d'água. Mas deve-se ressaltar que

a maioria dos sedimentos apresentam risco ambiental, exceto o ponto 4LB no período chuvoso. Assim é necessário investigar e açãoar algumas medidas mitigatórias, uma vez que mobilização de P a partir do sedimento ainda é incipiente.

As maiores concentrações de P ocorrem no BRF e à medida que se aproximam do centro do LP, essas diminuem. Esse caso é indicativo que a influência da principal fonte de P, ETE-Sul, é limitado a região do BRF. E também indicam a existência de barreiras ou mecanismos geoquímicos ou hidrodinâmicos, caso da diluição, que auxiliam no processo de retenção do P nessa região, que pode ser mais detalhadas em futuros estudos.

Desse modo, a proposta que investiga o compartimento sedimentar, incluindo o MPS, foi possível entender melhor todo o sistema. Esse estudo mostrou que a análise de P restrita à água ou a porção dissolvida, geralmente feita por instituições de saneamento básico e realizada por outros estudos como Barbosa et al., (2019), Mar da Costa (2016), entre outros, é limitada para as questões ambientais do LP. A implementação desta metodologia, da investigação de P no particulado e no sedimento, assim como seu fracionamento, na gestão de recursos hídricos fortalece a compreensão do processo de eutrofização e apoia de forma eficiente a tomada de decisões.

## 4. REFERÊNCIAS BIBLIOGRÁFICAS

- Abdel-Satar, A.M., Goher, M.E., 2009. Nutrient Status and Phosphorus Speciation of Manzalah Lake Sediment, Egypt. *Thalassia Salentina* 32, 32–2009. <https://doi.org/10.1285/i15910725v32p3>
- ADASA, 2017. Plano Distrital De Saneamento Básico E De Gestão Integrada De Resíduos Sólidos 2, 124.
- Adasa, 2011. Plano de Gerenciamento Integrado de Recurso Hídrico do DF 446.
- Amorim, A.M., Sodré, F.F., Rousseau, T.C.C., Maia, P.D., 2019. Assessing rare-earth elements and anthropogenic gadolinium in water samples from an urban artificial lake and its tributaries in the Brazilian Federal District. *Microchemical Journal* 148, 27–34. <https://doi.org/10.1016/j.microc.2019.04.055>
- Angelini, R., Bini, L.M., Starling, F.L.R.M., 2008. Efeitos De Diferentes Intervenções No Processo De Eutrofização Do Lago Paranoá (Brasília – Df). *Oecologia Australis* 12, 564–571. <https://doi.org/10.4257/oeco.2008.1203.14>
- Aquino, I.G. de, 2017. Estudo Da Variação Da Descarga Sólida Em Suspensão Da Sub- Bacia Do Riacho Fundo - Lago Paranoá, Brasília - DF. Dissertação (Mestrado) - Instituto de Geociências, Universidade de Brasília, Brasília.
- Ashley, K., Cordell, D., Mavinic, D., 2011. A brief history of phosphorus: From the philosopher's stone to nutrient recovery and reuse. *Chemosphere* 84, 737–746. <https://doi.org/10.1016/j.chemosphere.2011.03.001>
- Atinkpahoun, C.N.H., Le, N.D., Pontvianne, S., Poirot, H., Leclerc, J.P., Pons, M.N., Soclo, H.H., 2018. Population mobility and urban wastewater dynamics. *Science of the Total Environment* 622–623, 1431–1437. <https://doi.org/10.1016/j.scitotenv.2017.12.087>
- Avilés, A., Rodero, J., Amores, V., de Vicente, I., Rodríguez, M.I., Niell, F.X., 2006. Factors controlling phosphorus speciation in a Mediterranean basin (River Guadaleo, Spain). *Journal of Hydrology* 331, 396–408. <https://doi.org/10.1016/j.jhydrol.2006.05.024>

- Aydin, I., Aydin, F., Hamamci, C., 2010. Phosphorus Speciation in the Surface Sediment and River Water from the Orontes (Asi) River, Turkey. *Water Environment Research* 82, 2265–2271. <https://doi.org/10.2175/106143010X12609736967206>
- Aydin, I., Aydin, F., Saydut, A., Hamamci, C., 2009a. A sequential extraction to determine the distribution of phosphorus in the seawater and marine surface sediment. *Journal of Hazardous Materials* 168, 664–669. <https://doi.org/10.1016/j.jhazmat.2009.02.095>
- Aydin, I., Imamoglu, S., Aydin, F., Saydut, A., Hamamci, C., 2009b. Determination of mineral phosphate species in sedimentary phosphate rock in Mardin, SE Anatolia, Turkey by sequential extraction. *Microchemical Journal* 91, 63–69. <https://doi.org/10.1016/j.microc.2008.08.001>
- Baird, R.B., Eaton, A.D., Rice, E.W., 2017. Standard Methods for the Examination of Water and Wasterwater, 23rd ed, Encyclopedia of Forensic Sciences: Second Edition. American Public Health Association, Washington. <https://doi.org/10.1016/B978-0-12-382165-2.00237-3>
- Bao, L., Li, X., Cheng, P., 2018. Phosphorus retention along a typical urban landscape river with a series of rubber dams. *Journal of Environmental Management* 228, 55–64. <https://doi.org/10.1016/j.jenvman.2018.09.019>
- Barbosa, J.S.B., 2019. Balanço De Massa E Especiação De Fósforo Na Bacia Hidrográfica Do Lago Paranoá-DF. Tese (Doutorado) - Programa de Pós-Graduação em Tecnologias Química e Biológica, Universidade de Brasília, Brasília.
- Barbosa, J.S.B., Bellotto, V.R., da Silva, D.B., Lima, T.B., 2019. Nitrogen and Phosphorus Budget for a Deep Tropical Reservoir of the Brazilian Savannah. *Water* 11, 1205. <https://doi.org/10.3390/w11061205>
- Barik, S.K., Bramha, S., Bastia, T.K., Behera, D., Mohanty, P.K., Rath, P., 2019. Distribution of geochemical fractions of phosphorus and its ecological risk in sediment cores of a largest brackish water lake, South Asia. *International Journal of Sediment Research* 34, 251–261. <https://doi.org/10.1016/j.ijsrc.2018.11.004>

- Barik, S.K., Bramha, S.N., Mohanty, A.K., Bastia, T.K., Behera, D., Rath, P., 2016. Sequential extraction of different forms of phosphorus in the surface sediments of Chilika Lake. *Arabian Journal of Geosciences* 9, 1–12. <https://doi.org/10.1007/s12517-015-2217-5>
- Bennett, E.M., Carpenter, S.R., Caraco, N.F., 2001. Human impact on erodable phosphorus and eutrophication: A global perspective. *BioScience* 51, 227–234. [https://doi.org/10.1641/0006-3568\(2001\)051\[0227:HIOEPA\]2.0.CO;2](https://doi.org/10.1641/0006-3568(2001)051[0227:HIOEPA]2.0.CO;2)
- BERBEL, G.B.B., 2008. Estudo do fósforo sedimentar e de suas especiações químicas em dois sistemas costeiros e Plataforma Continental Sudeste (Brasil) e Baía do Almirantado (Região Antártica) considerando suas relações biogeoquímicas. Universidade de São Paulo. Tese (Doutorado) - Instituto Oceanográfico, Universidade de São Paulo, São Paulo.
- Berbel, G.B.B., Favaro, D.I.T., Braga, E.S., 2015. Impact of harbour, industry and sewage on the phosphorus geochemistry of a subtropical estuary in Brazil. *Marine Pollution Bulletin* 93, 44–52. <https://doi.org/10.1016/j.marpolbul.2015.02.016>
- Bernardi, J.V.E., Lacerda, L.D., Dórea, J.G., Landim, P.M.B., Gomes, J.P.O., Almeida, R., Manzatto, A.G., Bastos, W.R., 2012. APLICAÇÃO DAANÁLISE DAS COMPONENTES PRINCIPAIS NA ORDENAÇÃO DOS PARÂMETROS FÍSICO-QUÍMICOS NO ALTO RIO MADEIRA E AFLUENTES, AMAZÔNIA OCIDENTAL. *Geochimica Brasiliensis* 23. <https://doi.org/http://dx.doi.org/10.21715/gb.v23i1.296>
- Bhateria, R., Jain, D., 2016. Water quality assessment of lake water: a review. *Sustainable Water Resources Management* 2, 161–173. <https://doi.org/10.1007/s40899-015-0014-7>
- Bigaj, I., Łopata, M., Dunalska, J., Szymbański, D., Zieliński, R., 2013. Bottom sediments as a potential source of phosphorus in the riverine-lacustrine system of the Kośna River (Northeastern Poland). *Limnological Review* 12, 115–124. <https://doi.org/10.2478/v10194-011-0051-7>
- Bitschofsky, F., Nausch, M., 2019. Spatial and seasonal variations in phosphorus speciation along a river in a lowland catchment (Warnow, Germany). *Science of*

the Total Environment 657, 671–685.  
<https://doi.org/10.1016/j.scitotenv.2018.12.009>

Boisvert, J.P., To, T.C., Berrak, A., Jolicoeur, C., 1997. Phosphate adsorption in flocculation processes of aluminium sulphate and poly-aluminium-silicate-sulphate. Water Research 31, 1939–1946. [https://doi.org/10.1016/S0043-1354\(97\)00042-0](https://doi.org/10.1016/S0043-1354(97)00042-0)

Boström, B., Persson, G., Broberg, B., 1988. Bioavailability of different phosphorus forms in freshwater systems. Hydrobiologia 170, 133–155.  
<https://doi.org/10.1007/BF00024902>

Bramha, S.N., Mohanty, A.K., Padhi, R.K., Panigrahi, S.N., Satpathy, K.K., 2014. Phosphorus speciation in the marine sediment of Kalpakkam coast, southeast coast of India. Environmental Monitoring and Assessment 186, 6003–6015.  
<https://doi.org/10.1007/s10661-014-3836-0>

Broberg, O., Persson, G., 1988. Particulate and dissolved phosphorus forms in freshwater: composition and analysis. Hydrobiologia 170, 61–90.  
<https://doi.org/10.1007/BF00024899>

Caesb, 2019. Relatório da Qualidade da Água Distribuída pela Caesb em 2018.

Campos, J.E.G., Freitas-Silva, F.H., 1998. Hidrogeologia do Distrito Federal , in: Inventário Hidrogeológico e Dos Recursos Hídricos Superficiais Do Distrito Federal. IEMA-SEIMATEC/Universidade de Brasília., Brasília.

Cavalcante, H., Araújo, F., Noyma, N.P., Becker, V., 2018. Phosphorus fractionation in sediments of tropical semiarid reservoirs. Science of The Total Environment 619–620, 1022–1029. <https://doi.org/10.1016/j.scitotenv.2017.11.204>

CODEPLAN, 2017. Densidades Urbanas Nas Regiões Administrativas Do Distrito Federal 47.

CONAMA, 2005. Ministério do Meio Ambiente. Conselho Nacional do Meio Ambiente – CONAMA. Resolução nº 357 de 17 de março de 2005.

Cooper, R.J., Rawlins, B.G., Krueger, T., Lézé, B., Hiscock, K.M., Pedentchouk, N., 2015. Contrasting controls on the phosphorus concentration of suspended particulate matter under baseflow and storm event conditions in agricultural

- headwater streams. *Science of the Total Environment* 533, 49–59. <https://doi.org/10.1016/j.scitotenv.2015.06.113>
- Cordell, D., Drangert, J.O., White, S., 2009. The story of phosphorus: Global food security and food for thought. *Global Environmental Change* 19, 292–305. <https://doi.org/10.1016/j.gloenvcha.2008.10.009>
- Cunha, J.P.A. da, 2015. Qualidade Da Água Do Lago Paranoá E De Seus Tributários. Trabalho de Conclusão de Curso - Pós-graduação Lato Sensu em Análise ambiental e desenvolvimento sustentável, Centro Universitário de Brasília (UniCEUB/ICPD), Brasília.
- da Silva, A.C.R., Celino, J.J., Alva, J.C.R., Silva, M.D.J., 2013. Geoestatística E Geoquímica Dos Metais Traços Na Água De Fontes Naturais No Município De Salvador - Bahia, Brasil. *Águas Subterrâneas* 27, 16–26. <https://doi.org/10.14295/ras.v27i3.27405>
- de Aquino, I.G., Roig, H.L., Oliveira, E.S., Garnier, J., Guimarães, E.M., Koide, S., 2018. Temporal variation of suspended sediments and mineralogy using an improved automatic sampler system in the Riacho Fundo Stream, Brasília, Distrito Federal, Brazil. *Geologia USP - Serie Cientifica* 18, 171–185. <https://doi.org/10.11606/issn.2316-9095.v18-140500>
- Dias, D.F., 2017. Processos Geoquímicos Na Interface Sedimento-Água No Braço Riacho Fundo Do Lago Paranoá - DF. Dissertação (Mestrado) - Instituto de Geociências, Universidade de Brasília, Brasília.
- Dias, R.Z., 2013. Papel Da Wetland Do Riacho Fundo No Controle Da Eutrofização Do Lago Paranoá, Brasília - Distrito Federal. Dissertação (Mestrado) - Instituto de Geociências, Universidade de Brasília, Brasília.
- Dugopolski, R.A., Rydin, E., Brett, M.T., 2008. Short-term effects of a buffered alum treatment on green lake sediment phosphorus speciation. *Lake and Reservoir Management* 24, 181–189. <https://doi.org/10.1080/07438140809354059>
- Echeverria, R.M., 2007. Avaliação de impactos ambientais nos tributários do Lago Paranoá, Brasília, DF. Dissertação (Mestrado) - Instituto de Geociências, Universidade de Brasília, Brasília.

- EMBRAPA, 1978. Levantamento de Reconhecimento dos solos do Distrito Federal. Serviço Nacional de Levantamento e Conservação do Solo 455.
- Embrapa Solos, 2018. Sistema brasileiro de classificação de solos, Embrapa Solos.
- Feng, W., Yang, F., Zhang, C., Liu, J., Song, F., Chen, H., Zhu, Y., Liu, S., Giesy, J.P., 2020. Composition characterization and biotransformation of dissolved, particulate and algae organic phosphorus in eutrophic lakes. Environmental Pollution 265, 114838. <https://doi.org/10.1016/j.envpol.2020.114838>
- Fonseca, F.O., 2001. Olhares sobre o lago Paranoá, 1º. ed. Secretaria do Meio Ambiente Recursos Hídricos, Brasília.
- Fox, G.A., Purvis, R.A., Penn, C.J., 2016. Streambanks: A net source of sediment and phosphorus to streams and rivers. Journal of Environmental Management 181, 602–614. <https://doi.org/10.1016/j.jenvman.2016.06.071>
- Frankowski, L., Bolałek, J., 1999. Transformations and release of phosphorus forms at the sediment-water interface in the Pomeranian Bay (southern Baltic). Oceanologia 41, 429–444.
- Frankowski, L., Bolałek, J., Szostek, A., 2002. Phosphorus in bottom sediments of Pomeranian Bay (Southern Baltic - Poland). Estuarine, Coastal and Shelf Science 54, 1027–1038. <https://doi.org/10.1006/ecss.2001.0874>
- Franz, C., Makeschin, F., Weiß, H., Lorz, C., 2014. Sediments in urban river basins: Identification of sediment sources within the Lago Paranoá catchment, Brasilia DF, Brazil - using the fingerprint approach. Science of the Total Environment 466–467, 513–523. <https://doi.org/10.1016/j.scitotenv.2013.07.056>
- FREITAS, P.L. de, BLANCANEAUX, P., MOREAU, R., 1998. Caractérisation structurale de sols des cerrados brésiliens (Savanes) sous différents modes d'utilisation agricole. Étude et Gestion des Sols 5, 93–105.
- Frumin, G.T., Gildeeva, I.M., 2014. Eutrophication of water bodies - A global environmental problem. Russian Journal of General Chemistry 84, 2483–2488. <https://doi.org/10.1134/S1070363214130015>
- Gatiboni, L.C., Souza Junior, A.A. de, Dall'Orsoletta, D.J., Mumbach, G.L., Kulesza, S.B., Abdala, D.B., 2021. Phosphorus speciation in soils with low to high degree

of saturation due to swine slurry application. *Journal of Environmental Management* 282. <https://doi.org/10.1016/j.jenvman.2020.111553>

Grochowska, J., Augustyniak, R., Łopata, M., Parszuto, K., Tandyrik, R., Płachta, A., 2019. From Saprotrophic to Clear Water Status: the Restoration Path of a Degraded Urban Lake. *Water, Air, and Soil Pollution* 230. <https://doi.org/10.1007/s11270-019-4138-5>

Gunduz, B., Aydin, F., Aydin, I., Hamamci, C., 2011. Study of phosphorus distribution in coastal surface sediment by sequential extraction procedure (NE Mediterranean Sea, Antalya-Turkey). *Microchemical Journal* 98, 72–76. <https://doi.org/10.1016/j.microc.2010.11.006>

Hanrahan, G., Salmassi, T.M., Khachikian, C.S., Foster, K.L., 2005. Reduced inorganic phosphorus in the natural environment: Significance, speciation and determination. *Talanta* 66, 435–444. <https://doi.org/10.1016/j.talanta.2004.10.004>

Holtan, H., Kamp-Nielsen, L., Stuanes, A.O., 1988. Phosphorus in soil, water and sediment: an overview. *Hydrobiologia* 170, 19–34. <https://doi.org/10.1007/BF00024896>

Hosomi, M., Okada, M., Sudo, R., 1982. Release of phosphorus from lake sediments. *Environment International* 7, 93–98. [https://doi.org/10.1016/0160-4120\(82\)90078-2](https://doi.org/10.1016/0160-4120(82)90078-2)

Hupfer, M., Gächter, R., Giovanoli, R., 1995. Transformation of phosphorus species in settling seston and during early sediment diagenesis. *Aquatic Sciences* 57, 305–324. <https://doi.org/10.1007/BF00878395>

Huser, B.J., 2012. Variability in phosphorus binding by aluminum in alum treated lakes explained by lake morphology and aluminum dose. *Water Research* 46, 4697–4704. <https://doi.org/10.1016/j.watres.2012.06.005>

IBGE, 2016. IBGE Censo 2010 [WWW Document]. Instituto Brasileiro de Geografia e Estatística.

Jarvie, H.P., Neal, C., Williams, R.J., Neal, M., Wickham, H.D., Hill, L.K., Wade, A.J., Warwick, A., White, J., 2002. Phosphorus sources, speciation and dynamics in

- the lowland eutrophic River Kennet, UK. *Science of the Total Environment* 282–283, 175–203. [https://doi.org/10.1016/S0048-9697\(01\)00951-2](https://doi.org/10.1016/S0048-9697(01)00951-2)
- Jarvie, H.P., Sharpley, A.N., Flaten, D., Kleinman, P.J.A., Jenkins, A., Simmons, T., 2015. The Pivotal Role of Phosphorus in a Resilient Water-Energy-Food Security Nexus. *Journal of Environmental Quality* 44, 1049–1062. <https://doi.org/10.2134/jeq2015.01.0030>
- Jiang, C., Hu, J., Huang, X., Li, C., Deng, J., Zhang, J., Liu, F., 2011. Phosphorus speciation in sediments of Lake Hongfeng, China. *Chinese Journal of Oceanology and Limnology* 29, 53–62. <https://doi.org/10.1007/s00343-011-9047-4>
- Karim Morsy, Amr Morsy, Mohamed Morsy, Hoda Thakeb, 2017. Eutrophication of Aquatic Ecosystems: A Viewpoint on the Environmental Impact of Climate Change. *Journal of Environmental Science and Engineering B* 6, 506–514. <https://doi.org/10.17265/2162-5263/2017.10.002>
- Kleeberg, A., Grüneberg, B., 2005. Phosphorus mobility in sediments of acid mining lakes, Lusatia, Germany. *Ecological Engineering* 24, 89–100. <https://doi.org/10.1016/j.ecoleng.2004.12.010>
- Li, M., Dong, J., Zhang, Y., Yang, H., van Zwieten, L., Lu, H., Alshameri, A., Zhan, Z., Chen, X., Jiang, X., Xu, W., Bao, Y., Wang, H., 2021. A critical review of methods for analyzing freshwater eutrophication. *Water (Switzerland)* 13, 1–20. <https://doi.org/10.3390/w13020225>
- Lidiane Tomaz Dias, 2011. Modelagem dinâmica espacial do uso e ocupação do solo na bacia hidrográfica do lago Paranoá-DF : 1998–2020. Dissertação (Mestrado) - Instituto de Geociências, Universidade de Brasília, Brasília.
- Lin, J., Sun, Q., Ding, S., Wang, D., Wang, Y., Chen, M., Shi, L., Fan, X., Tsang, D.C.W., 2017. Mobile phosphorus stratification in sediments by aluminum immobilization. *Chemosphere* 186, 644–651. <https://doi.org/10.1016/j.chemosphere.2017.08.005>
- Liporoni, L.M., 2012. Estudo Preliminar Da Qualidade Da Água Do Lago Paranoá , Brasília – DF , Utilizando Um Modelo De Qualidade Da Água Bidimensional.

Dissertação (Mestrado) - Faculdade de Tecnologia, Universidade de Brasília, Brasília.

Liu, Q., Liu, S., Zhao, H., Deng, L., Wang, C., Zhao, Q., Dong, S., 2015. The phosphorus speciations in the sediments up- and down-stream of cascade dams along the middle Lancang River. *Chemosphere* 120, 653–659. <https://doi.org/10.1016/j.chemosphere.2014.10.012>

Loska, K., Wiechuła, D., 2003. Application of principal component analysis for the estimation of source of heavy metal contamination in surface sediments from the Rybnik Reservoir. *Chemosphere* 51, 723–733. [https://doi.org/10.1016/S0045-6535\(03\)00187-5](https://doi.org/10.1016/S0045-6535(03)00187-5)

Louis, P., Messaoudene, A., Jrad, H., Abdoul-Hamid, B.A., Vignati, D.A.L., Pons, M.N., 2020. Understanding Rare Earth Elements concentrations, anomalies and fluxes at the river basin scale: The Moselle River (France) as a case study. *Science of the Total Environment* 742, 140619. <https://doi.org/10.1016/j.scitotenv.2020.140619>

Lürling, M., van Oosterhout, F., 2013. Case study on the efficacy of a lanthanum-enriched clay (Phoslock®) in controlling eutrophication in Lake Het Groene Eiland (The Netherlands). *Hydrobiologia* 710, 253–263. <https://doi.org/10.1007/s10750-012-1141-x>

Lyra, W. da S., Silva, E.C. da, Araújo, M.C.U. de, Fragoso, W.D., Veras, G., 2010. Classificação periódica: um exemplo didático para ensinar análise de componentes principais. *Química Nova* 33, 1594–1597. <https://doi.org/10.1590/s0100-40422010000700030>

Macintosh, K.A., Mayer, B.K., McDowell, R.W., Powers, S.M., Baker, L.A., Boyer, T.H., Rittmann, B.E., 2018. Managing Diffuse Phosphorus at the Source versus at the Sink. *Environmental Science & Technology* 52, 11995–12009. <https://doi.org/10.1021/acs.est.8b01143>

Maia, P.D., 2003. Estudo Geoquímico De Metais Em Sedimentos Do Lago Paranoá - DF. Dissertação (Mestrado) - Instituto de Geociências, Universidade de Brasília, Brasília.

- Mao, C., Li, T., Rao, W., Tang, Z., Song, Y., Wang, S., 2021. Chemical speciation of phosphorus in surface sediments from the Jiangsu Coast, East China: Influences, provenances and bioavailabilities. *Marine Pollution Bulletin* 163, 111961. <https://doi.org/10.1016/j.marpolbul.2020.111961>
- Mar da Costa, N.Y., Boaventura, G.R., Mulholland, D.S., Araújo, D.F., Moreira, R.C.A., Faial, K.C.F., Bomfim, E. de O., 2016a. Biogeochemical mechanisms controlling trophic state and micropollutant concentrations in a tropical artificial lake. *Environmental Earth Sciences* 75. <https://doi.org/10.1007/s12665-016-5629-y>
- Mar da Costa, N.Y., Boaventura, G.R., Mulholland, D.S., Araújo, D.F., Moreira, R.C.A., Faial, K.C.F., Bomfim, E. de O., 2016b. Biogeochemical mechanisms controlling trophic state and micropollutant concentrations in a tropical artificial lake. *Environmental Earth Sciences* 75. <https://doi.org/10.1007/s12665-016-5629-y>
- Meinikmann, K., Lewandowski, J., Hupfer, M., 2015. Phosphorus in groundwater discharge - A potential source for lake eutrophication. *Journal of Hydrology* 524, 214–226. <https://doi.org/10.1016/j.jhydrol.2015.02.031>
- Merschel, G., Bau, M., Baldewein, L., Dantas, E.L., Walde, D., Bühn, B., 2015. Tracing and tracking wastewater-derived substances in freshwater lakes and reservoirs: Anthropogenic gadolinium and geogenic REEs in Lake Paranoá, Brasilia. *Comptes Rendus - Geoscience* 347, 284–293. <https://doi.org/10.1016/j.crte.2015.01.004>
- Moreira, R.C.A., Boaventura, G.R., 2003. Referência geoquímica regional para a interpretação das concentrações de elementos químicos nos sedimentos da bacia do Lago Paranoá - DF. *Química Nova* 26, 812–820. <https://doi.org/10.1590/s0100-40422003000600006>
- Moura, D.S., Lima Neto, I.E., Clemente, A., Oliveira, S., Pestana, C.J., Aparecida de Melo, M., Capelo-Neto, J., 2020. Modeling phosphorus exchange between bottom sediment and water in tropical semiarid reservoirs. *Chemosphere* 246. <https://doi.org/10.1016/j.chemosphere.2019.125686>
- Moura, L.H.A., 2008. Estudo Geoquímico da Bacia do Gama e Avaliação da Qualidade de Água. Dissertação (Mestrado) - Instituto de Geociências, Universidade de Brasília, Brasília.

- Moura, L.H.A., Boaventura, G.R., Pinelli, M.P., 2010. A qualidade de água como indicador de uso e ocupação do solo: bacia do Gama - Distrito Federal. *Química Nova* 33, 97–103. <https://doi.org/10.1590/S0100-40422010000100018>
- Némery, J., Garnier, J., 2007. Origin and fate of phosphorus in the Seine watershed (France): Agricultural and hydrographic P budgets. *Journal of Geophysical Research: Biogeosciences* 112. <https://doi.org/10.1029/2006JG000331>
- Ni, J., Lin, P., Zhen, Y., Yao, X., Guo, L., 2015. Distribution, source and chemical speciation of phosphorus in surface sediments of the central Pacific Ocean. *Deep-Sea Research Part I: Oceanographic Research Papers* 105, 74–82. <https://doi.org/10.1016/j.dsr.2015.08.008>
- Nunes, R. de S., 2010. Distribuição Do Fósforo No Solo Sob Dois Sistemas De Cultivo E Diferentes Manejos Da Adubação Fosfatada. Dissertação (Mestrado) - Faculdade de Agronomia e Medicina Veterinária, Universidade de Brasília, Brasília.
- OECD. 1982. Eutrophication of waters: Monitoring, assessment and control. OECD.
- Oliveira, E.S., 2021. QUALIDADE DOS SEDIMENTOS E ANÁLISE MULTITEMPORAL DO ASSOREAMENTO DO LAGO PARANOÁ - DF. Tese (Doutorado) - Instituto de Geociências, Universidade de Brasília, Brasília.
- Owens, P.N., Walling, D.E., 2002. The phosphorus content of fluvial sediment in rural and industrialized river basins. *Water Research* 36, 685–701.
- Pardo, P., López Sánchez, J.F., Rauret, G., Ruban, V., Muntau, H., Quevauviller, Ph., 1999. Study of the stability of extractable phosphate content in a candidate reference material using a modified Williams extraction procedure. *The Analyst* 124, 407–411. <https://doi.org/10.1039/a808693a>
- Pavinato, P.S., Cherubin, M.R., Soltangheisi, A., Rocha, G.C., Chadwick, D.R., Jones, D.L., 2020. Revealing soil legacy phosphorus to promote sustainable agriculture in Brazil. *Scientific Reports* 10, 1–11. <https://doi.org/10.1038/s41598-020-72302-1>

- Pedreira, R.M.A., Pahnke, K., Böning, P., Hatje, V., 2018. Tracking hospital effluent-derived gadolinium in Atlantic coastal waters off Brazil. *Water Research* 145, 62–72. <https://doi.org/10.1016/j.watres.2018.08.005>
- Persson, G., Jansson, M., 1988. Phosphorus in Freshwater Ecosystems, *Hydrobiologia*. Springer Netherlands, Dordrecht. <https://doi.org/10.1007/978-94-009-3109-1>
- Petrere, M., Walter, T., Minte-Vera, C. v., 2006. Income evaluation of small - Scale fishers in two Brazilian urban reservoirs: Represa Billings (SP) and Lago Paranoá (DF). *Brazilian Journal of Biology* 66, 817–828. <https://doi.org/10.1590/s1519-69842006000500007>
- Philomeno, G.M., 2007. A Comunidade Fitoplânctonica E a Restauração Do Lago Paranoá , Brasília-Df. Tese (Doutorado) - Departamento de Ecologia, Universidade de Brasília, Brasília.
- Pinho, A.L.V. de, Santos, D.S., 2016. Avaliação qualitativa da pluma de contaminação do Braço do Riacho Fundo, Lago Paranoá - DF. Trabalho de Conclusão de Curso (Bacharel) - Departamento de Engenharia Civil e Ambiental, Universidade de Brasília, Brasília.
- Rauret, G., López-Sánchez, J.F., Sahuquillo, A., Rubio, R., Davidson, C., Ure, A., Quevauviller, P., 1999. Improvement of the BCR three step sequential extraction procedure prior to the certification of new sediment and soil reference materials. *Journal of Environmental Monitoring* 1, 57–61. <https://doi.org/10.1039/a807854h>
- REATTO, A., 2004. Mapa pedológico digital - SIG atualizado do Distrito Federal Escala 1:100.000 e uma síntese do texto explicativo, Documentos - EMBRAPA Cerrados (Brazil).
- Reatto-Braga, A., Correia, J.R., 2000. Levantamento semidetalhado dos solos da bacia do rio Jardim-DF, escala 1:50.000 Environmental Education View project Número Temático de Solos da revista PAB View project. <https://doi.org/10.13140/RG.2.1.4603.0329>

- Reitzel, K., Jensen, H.S., Egemose, S., 2013. PH dependent dissolution of sediment aluminum in six Danish lakes treated with aluminum. *Water Research* 47, 1409–1420. <https://doi.org/10.1016/j.watres.2012.12.004>
- Rönspieß, L., Dellwig, O., Lange, X., Nausch, G., Schulz-Bull, D., 2020. Spatial and seasonal phosphorus dynamics in a eutrophic estuary of the southern Baltic Sea. *Estuarine, Coastal and Shelf Science* 233. <https://doi.org/10.1016/j.ecss.2019.106532>
- Rott, E., Minke, R., Steinmetz, H., 2017. Removal of phosphorus from phosphonate-loaded industrial wastewaters via precipitation/flocculation. *Journal of Water Process Engineering* 17, 188–196. <https://doi.org/10.1016/j.jwpe.2017.04.008>
- Salles, P., Bredeweg, B., 2009. A qualitative model of Riacho Fundo (DF, Brazil) water basin sustainability. *Ecological Informatics* 4, 320–338. <https://doi.org/10.1016/j.ecoinf.2009.09.012>
- Sandström, S., Futter, M.N., Kyllmar, K., Bishop, K., O'Connell, D.W., Djodjic, F., 2020. Particulate phosphorus and suspended solids losses from small agricultural catchments: Links to stream and catchment characteristics. *Science of the Total Environment* 711. <https://doi.org/10.1016/j.scitotenv.2019.134616>
- Sarvajayakesavalu, S., Lu, Y., Withers, P.J.A., Pavinato, P.S., Pan, G., Chareonsudjai, P., 2018. Phosphorus recovery: a need for an integrated approach. *Ecosystem Health and Sustainability* 4, 48–57. <https://doi.org/10.1080/20964129.2018.1460122>
- Savage, C., Leavitt, P.R., Elmgren, R., 2010. Effects of land use, urbanization, and climate variability on coastal eutrophication in the Baltic Sea. *Limnology and Oceanography* 55, 1033–1046. <https://doi.org/10.4319/lo.2010.55.3.1033>
- Shilla, D.A., Asaeda, T., Kalibbala, M., 2009. Phosphorus speciation in Myall Lake sediment, NSW, Australia. *Wetlands Ecology and Management* 17, 85–91. <https://doi.org/10.1007/s11273-008-9087-5>
- Sobral, L.F., Barreto, M.C. v, Silva, A.J. da, Anjos, J.L. dos, 2015. Guia Prático para Interpretação de Resultados de Análises de Solo. Embrapa Tabuleiros Costeiros-Documentos (INFOTECA-E). 13.

- Søndergaard, M., Windolf, J., Jeppesen, E., 1996. Phosphorus fractions and profiles in the sediment of shallow Danish lakes as related to phosphorus load, sediment composition and lake chemistry. *Water Research* 30, 992–1002. [https://doi.org/10.1016/0043-1354\(95\)00251-0](https://doi.org/10.1016/0043-1354(95)00251-0)
- Spivakov, B.Y.A., Maryutina, T.A., Muntau, H., 1999. Phosphorus speciation in water and sediments (Technical Report). *Pure and Applied Chemistry* 71, 2161–2176. <https://doi.org/10.1351/pac199971112161>
- Starling, F., Lazzaro, X., Cavalcanti, C., Moreira, R., 2002. Contribution of omnivorous tilapia to eutrophication of a shallow tropical reservoir: Evidence from a fish kill. *Freshwater Biology* 47, 2443–2452. <https://doi.org/10.1046/j.1365-2427.2002.01013.x>
- Tang, W., Shan, B., Zhang, H., 2010. Phosphorus buildup and release risk associated with agricultural intensification in the estuarine sediments of Chaohu Lake Valley, Eastern China. *Clean - Soil, Air, Water* 38, 336–343. <https://doi.org/10.1002/clen.200900275>
- Tang, X., Li, R., Wu, M., Zhao, W., Zhao, L., Zhou, Y., Bowes, M.J., 2019. Influence of turbid flood water release on sediment deposition and phosphorus distribution in the bed sediment of the Three Gorges Reservoir, China. *Science of the Total Environment* 657, 36–45. <https://doi.org/10.1016/j.scitotenv.2018.12.011>
- Thin, M.M., Sacchi, E., Setti, M., Re, V., 2020. A Dual Source of Phosphorus to Lake Sediments Indicated by Distribution, Content, and Speciation: Inle Lake (Southern Shan State, Myanmar). *Water* 12. <https://doi.org/10.3390/w12071993>
- Tiecher, T., Schenato, R.B., Santanna, M.A., Caner, L., dos Santos, D.R., 2017. Phosphorus forms in sediments as indicators of anthropic pressures in an agricultural catchment in Southern Brazil. *Revista Brasileira de Ciencia do Solo* 41, 1–17. <https://doi.org/10.1590/18069657rbcs20160569>
- Tu, L., Jarosch, K.A., Schneider, T., Grosjean, M., 2019. Phosphorus fractions in sediments and their relevance for historical lake eutrophication in the Ponte Tresa basin (Lake Lugano, Switzerland) since 1959. *Science of the Total Environment* 685, 806–817. <https://doi.org/10.1016/j.scitotenv.2019.06.243>

USEPA, 2000. National Recommended Water Quality Criteria, in: Applications of Environmental Chemistry. CRC Press.  
<https://doi.org/10.1201/9781420032963.axb>

Wan, J., Wang, Z., Qian, S.Q., 2011. Distribution of bioavailable phosphorus between overlying water and SPM under abrupt expansion condition. *Journal of Hydrodynamics* 23, 398–406. [https://doi.org/10.1016/S1001-6058\(10\)60129-1](https://doi.org/10.1016/S1001-6058(10)60129-1)

Wang, C., Bai, L., Pei, Y., 2013. Assessing the stability of phosphorus in lake sediments amended with water treatment residuals. *Journal of Environmental Management* 122, 31–36. <https://doi.org/10.1016/j.jenvman.2013.03.007>

WHO, 2017. Guidelines for drinking-water quality. World Health Organization.

Wildung, R.E., Schmidt, R.L., 1973. Phosphorus Release from Lake Sediments.

Williams, J.D.H., Jaquet, J.-M., Thomas, R.L., 1976. Forms of Phosphorus in the Surficial Sediments of Lake Erie. *Journal of the Fisheries Research Board of Canada* 33, 413–429. <https://doi.org/10.1139/f76-063>

Withers, P.J.A., 2019. Closing the phosphorus cycle. *Nature Sustainability* 2, 1001–1002. <https://doi.org/10.1038/s41893-019-0428-6>

Withers, P.J.A., Jarvie, H.P., 2008. Delivery and cycling of phosphorus in rivers: A review. *Science of the Total Environment* 400, 379–395. <https://doi.org/10.1016/j.scitotenv.2008.08.002>

WMO, 2010. World Meteorological Organization. World Weather Information Service 2010: Brasília.

Worsfold, P., McKelvie, I., Monbet, P., 2016. Determination of phosphorus in natural waters: A historical review. *Analytica Chimica Acta* 918, 8–20. <https://doi.org/10.1016/j.aca.2016.02.047>

Xiang, S.L., Zhou, W. bin, 2011. Phosphorus forms and distribution in the sediments of Poyang Lake, China. *International Journal of Sediment Research* 26, 230–238. [https://doi.org/10.1016/S1001-6279\(11\)60089-9](https://doi.org/10.1016/S1001-6279(11)60089-9)

Yang, B., Lin, H., Bartlett, S.L., Houghton, E.M., Robertson, D.M., Guo, L., 2021. Partitioning and transformation of organic and inorganic phosphorus among

- dissolved, colloidal and particulate phases in a hypereutrophic freshwater estuary. *Water Research* 196, 117025. <https://doi.org/10.1016/j.watres.2021.117025>
- Yang, B., Liu, S.M., Wu, Y., Zhang, J., 2016. Phosphorus speciation and availability in sediments off the eastern coast of Hainan Island, South China Sea. *Continental Shelf Research* 118, 111–127. <https://doi.org/10.1016/j.csr.2016.03.003>
- Yin, H., Du, Y., Kong, M., Liu, C., 2017. Interactions of riverine suspended particulate matter with phosphorus inactivation agents across sediment-water interface and the implications for eutrophic lake restoration. *Chemical Engineering Journal* 327, 150–161. <https://doi.org/10.1016/j.cej.2017.06.099>
- Yin, H., Kong, M., Fan, C., 2013. Batch investigations on P immobilization from wastewaters and sediment using natural calcium rich sepiolite as a reactive material. *Water Research* 47, 4247–4258. <https://doi.org/10.1016/j.watres.2013.04.044>
- Yu, B., Luo, J., Xie, H., Yang, H., Chen, S., Liu, J., Zhang, R., Li, Y.Y., 2021. Species, fractions, and characterization of phosphorus in sewage sludge: A critical review from the perspective of recovery. *Science of the Total Environment* 786, 147437. <https://doi.org/10.1016/j.scitotenv.2021.147437>
- Yu, J., Ding, S., Zhong, J., Fan, C., Chen, Q., Yin, H., Zhang, L., Zhang, Y., 2017. Evaluation of simulated dredging to control internal phosphorus release from sediments: Focused on phosphorus transfer and resupply across the sediment-water interface. *Science of the Total Environment* 592, 662–673. <https://doi.org/10.1016/j.scitotenv.2017.02.219>
- Zhang, W., Jin, X., Zhu, X., Shan, B., 2016. Characteristics and distribution of phosphorus in surface sediments of limnetic ecosystem in Eastern China. *PLoS ONE* 11, 1–14. <https://doi.org/10.1371/journal.pone.0156488>
- Zhao, J., Gao, Q., Liu, Q., Fu, G., 2020. Lake eutrophication recovery trajectories: Some recent findings and challenges ahead. *Ecological Indicators* 110. <https://doi.org/10.1016/j.ecolind.2019.105878>
- Zhu, Y., Zhang, R., Wu, F., Qu, X., Xie, F., Fu, Z., 2013. Phosphorus fractions and bioavailability in relation to particle size characteristics in sediments from Lake

Hongfeng, Southwest China. Environmental Earth Sciences 68, 1041–1052.  
<https://doi.org/10.1007/s12665-012-1806-9>

## ANEXOS

Tabela 2 - Coordenadas dos pontos de amostragem.

<b>ID</b>	<b>Nome</b>	<b>Y</b>	<b>X</b>
1LA	Braço do Bananal - LP	194576,3931	8255659,524
1LB	Braço do Bananal - ETE Norte - 1 - LP	191565,2634	8257568,496
1LC	Braço do Bananal - ETE Norte - 2 - LP	191574,5238	8257588,781
1SA	Córrego do Bananal - Ponte na EPIA	188125,8495	8258957,165
1SB	Córrego do Bananal - EPIA - Montante	188164,352	8258367,826
1SC	Córrego do Bananal - EPIA - Jusante	188660,447	8258566,264
1SD	Córrego do Bananal - depois da ponte	190197,093	8258515,708
2L	Braço do Gama - LP	194100,2854	8247165,941
2SA	Braço do Gama - Clube dos Oficiais da Base Aérea	190066,681	8242555,437
2SB	Córrego do Gama - Montante / Entrada da FAL	185704,372	8235221,026
2SC	Ribeirão do Gama - Jusante	186590,3371	8238347,184
2SD	Córrego Mato Seco	184341,3743	8237197,126
2SE	Córrego Mato Seco - Ponte	186383,9617	8238551,796
2SF	Córrego Taquara	188509,452	8238791,685
2SG	Córrego do Cedro - Montante	184097,9571	8239003,352
2SH	Córrego do Cedro - Jusante	185024,0006	8240340,382
2SI	Córrego Capetinga	185477,321	8234817,635
3L	Centro do Lago Paranoá	199264,2198	8252285,455
4LB	Braço do Riacho Fundo - Saída do Córrego RF - LP	189037,5028	8246294,613
4LC	Braço do Riacho Fundo - ETE Sul - LP	188622,8155	8246319,151
4LD	Braço do Riacho Fundo - Antes da 1ª ponte	189425,1609	8246632,746
4LE	Braço do Riacho Fundo - Depois da 2ª ponte	193470,5698	8248490,078
4LF	Braço do Riacho Fundo - Depois da 1ª ponte	189799,53	8246771,85
4SA	Correjo Riacho Fudno - ETE/R.F. Montante	175871,803	8240736,131
4SB	Correjo Riacho Fundo - ETE/R.F. Jusante	176244,2938	8240174,953
4SC	Correjo Riacho Fundo - Ponte	179341,8504	8241135,755
4SD	Córrego Riacho Fundo - Vila Cauy / Jusante	182889,7128	8243241,012
4SE	Córrego do Valo - Lixão Jusante	178190,605	8252470,344
4SF	Córrego Vicente Pires - Parque Bandeirante	183136,2065	8243744,633
4SG	Córrego Guará - Linda do Metrô	181787,111	8248495,783
4SH	Correjo do Valo - Lixão Montante	178102,822	8252776,891
4SI	Correjo do Riacho Fundo - Nascente	174415,774	8241739,162
4SJ	Correjo Açuinho	177475,3907	8239103,7
4SK	Correjo do Valo - Juante Vicente Pires	178114,7576	8249199,206
4SL	Braço do Riacho Fundo - Zoológico/Ponte na EPAR	185967,6352	8245311,271
4SM	Córrego Riacho Fundo - Zoológico Montante	183337,4682	8243686,841
4SN	Córrego Riacho Fundo - Pivô / Jusante	177537,2877	8239113,835
4SO	Correjo do Valo - Nascente	177759,127	8254834,711

4SP	Galeria - Montante estação Riacho Fundo	183236,597	8243707,214
4SQ	Córrego Vicente Pires - Arriqueiras/Ponte	181075,892	8244520,481
4SR	Córrego Riacho Fundo - Vila Cauy / Montante	182377,7613	8242640,033
4SS	Córrego Riacho Fundo - Metropolitana / Ponte	181257,3368	8242213,876
4SU	Córrego Coqueiros - Granja Ipê / Montante	180713,5003	8237519,195
5LB	Braço do Torto - LP	197526,34	8255785,882
5SA	Córrego do Torto Montante	188447,4512	8262159,291
5SB	Braço do Torto - Ponte na EPIA	190003,2043	8261370,831
5SC	Córrego do Torto - Ponte do Varjão	191851,99	8260170,303
5SD	Córrego do Urubu	192927,738	8260240,176
CX	CX	195942,00000	8278990
Ox 1	Ox1	193938,00000	8263920
Ox 2	Ox2	216841,00000	8273220

Tabela 3 - Composição amostras dissolvidas

ID	Data mês/ano	Na mg/L	Mg mg/L	Al mg/L	Si mg/L	K mg/L	Ca mg/L	P µg/L	Mn µg/L	Fe µg/L	Ni µg/L	Cu µg/L	Zn µg/L	Sr µg/L	Gd µg/L	Pb µg/L	Cl mg/L	NO3 mg/L	SO4 mg/L
1LA	jun/16	8,44	1,09	0,01	1,94	2,39	9,28	8,85	0,24	2,45	0,13	0,13	0,50	40,90	0,03	0,06	<LD	<LD	<LD
1LA	jul/18	4,57	1,15	0,02	2,88	1,41	8,49	7,35	3,83	5,66	0,11	0,15	0,50	20,49	0,01	0,02	<LD	<LD	<LD
1LA	abr/18	0,30	0,59	0,00	2,92	0,17	4,64	1,74	0,02	4,74	0,18	0,41	0,79	6,39	0,00	0,00	0,52	<LD	0,41
1LB	jul/18	40,10	1,29	0,02	4,13	11,52	10,47	289,69	7,14	6,16	0,90	0,48	1,67	42,60	0,31	0,03	<LD	<LD	<LD
1LB	abr/18	10,04	1,02	0,00	1,89	2,94	8,89	1,97	0,18	0,34	0,15	0,22	3,78	37,77	0,05	0,00	9,60	11,64	14,27
1LC	abr/18	62,99	2,45	0,03	5,02	18,04	20,48	28,27	19,18	9,73	1,42	0,37	6,13	94,97	1,01	0,02	65,23	3,08	128,58
2L	jul/18	2,50	0,58	0,01	2,33	0,72	6,63	5,46	0,70	1,27	0,05	0,09	0,29	14,69	0,00	0,01	<LD	<LD	<LD
2L	ago/16	9,15	1,10	0,02	1,10	2,47	9,34	7,78	0,28	1,69	0,92	0,35	0,47	40,90	0,03	0,03	<LD	<LD	<LD
2L	abr/18	0,66	0,25	0,00	2,07	0,21	1,80	0,46	1,36	2,03	0,05	0,11	2,00	6,10	0,00	0,01	1,08	<LD	1,17
3L	jul/18	9,34	1,11	0,00	1,84	2,67	9,56	4,80	0,13	<LD	0,07	0,09	0,33	38,00	0,02	0,01	<LD	<LD	<LD
3L	ago/16	9,67	1,21	0,01	1,42	2,74	10,22	7,46	0,21	2,48	0,22	1,14	0,88	44,54	0,03	0,09	<LD	<LD	<LD
3L	abr/18	8,64	1,03	0,00	1,82	2,50	8,73	0,50	0,01	0,10	0,07	0,15	2,99	37,84	0,02	<LD	8,12	3,11	10,09
4LB	abr/18	7,63	1,13	0,00	2,32	1,91	12,02	2,08	0,47	0,24	0,09	0,15	0,52	51,25	0,02	0,01	6,77	7,30	8,72
4LB	jun/16	7,06	1,18	0,01	2,82	1,11	12,10	8,78	27,60	2,50	0,15	0,21	0,53	45,71	0,01	0,05	<LD	<LD	<LD
4LB	fev/16	5,41	1,33	0,07	2,72	1,63	19,97	25,03	9,04	63,33	0,00	5,83	22,27	59,42	0,01	6,69	4,1	2,05	4,91
4LC	abr/18	40,44	1,18	0,01	3,60	10,04	11,58	14,54	16,31	12,42	0,68	0,27	1,80	57,17	0,63	0,04	43,66	12,66	52,48
4LC	abr/18	41,16	1,20	0,01	3,73	10,16	11,84	11,45	15,85	8,09	0,69	0,30	2,02	57,63	0,62	0,03	43,66	12,66	52,48
4LC	jun/16	20,46	0,60	0,01	2,01	5,64	5,15	30,76	17,45	11,95	1,06	0,31	2,25	21,66	0,11	0,06	<LD	<LD	<LD
4LC	jun/16	31,77	1,16	0,03	3,22	7,66	10,25	23,22	29,52	13,89	1,55	0,39	2,85	44,51	0,19	0,08	<LD	<LD	<LD
4LC	fev/16	23,39	1,45	0,05	2,90	5,64	11,65	36,05	23,13	24,76	0,00	4,62	7,31	52,65	0,13	7,93	17,98	13,84	33,98
4LC	jul/18	47,45	1,38	0,01	4,19	13,24	10,34	30,74	19,15	6,38	1,56	0,56	7,93	42,09	0,50	0,02	<LD	<LD	<LD
4LD	jun/16	13,26	1,14	0,02	2,13	3,32	10,00	12,64	0,93	5,26	0,31	0,30	0,70	43,91	0,07	0,45	<LD	<LD	<LD
4LD	abr/18	9,13	1,06	0,01	1,92	2,55	9,76	1,36	0,21	0,08	0,09	0,24	1,13	42,91	0,03	0,00	8,82	4,18	11,14
4LD	fev/16	7,80	1,00	0,03	1,97	2,25	9,62	0,00	0,72	50,66	0,00	1,26	1,26	41,44	0,02	4,67	6,83	3,55	10,28
4LD	abr/18	9,21	1,04	0,01	1,93	2,57	9,83	1,45	0,18	0,14	0,12	0,24	1,32	43,40	0,04	0,00	8,82	4,18	11,14
4LE	jun/16	10,13	1,10	0,01	2,05	2,67	9,67	8,15	0,42	4,85	0,18	0,19	0,64	42,95	0,04	0,06	<LD	<LD	<LD
4LF	fev/16	8,12	1,03	0,04	2,05	2,33	9,80	0,00	0,52	33,84	0,00	1,29	3,26	41,69	0,02	5,53	6,95	1,87	10,76

ID	Data mês/ano	Na mg/L	Mg mg/L	Al mg/L	Si mg/L	K mg/L	Ca mg/L	P µg/L	Mn µg/L	Fe µg/L	Ni µg/L	Cu µg/L	Zn µg/L	Sr µg/L	Gd µg/L	Pb µg/L	Cl mg/L	NO3 mg/L	SO4 mg/L
4SA	mar/17	1,59	0,79	0,00	2,02	0,54	6,06	3,05	0,04	<LD	0,05	0,39	0,33	26,97	0,00	0,00	1,07	0,51	1,89
4SA	set/17	1,56	0,43	0,00	2,81	0,19	2,29	<LD!	0,02	<LD	0,06	0,57	0,45	9,19	0,00	0,00	1,32	2,21	0,61
4SA	set/17	1,56	0,42	0,00	2,60	0,21	2,24	0,80	0,03	1,68	0,05	0,28	0,54	10,12	0,00	0,00	1,15	1,44	0,68
4SA	set/17	0,78	0,24	0,00	1,42	0,10	1,39	5,78	0,02	<LD	0,04	0,29	0,54	5,57	0,00	0,02	1,32	2,21	0,61
4SA	nov/16	1,20	0,51	0,01	2,39	0,16	3,88	2,83	3,54	2,15	0,88	0,35	1,13	16,32	0,00	0,02	2,41	0,55	0,48
4SA	set/20	2,94	0,62	0,04	2,58	1,08	7,65	4,62	0,71	30,65	0,16	0,73	1,71	37,55	0,00	0,03	2,49	2,55	3,19
4SB	set/17	11,08	0,40	0,01	1,85	2,12	2,52	57,04	1,11	2,09	0,17	0,14	0,78	9,22	0,01	0,02	14,99	0,83	0,00
4SB	mar/17	2,61	0,73	0,00	1,95	0,90	6,14	14,05	0,14	<LD	0,08	0,37	0,86	28,24	0,00	0,00	3,22	0,72	2,93
4SB	set/17	21,41	0,71	0,01	3,56	4,16	4,00	153,19	1,86	4,01	0,34	0,23	1,23	14,90	0,03	0,00	14,99	0,83	0,00
4SB	nov/16	50,49	1,41	0,13	4,18	8,51	11,63	24,41	19,46	22,26	2,07	0,41	3,23	44,34	0,07	0,10	44,07	1,78	110,28
4SB	set/17	4,43	0,68	0,01	2,75	1,48	4,16	200,81	5,34	3,11	0,20	0,78	7,51	16,77	0,01	0,00	3,05	13,35	4,69
4SB	set/20	40,77	1,35	0,03	3,77	8,51	14,09	19,14	18,81	21,49	2,02	0,81	8,65	60,71	0,09	0,07	33,70	2,21	68,98
4SC	mar/17	6,63	0,76	0,01	2,88	1,70	5,70	15,06	9,80	1,19	0,12	0,28	0,91	25,71	0,01	0,00	5,69	7,52	12,38
4SC	set/17	8,16	0,38	0,01	1,80	1,45	1,96	12,30	0,44	2,87	0,15	0,10	1,01	7,46	0,01	0,02	6,28	16,66	10,92
4SC	set/20	12,52	0,92	0,02	3,19	3,18	9,05	16,40	5,29	75,88	0,72	0,90	1,16	40,71	0,02	0,08	12,28	2,69	23,94
4SC	set/17	16,04	0,73	0,01	3,52	2,94	3,77	27,18	0,83	2,37	0,26	0,12	1,66	14,55	0,02	0,00	6,28	16,66	10,92
4SC	nov/16	13,47	0,73	0,02	3,38	2,35	4,89	16,99	18,85	9,15	0,59	0,27	1,74	19,96	0,03	0,02	10,81	8,66	23,77
4SD	mar/17	5,25	0,74	0,00	2,91	1,20	6,64	7,10	0,20	<LD	0,13	0,21	0,21	27,77	0,00	0,00	4,17	3,69	7,98
4SD	nov/16	5,09	0,74	0,01	3,10	0,92	6,87	10,22	9,66	3,33	0,27	0,22	0,53	24,66	0,01	0,01	3,75	6,79	6,48
4SD	set/17	4,25	0,39	0,00	1,86	0,79	3,15	8,99	0,11	<LD	0,08	0,13	0,72	10,30	0,01	0,02	12,56	8,28	0,00
4SD	set/17	8,24	0,75	0,00	3,35	1,58	5,99	15,02	0,04	<LD	0,19	0,15	0,73	19,89	0,01	0,00	12,56	8,28	0,00
4SD	set/17	7,92	1,07	0,00	2,95	3,10	10,59	17,79	2,07	2,17	0,26	0,63	1,67	47,40	0,01	0,00	6,59	3,32	11,85
4SE	set/20	8,28	0,52	0,03	2,69	1,70	5,25	1,95	30,04	10,98	0,15	0,11	0,09	17,65	0,00	0,00	15,53	7,03	2,76
4SE	mar/17	5,26	0,43	0,00	2,85	0,96	3,55	1,88	1,41	<LD	0,08	0,15	0,12	9,59	0,00	0,00	10,06	2,09	1,04
4SE	set/17	8,76	0,51	0,00	2,77	1,68	5,00	0,85	44,37	<LD	0,14	0,14	0,25	7,06	0,00	0,00	16,63	3,00	1,41
4SE	set/17	6,46	0,60	0,01	1,30	1,61	5,50	6,44	0,47	2,54	0,14	0,16	0,59	20,40	0,03	0,02	16,63	3,00	1,41
4SE	nov/16	8,43	0,51	0,00	2,62	1,37	5,46	2,98	55,53	1,72	0,23	0,12	0,77	11,50	0,00	0,00	14,88	3,02	1,14
4SE	set/19	8,46	0,54	0,01	2,85	1,49	6,35	4,22	26,71	<LD	0,46	0,35	5,22	13,95	0,00	0,03	13,57	1,93	0,64

ID	Data mês/ano	Na mg/L	Mg mg/L	Al mg/L	Si mg/L	K mg/L	Ca mg/L	P µg/L	Mn µg/L	Fe µg/L	Ni µg/L	Cu µg/L	Zn µg/L	Sr µg/L	Gd µg/L	Pb µg/L	Cl mg/L	NO3 mg/L	SO4 mg/L
4SE	out/19	7,85	0,51	0,03	2,76	1,37	5,98	19,44	40,51	99,50	0,99	3,24	21,44	14,14	0,01	0,20	3,06	3,83	5,91
4SF	mar/17	6,83	1,35	0,01	2,98	1,58	16,81	2,15	0,10	<LD	0,08	0,32	0,14	68,78	0,00	0,00	5,57	3,93	5,46
4SF	set/20	8,86	1,75	0,02	2,89	3,83	23,29	6,51	1,16	10,17	0,22	0,93	0,21	90,07	0,01	0,00	12,07	7,10	11,91
4SF	set/17	7,47	1,40	0,00	2,93	1,05	15,77	9,13	0,01	<LD	0,09	0,15	0,31	49,54	0,00	0,00	6,32	4,46	0,00
4SF	nov/16	8,27	1,58	0,03	3,09	1,42	19,67	7,32	3,55	6,74	0,30	0,54	0,51	73,48	0,01	0,02	6,57	5,75	4,31
4SF	set/17	7,24	1,56	0,01	2,61	2,63	25,62	13,75	0,03	2,32	0,40	1,95	3,19	108,43	0,02	0,00	6,22	4,59	8,05
4SF	out/19	8,63	1,78	0,04	3,15	2,03	25,58	9,05	1,49	17,26	0,26	0,63	4,87	78,57	0,01	0,05	<LD	0,49	<LD
4SF	set/19	8,67	1,56	0,04	2,69	1,35	20,43	8,60	0,21	4,89	0,47	0,67	8,38	57,23	0,00	0,03	6,53	5,11	2,14
4SG	set/17	10,53	2,12	0,00	2,28	2,51	25,56	15,95	0,14	<LD	0,15	0,19	0,52	97,21	0,01	0,00	10,00	15,21	2,49
4SG	mar/17	3,73	1,27	0,00	2,22	1,41	15,61	5,43	0,14	7,48	0,17	0,40	0,88	72,96	0,00	0,00	3,68	2,46	2,55
4SG	nov/16	9,80	1,93	0,01	2,70	2,31	21,43	97,91	1,52	19,39	0,35	0,50	1,78	102,09	0,01	0,02	11,39	12,43	6,74
4SG	set/20	5,62	1,69	0,03	2,46	3,90	19,95	18,36	1,49	38,90	0,38	1,72	1,98	95,14	0,02	0,01	8,33	1,22	24,54
4SG	set/19	11,73	2,42	0,01	3,16	2,94	27,99	15,19	0,09	7,38	0,48	0,30	5,61	107,39	0,02	0,03	9,37	8,17	1,20
4SG	out/19	8,14	1,96	0,01	2,85	2,87	25,52	25,90	0,61	20,93	0,49	0,60	8,43	105,90	0,02	0,05	2,86	3,35	8,41
4SH	set/20	9,50	0,16	0,03	2,07	2,03	0,96	1,36	1,78	24,93	0,13	0,18	0,10	2,45	0,01	0,01	19,47	2,61	1,09
4SI	set/20	1,14	0,30	0,10	2,10	0,55	2,15	1,59	0,81	28,04	0,30	1,62	1,28	11,23	0,01	0,06	1,06	0,12	2,44
4SJ	set/20	0,39	0,14	0,03	2,38	0,23	0,26	0,00	7,23	29,74	0,07	0,28	0,93	1,31	0,00	0,01	0,40	<LD	<LD
4SJ	nov/16	0,31	0,12	0,00	2,46	0,07	0,29	2,28	5,73	3,60	0,12	0,24	1,20	1,49	0,00	0,00	0,56	<LD	0,32
4SK	set/20	6,77	0,93	0,01	2,66	1,72	12,75	2,01	8,99	4,71	0,12	0,33	0,00	43,83	0,00	0,00	9,26	3,45	3,83
4SK	nov/16	6,27	1,01	0,01	2,66	0,92	11,69	4,61	4,91	5,00	0,19	0,26	0,37	38,61	0,01	0,00	6,62	3,64	2,15
4SL	nov/16	6,10	1,24	0,02	2,85	1,11	13,65	8,41	12,38	2,60	0,34	0,24	0,26	51,56	0,01	0,01	4,86	6,03	4,54
4SL	out/16	5,92	1,27	0,02	2,23	2,24	16,19	5,35	6,69	5,51	0,30	0,75	0,49	64,10	0,01	0,03	5,25	6,90	5,28
4SL	out/16	5,88	1,29	0,02	2,15	2,21	16,08	5,85	6,86	6,04	0,40	0,75	0,72	63,96	0,01	0,04	5,25	6,90	5,28
4SL	set/20	7,95	1,59	0,01	2,81	3,92	19,91	8,14	19,85	12,48	0,36	1,30	0,76	82,25	0,01	0,01	9,97	4,27	15,72
4SM	set/20	8,55	1,53	0,02	2,94	3,29	19,50	8,98	1,62	16,48	0,29	0,82	0,40	76,38	0,01	0,01	10,21	4,41	10,72
4SM	nov/16	7,39	1,27	0,02	2,92	1,28	14,39	10,13	9,29	5,07	0,25	0,34	0,51	54,78	0,01	0,02	5,76	3,11	6,40
4SM	set/17	9,26	1,35	0,00	3,08	2,33	14,17	5,30	23,55	0,00	0,21	0,52	0,53	49,23	0,01	0,00	7,12	3,90	12,61
4SM	set/17	3,98	0,60	0,01	1,27	0,97	6,34	4,96	4,51	<LD	0,09	0,36	0,57	21,28	0,00	0,04	7,12	3,90	12,61
4SM	mar/17	5,48	1,07	0,00	2,36	1,60	13,18	31,50	0,04	<LD	0,13	0,61	0,98	59,44	0,00	0,00	3,92	4,86	6,55

ID	Data mês/ano	Na mg/L	Mg mg/L	Al mg/L	Si mg/L	K mg/L	Ca mg/L	P µg/L	Mn µg/L	Fe µg/L	Ni µg/L	Cu µg/L	Zn µg/L	Sr µg/L	Gd µg/L	Pb µg/L	Cl mg/L	NO3 mg/L	SO4 mg/L
4SM	set/17	8,62	1,38	0,01	2,62	3,22	24,23	14,96	1,04	2,06	0,56	1,17	3,18	105,26	0,02	0,00	7,12	3,90	12,61
4SM	out/19	8,53	1,33	0,04	3,18	1,89	17,35	12,70	1,86	30,24	0,23	0,39	3,21	53,63	0,01	0,04	2,37	1,22	3,33
4SM	set/19	8,49	1,32	0,07	3,20	2,02	17,59	24,59	2,67	42,02	1,49	4,96	42,10	58,09	0,02	0,34	5,83	5,06	6,72
4SN	nov/16	5,94	0,65	0,02	3,12	1,17	4,75	16,45	17,64	6,80	0,36	0,26	0,88	17,91	0,01	0,01	4,06	3,32	7,50
4SN	set/20	4,48	0,78	0,05	2,88	1,74	8,99	12,75	13,33	102,85	0,37	0,81	1,54	41,82	0,01	0,10	3,93	2,09	5,48
4SN	out/19	14,66	0,79	0,04	3,28	2,95	5,77	31,09	14,62	65,51	0,41	1,06	5,91	19,12	0,05	0,06	3,42	3,65	7,12
4SN	set/19	6,17	0,75	0,05	2,88	1,43	6,36	57,08	4,45	12,03	1,66	5,29	55,96	21,99	0,01	0,32	3,99	1,52	5,36
4SO	set/20	0,89	0,11	0,03	1,90	0,65	0,29	1,17	2,50	39,29	0,06	0,05	0,09	1,31	0,00	0,01	1,31	<LD	0,29
4SO	out/19	0,63	0,09	0,02	1,64	0,09	0,41	4,76	3,18	161,99	0,33	0,53	8,95	1,80	0,00	0,05	3,49	3,95	6,33
4SO	set/19	0,70	0,09	0,01	1,71	0,14	0,49	4,01	2,83	13,40	0,32	1,10	16,08	2,62	0,00	0,08	0,15	0,08	0,06
4SP	set/17	2,72	0,91	0,01	0,65	2,71	21,57	11,83	31,39	3,25	0,80	4,71	6,47	101,72	0,00	0,00	4,02	0,93	10,48
4SP	set/17	2,45	0,89	0,04	0,69	2,25	13,46	11,18	15,05	6,62	1,61	24,89	14,29	68,32	0,01	0,04	4,02	0,93	10,48
4SP	set/17	4,76	1,69	0,04	1,27	4,46	27,24	18,43	26,22	7,47	2,88	38,04	15,43	131,72	0,01	0,02	4,02	0,93	10,48
4SQ	nov/16	8,88	1,57	0,02	3,00	1,64	19,71	9,42	0,25	15,68	0,25	0,41	0,36	74,59	0,01	0,02	7,27	5,36	5,52
4SR	nov/16	4,95	0,71	0,01	3,12	0,86	6,09	8,10	11,80	3,65	0,32	0,23	0,72	21,35	0,01	0,01	3,70	6,73	6,06
4SS	nov/16	8,07	0,65	0,01	3,17	1,39	4,55	9,73	12,38	4,48	0,36	0,29	0,83	18,67	0,01	0,02	6,14	7,14	11,71
5L	jul/18	8,61	1,05	0,01	1,76	2,47	9,05	5,58	0,06	<LD	0,06	0,09	0,22	36,23	0,02	0,01	<LD	<LD	<LD
5L	abr/18	7,22	0,89	0,00	1,95	2,08	7,53	0,67	0,05	0,06	0,07	0,19	0,40	32,71	0,02	0,00	6,49	2,58	8,09
5L	jun/16	7,64	1,03	0,01	2,02	2,16	8,90	7,47	0,13	3,29	0,12	0,13	0,56	39,84	0,02	0,05	<LD	<LD	<LD

Tabela 4 – Composição do SPM

ID	Massa amostra (g)	Data mês/ano	Na (mg/kg)	Mg (mg/kg)	Al (mg/kg)	P (mg/kg)	K (mg/kg)	Ca (mg/kg)	Ti (mg/kg)	Mn (mg/kg)	Fe (mg/kg)	Pb (mg/kg)	Th (mg/kg)	Cu (mg/kg)	Zn (mg/kg)	Sr (mg/kg)	REE SUM (mg/kg)	Gd (mg/kg)
1L	0,0040	jul/17	7657	6289	85754	9181	5735	61772	467	578	87663	26	19	49	308	149	119	3
2L	0,0013	jul/17	22897	17640	238228	26967	15200	191803	924	1918	309202	68	49	112	476	471	404	10
4LB	0,0037	jul/17	7816	7116	103899	41289	6327	67891	309	196	43117	28	7	80	786	191	199	10
4LE	0,0044	jul/17	6921	5952	91290	10745	4863	58809	288	1735	60374	31	17	59	234	157	156	4
4SA	0,1065	mar/17	251	1742	73593	901	984	6742	238	159	41349	36	11	45	243	28	126	3
4SA	0,0052	set/20	1400	2831	134333	3050	5675	9398	5740	763	66465	68	21	103	1014	62	234	4
4SB	0,0817	mar/17	288	1142	49437	1377	747	6191	96	84	25825	29	7	37	194	24	98	2
4SB	0,0317	set/20	1304	2825	56011	11295	5253	6596	2789	245	26955	33	10	89	614	45	128	2
4SB	0,0477	nov/16	733	2562	48776	20291	4775	11675	144	79	12253	15	1	87	492	56	59	1
4SB	0,0017	set/17	12650	17317	224958	100781	14468	143711	423	428	121089	57	30	344	2370	458	254	5
4SC	0,0090	mar/17	2512	2937	54471	5307	1065	28161	157	128	33604	14	11	33	89	78	111	3
4SC	0,0267	set/20	929	2932	90090	5834	11735	4861	5124	570	44681	39	16	71	425	42	195	4
4SC	0,0158	nov/16	2626	2510	68256	8716	1817	19525	230	462	52246	35	7	67	287	64	151	3
4SC	0,0034	set/17	4895	6525	62902	17111	1246	68626	144	1179	49117	19	13	59	443	179	98	2
4SD	0,0217	nov/16	3204	3219	33237	3468	1272	33600	196	426	26222	13	9	25	110	85	57	2
4SD	0,0021	set/17	10947	11044	109945	35418	3154	116626	297	2826	166871	53	38	107	816	304	231	6
4SE	0,0067	set/20	1361	698	70065	964	3131	4347	3732	2051	75286	32	12	24	110	24	183	4
4SE	0,0151	set/17	1449	1192	14144	2023	181	13236	23	543	40885	5	3	8	83	31	26	1
4SE	0,0074	mar/17	2188	2657	62550	2653	430	29007	225	87	63793	14	32	29	0	70	88	2
4SF	0,0212	set/20	1069	2309	107189	1002	12080	5637	6138	428	46959	29	19	36	117	39	146	4
4SF	0,0052	set/17	3926	4207	41908	5704	924	45786	109	634	31852	13	9	27	236	118	68	3
4SG	0,0050	set/20	1620	1720	79688	3634	5810	9434	3642	741	33183	51	15	67	398	69	157	3
4SG	0,0050	nov/16	5949	5482	63640	17320	3792	57393	123	603	41083	20	9	59	317	188	129	3
4SH	0,0043	set/20	1236	717	127605	1548	1470	3583	5928	1628	50890	58	19	39	137	17	350	8
4SI	0,0055	set/20	896	1240	175456	1574	2146	5036	5920	171	29760	36	25	57	394	40	205	5
4SJ	0,0040	set/20	998	1573	110694	2288	3784	3909	4872	3053	80932	35	18	42	187	34	159	4

ID	Massa amostra)	Data	Na	Mg	Al	P	K	Ca	Ti	Mn	Fe	Pb	Th	Cu	Zn	Sr	REE SUM	Gd
	(g)	mês/ano	(mg/kg)															
4SK	0,0047	set/20	1876	1952	163026	1270	5856	8300	8606	1016	91684	31	28	68	184	43	158	4
4SL	0,0495	set/20	668	2177	89354	1587	10663	4585	5234	521	40974	25	17	39	137	36	142	3
4SM	0,0368	set/20	836	2440	99849	1993	11271	5961	5744	435	45659	31	18	42	161	42	153	4
4SN	0,0223	set/20	949	3192	82350	6094	9028	6453	4454	441	49289	44	14	91	655	51	174	3
4SO	0,0052	set/20	847	685	47398	1897	2344	4274	1146	160	84793	16	7	18	72	22	96	1
4SQ	0,0035	mar/17	5464	6191	64590	6940	1635	65888	220	294	96458	<LD	14	41	<LD	160	137	3
5L	0,0088	jul/17	3195	2919	41261	3717	2817	30098	203	876	46308	15	11	25	94	79	95	2

Tabela 5 - Concentração química dos sedimentos

ID	Profundidade (cm)	P (mg/kg)	Al (mg/kg)	Fe (mg/kg)	Mn (mg/kg)	Ca (mg/kg)	Cu (mg/kg)	Zn (mg/kg)	Mg (mg/kg)	As (mg/kg)	V (mg/kg)	Ti (mg/kg)
1L	1	783,32	111933,39	46441,89	331,01	2512,55	41,99	105,09	1864,86	8,32	106,50	7683,55
2L	1	857,71	132368,42	56614,78	330,71	2005,67	34,38	62,09	2024,17	8,15	143,73	7461,92
4LC	1	7753,95	81662,05	38243,04	104,87	5594,77	58,07	333,12	2855,17	7,74	87,28	5205,57
4LC	4	4436,22	79780,53	30737,15	118,93	4284,88	45,66	200,61	2133,51	6,04	74,63	4387,15
4LC	9	6763,10	84224,60	40754,42	95,24	7988,55	59,57	293,86	2832,14	8,56	75,52	4958,28
4LC	15	6176,84	97853,65	41013,36	100,28	7166,36	54,05	304,04	3360,96	8,22	84,41	5732,84
4LB	1	406,64	64272,33	22068,23	88,11	2592,19	19,30	39,65	1390,58	4,38	69,22	4170,05
4LB	1	530,41	70074,25	23735,63	167,10	3325,81	22,96	49,24	1655,59	5,45	71,03	4726,09
4LB	9	678,50	58269,26	21116,42	72,54	3290,87	18,00	36,21	1358,05	3,99	58,77	4111,84
4LB	15	801,59	75906,49	28758,37	107,06	2894,00	22,70	46,83	1704,91	5,71	71,90	5312,74
4LD	1	667,12	68196,55	25603,39	96,92	4116,10	27,05	69,52	1697,58	6,71	68,57	4230,27
4LD	5	590,04	77525,19	27581,08	98,21	4042,76	24,49	68,25	1826,39	6,11	76,34	4703,83
4LD	9	759,12	98941,19	36006,82	107,99	4162,00	31,32	86,07	2412,24	8,01	90,80	6023,88
4LD	15	808,82	98885,68	37136,18	96,31	4110,76	30,25	90,38	2357,39	7,33	83,82	5874,84
4LF	1	780,24	81864,72	26416,73	79,07	2611,44	22,12	64,99	1710,75	7,25	81,08	4711,83
4LF	5	781,35	73347,37	26877,72	84,11	2361,54	21,76	65,02	1785,54	<LD	77,97	4481,84
4LF	9	864,15	70593,98	26776,96	76,52	2262,71	21,80	70,26	1731,96	6,05	75,69	4377,45
4LF	12	912,98	68088,76	29295,98	74,00	1895,93	23,35	75,53	1584,67	6,48	80,10	4753,94
4LF	17	829,08	67364,73	28770,36	67,48	1885,28	22,10	70,15	1616,69	<LD	79,00	4644,73
4LE	1	1014,07	132949,99	47864,75	191,88	3306,11	37,47	108,34	3005,45	9,47	136,69	7789,17
4LE	9	1216,36	130876,89	49164,49	150,17	3548,86	35,25	100,06	2765,94	9,02	115,49	7447,55
4LE	15	1163,08	127807,57	51720,51	139,88	3381,00	35,01	104,63	2996,81	8,76	116,38	7520,60
5L	1	535,76	109883,60	55197,52	270,68	1812,45	25,31	52,32	2975,93	8,50	114,48	6478,82
3L	1	1302,43	119799,46	59861,65	226,33	1803,57	35,55	69,32	2005,78	8,68	120,57	5242,33
3L	9	1199,71	106390,56	62446,16	164,93	1162,80	52,50	65,31	1562,03	9,15	126,73	7378,66
3L	15	1228,68	95503,21	54437,11	154,76	1025,14	52,52	61,96	1633,48	8,69	118,94	6628,46
CX	10	826,17	89901,15	137573,76	88,33	1361,48	58,30	186,65	755,51	10,36	156,37	5471,87
CX	4	875,68	86854,10	161871,78	89,90	2088,17	46,32	192,78	934,24	10,23	154,73	5405,89

ID	Profundidade (cm)	P (mg/kg)	Al (mg/kg)	Fe (mg/kg)	Mn (mg/kg)	Ca (mg/kg)	Cu (mg/kg)	Zn (mg/kg)	Mg (mg/kg)	As (mg/kg)	V (mg/kg)	Ti (mg/kg)
OX1	20	910,67	135164,88	68912,72	57,31	371,56	6,45	20,13	161,83	21,18	188,58	9473,02
OX1	5	861,14	125916,82	63034,46	55,45	369,18	6,15	16,62	163,47	20,48	172,47	8965,29
OX2	20	789,60	84352,44	32043,15	40,31	110,85	8,29	16,19	661,18	8,40	71,60	4200,96
RF1	10	209,08	30527,50	13838,31	43,33	963,95	10,36	19,20	665,29	2,93	36,72	2183,67
RF2	73,5	430,92	48851,23	24672,40	73,74	899,75	10,92	31,45	875,03	5,54	58,87	3508,69
RF3	129	471,87	65547,22	31612,29	35,92	614,98	9,77	30,99	1188,40	5,60	70,74	4345,32
RF4	235	1497,73	97997,39	41332,47	108,25	1238,09	19,84	31,80	1833,88	5,36	99,39	6508,87
RF5	213	801,85	75847,81	32835,80	73,12	1036,76	16,68	42,93	1767,23	5,92	84,65	4857,87
RF6	329	1021,06	80249,00	22312,98	28,64	1682,16	15,30	21,69	1300,82	3,46	97,72	5230,22
RF7	324,5	460,53	63471,78	38345,66	107,11	451,83	12,99	40,52	1156,17	5,28	80,45	4688,28
RF8	361	225,80	39090,24	19182,76	43,68	365,55	9,13	16,28	531,87	3,38	43,78	2632,20
RF9	387	1110,98	81012,13	21178,42	38,48	1537,44	15,88	43,77	1135,26	3,74	106,13	5016,33
RF10	445,7	531,37	55929,96	11047,30	21,56	2685,20	11,26	29,16	793,74	<LD	70,46	3338,82
RF11	579,6	219,46	32960,19	3256,49	10,66	1088,58	6,00	22,63	630,71	<LD	34,99	2289,66
RF12	523,4	121,52	33871,87	5063,79	11,03	522,33	6,22	13,67	551,09	<LD	32,15	2292,81

Tabela 6 - Concentração química de P e suas frações nos sedimentos

ID	Profundidade (cm)	Lo-P (mg/kg)	Al-P (mg/kg)	Fe-P (mg/kg)	Ca-P (mg/kg)	$\sum$ Frações de P (mg/kg)	P-Org	TP (mg/kg)
1L	1	3,6	95,3	291,4	105,1	495,4		783,3
2L	1	3,4	95,3	437,2	81,2	617,1		857,7
4LC	1	27,4	5463,7	1489,2	688,4	7668,7	747,7	7754,0
4LC	4	11,1	1477,5	670,7	160,5	2319,8		4436,2
4LC	9	9,0	2918,4	822,4	1571,2	5321,0		6763,1
4LC	15	2,1	5977,7	1040,5	3302,1	10322,4	999,8	6176,8
4LB	1	3,4	138,0	138,5	33,7	313,6		406,6
4LB	1	2,4	169,9	180,8	70,0	423,1	85,7	530,4
4LB	9	1,3	109,5	141,7	51,6	304,1		678,5
4LB	15	<LD	258,7	41,7	118,3	418,8		801,6
4LD	1	2,4	211,3	230,2	142,7	586,6		667,1
4LD	5	2,1	216,4	232,2	79,7	530,4		590,0
4LD	9	2,1	228,1	224,7	110,3	565,2		759,1
4LD	15	1,7	222,3	202,9	98,3	525,3		808,8
4LF	1	2,8	287,3	320,9	91,2	702,3	111,3	780,2
4LF	5	2,9	256,7	305,2	94,7	659,5		781,3
4LF	9	4,1	306,9	351,8	104,3	767,2		864,1
4LF	12	5,6	295,8	379,9	113,0	794,4		913,0
4LF	17	5,4	224,7	391,0	108,7	729,8	121,3	829,1
4LE	1	4,2	244,4	399,1	123,0	770,8		1014,1
4LE	9	2,1	185,8	338,6	123,8	650,3		1216,4
4LE	15	1,7	161,4	310,1	95,5	568,7		1163,1
5L	1	1,7	41,9	160,3	55,7	259,6		535,8
3L	1	7,9	128,0	685,9	177,5	999,4	234,8	1302,4
3L	9	1,7	85,8	475,3	212,3	775,1		1199,7
3L	15	1,0	89,6	375,8	252,6	719,1	146,9	1228,7

ID	Profundidade (cm)	Lo-P (mg/kg)	Al-P (mg/kg)	Fe-P (mg/kg)	Ca-P (mg/kg)	$\sum$ Frações de P (mg/kg)	P-Org (mg/kg)	TP
								(mg/kg)
CX	10	0,4	11,7	71,5	12,7	96,3		826,2
CX	4	1,3	15,3	75,6	22,1	114,3	93,5	875,7
OX1	20	0,9	14,2	70,0	10,2	95,3	1,4	910,7
OX1	5	0,4	15,2	77,7	11,0	104,3		861,1
OX2	20	1,3	17,9	65,2	9,7	94,1	6,1	789,6
RF1	10	1,9	49,8	168,2	26,4	246,3		209,1
RF2	73,5	1,7	28,1	126,6	18,1	174,6	69,9	430,9
RF3	129	<LD	21,9	125,5	14,9	162,2		471,9
RF4	235	0,7	61,8	153,5	31,7	247,7		1497,7
RF5	213	<LD	109,5	306,5	69,4	485,4		801,8
RF6	329	2,0	47,9	77,7	26,6	154,1		1021,1
RF7	324,5	4,4	25,1	139,8	35,6	204,8		460,5
RF8	361	2,5	60,2	35,7	6,1	104,6		225,8
RF9	387	2,9	92,6	190,9	18,5	304,8		1111,0
RF10	445,7	4,3	130,3	136,9	22,6	294,1	168,2	531,4
RF11	579,6	<LD	11,6	31,8	0,0	43,4		219,5
RF12	523,4	<LD	29,4	28,1	0,0	57,6		121,5

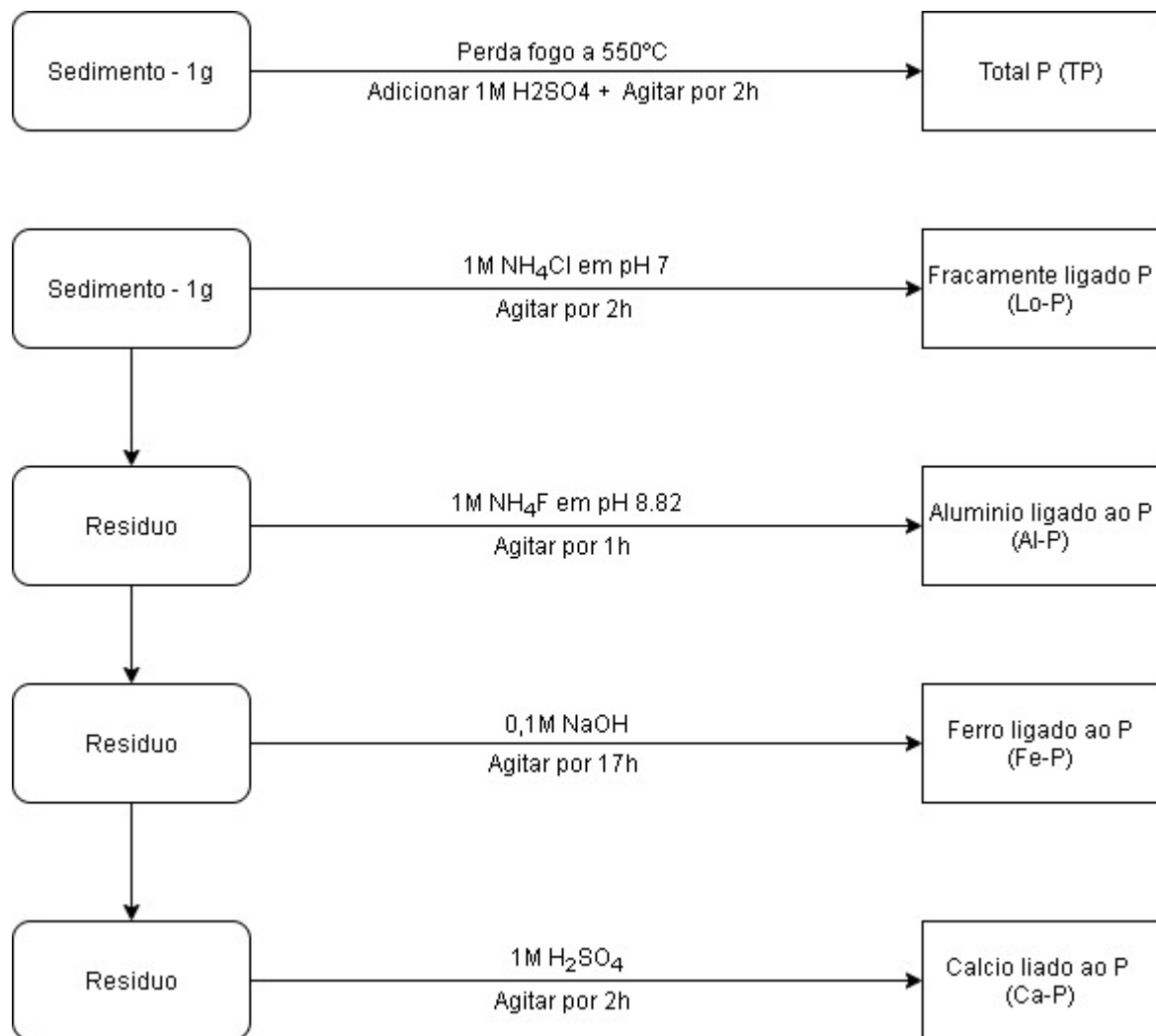


Figura 13 – Esquema do método para determinação de formas de fósforo inorgânico em sedimentos superficiais.

